Department of Earth Sciences
UNIVERSITEIT UTRECHT

Thin-skinned versus thick-skinned tectonics in the Friuli Alps (NE Italy) in relation to the Alpine-Dinaridic orogenic system

MSc Thesis

Dominique Engelen

February 2016

Supervisors

1st Dr. Ernst Willingshofer
2nd Drs. Inge van Gelder
3rd Dr. Liviu Matenco

In collaboration with

Anissa Smits

Abstract

The Friuli Alps, located in the easternmost part of the eastern Southern Alps in north-eastern Italy, represent the interference area of the Dinaric and Alpine mountain chains. There is a wide agreement on the general evolution of the eastern Southern Alps, which would consist of a poly-phase compressional evolution involving three main thrust systems. However, the amount and initiation of the total amount of shortening is still poorly constraint. In this study we investigate the kinematic evolution by means of structural fieldwork and by the balancing and reconstruction of a N-S cross-section by use of MOVE software for 2D modeling. Interpretation of the data led to the definition of five deformation phases (D1- D5), in which a clear distinction could be made between thin- and a thick-skinned phases of deformation. Prior to the compressional phases is the D1 NW-SE extensional phase, which is expressed by NNW-SSE oriented normal faults, related to the NE-SW separation of the Friuli platform during the Early-Jurassic. The D2 NE-SW to E-W directed Dinaric shortening started during the Eocene and is expressed by SW to W-vergent thrusting and folding. Dinaric deformation is largely overprinted by three Alpine phases; D3 – N-S thin-skinned Alpine shortening (Middle- to Late-Miocene), characterized by large scale S-vergent thrusting along flat-ramp-flat trajectories, which resulted in great amounts of transport of the Upper-Triassic and Jurassic platform formations along four main décollements (the Bellerophon, Raibl and Biancone Formation, and the Eocene flysch) and ultimately to tripling and folding of the sedimentary cover. The D4 – NE-SW thick-skinned Alpine shortening (Late Miocene – Pliocene), which is expressed by the reactivation and cross-cutting of thin-skinned structures and basement involved thrusting. The D5 – Transpressional phase (initiated during the Early –Miocene and is still active), which has been interpreted as the transpressional continuation of the D4 thick-skinned deformation and involves large scale strike-slip deformation and minor normal faulting. Due to the clear distinction between thin- and thick-skinned deformation, we were able to make an estimation of the total amount of N-S shortening since the Eocene. The balancing and reconstruction of the thin-skinned dominated model in MOVE indicates a minimum shortening of 57,2 km (51%) for the Friuli Alps. The maximum shortening is estimated on ~78,4 km. These newly proposed shortening estimates are significantly higher than the previously proposed 30 – 50 km of N-S shortening for the eastern Southern Alps during the Miocene and provide new insights on the plate tectonic setting below the Eastern Alps. This higher amount of shortening enhances the differentiation between the western and eastern Southern Alps even further and may indicate the horizontal decoupling of the Adriatic upper crust and underthrusting of the lower crust, associated to the subduction of the Adriatic plate beneath the Eastern Alps.

TABLE OF CONTENTS

1. Introduction

The Friuli Alps represent the easternmost part of the eastern Southern Alps, located in North-Eastern Italy. The present-day S-vergent fold-and-thrust belt in the Southern Alps is the result of four major tectonic events, including Miocene to recent deformations related to convergence of Apulia and Europe (Laubscher, 1985, 1990; Roeder, 1989, 1992; Schönborn, 1992).

There is a wide agreement on the general evolution of the eastern Southern Alps during the Neogene, which would consist of a poly-phase compressional evolution involving three main thrust systems (Schönborn, 1999; Castellarin & Cantelli, 2000; Nussbaum, 2002), followed by a phase of strike-slip deformation associated to the lateral extrusion of the area. The current models propose a southward in sequence propagation of the three thrust systems, which includes décollement thrusting, but it is also indicated that each system involves its own basement unit. (Schönborn, 1999; Castellarin & Cantelli, 2000; Nussbaum, 2002). No clear temporal or spatial discrimination between décollement thrusting and basement thrusting is indicated.

Apart from the general structural evolution of the area, is the paleogeographic evolution of the Friuli also well studied by Stefani et al. (2007).

The amount of shortening however, is poorly constrained and is currently still at the center of discussion. For a period of time an estimate of 50 km of Miocene shortening was generally applied for the Friuli Alps (Schönborn, 1999; Schmid et al., 1996). However, more recent studies of Nussbaum (2002) and Ustaszewski et al. (2008) propose significantly higher amounts of shortening. Nussbaum (2009) considers the 50 km of shortening as a underestimation, but does not provide an alternative number. But the crustal shortening estimate proposed by Ustaszewski et al. (2008), indicates an amount of 190 km for the last 20 Ma, based on teleseismic tomographic research which indicates the subduction of ~210 km of Adriatic slab blow the Eastern Alps.

As the spatial and temporal interaction of thin- and thick-skinned tectonics is crucial for the understanding of the dynamics and the sequence of foreland deformation in a collisional orogenic setting (Madritisch, 2008), it is also the main factor controlling the amount of shortening in the area, which makes this is the main point of attention during this study. The construction of a N-S cross-section, constrained by extrapolated field-data and characteristics of the examined surface geology, enables a critical evaluation as to whether deformation was by thin- or thick-skinned tectonics in order to explain the deeper structure of the Friuli Alps.

The N-S striking cross-section will be balanced and restored in MOVE (software for 2D/3D kinematic modelling & reconstruction, by Midland Valley). Forward modelling of the restored section will tests its validity and provides snap shots of the intermediate steps and gives new insights on the kinematic evolution of the Friuli Alps which enables us to address the different styles of deformation: thin-skinned versus thick-skinned tectonics in an Alpine-Dinaridic orogenic system.

The interpretation of the field data and the information obtained from the Kinematic model, allows us to shed new light on the recently proposed subduction polarity switch beneath the Eastern Alps, and my lead to a better understanding of the tectonic evolution of this earthquake-prone region of the Alpine-Dinaridic orogenic system.

2. Geological setting

The area of interest is located within the southern part of the larger Alpine mountain chain which formed due to the convergent movement between Europe and Africa, resulting in the closure of former oceans and ultimately to continental collision. The study area is located in the Friuli Alps, which covers the easternmost part of the eastern Southern Alps (fig.1). The Southern Alps, which represents one of the main structural subdivided regions of the larger Alpine Chain, is that part of the Alps that is found South of the Periadriatic Lineament, a major geological fault zone across the Alps representing the separation between the Apulian units (Adria) in the South, and the Apulian Austroalpine units (and Europe derived units) in the North. The crustal collision and indentation of Adria underneath the Alpine chain resulted in the South-verging fold-and-thrust belt of the Southern Alps (Schmid et al., 1996; Castellarin et al., 2006b; Caputo et al., 2010). The eastern part of the Southern Alps is affected by three main orogenic processes.

The Eo-Alpine deformation during the Cretaceous, the Dinaric deformation during the Paleogene and the Alpine deformation during Neogene times. The area is widely described as an important interference zone between Alpine and Dinaric structures.

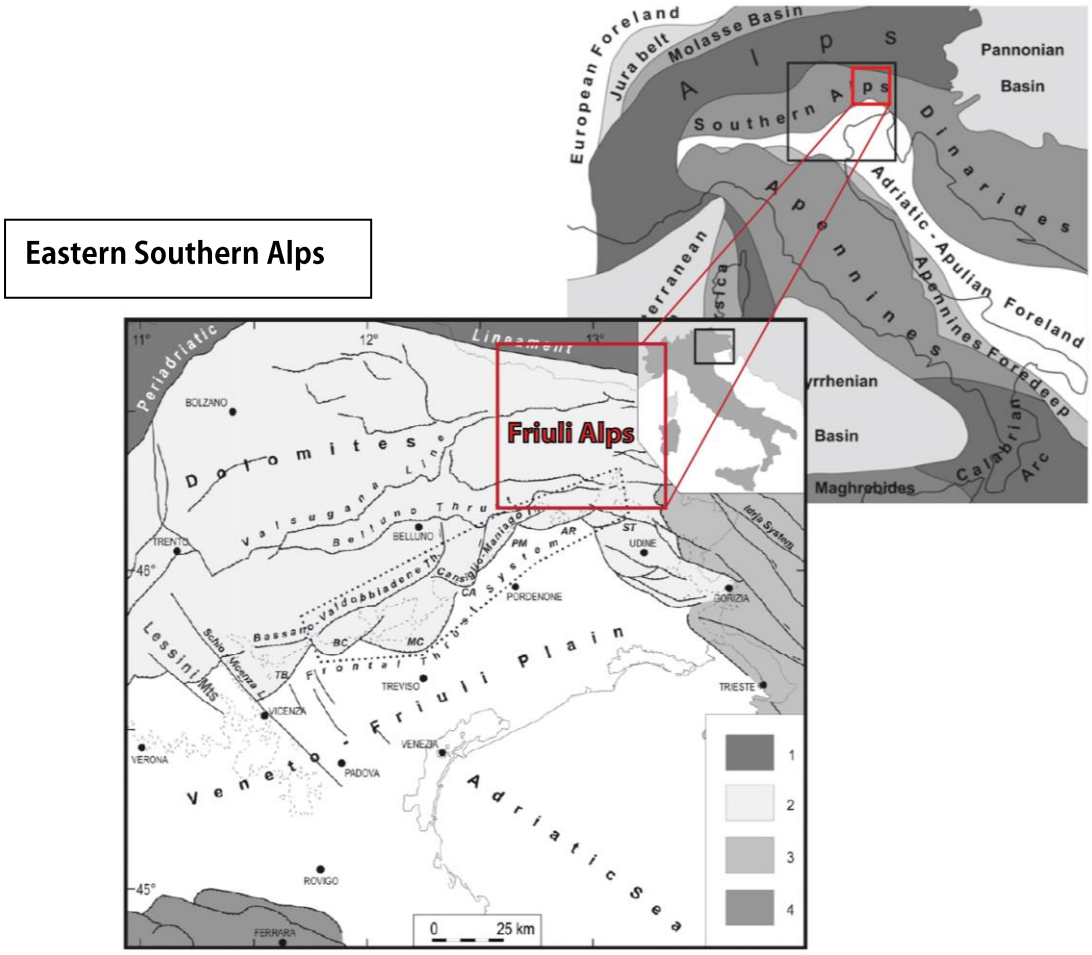

Figure 1. *Overview of the mountain chains of central and southern Europe. The red box indicates the research area, the Friuli Alps, located in Northeastern Italy (The North Italian geodynamic framework, modified from (Bigi et al., 1990 and Caputo et al., 2010).*

2.1 The Alps

The European Alps comprise an elongated arc shaped mountain range that covers parts of south-eastern France in the west to Slovenia in the east. The Alpine mountain chain formed due to the Europe – Africa convergence, which was responsible for the closure of former oceanic domains (fig. 3) and was followed by continental collision. The Alps formed by two orogenic phases, a Cretaceous orogeny (Eo-Alpine) and a Tertiary orogeny. The Eo-Alpine phase was caused by intracontinental subduction within the Austroalpine unit (Stüwe & Schuster, 2010) and started during the Valanginian in the Early Cretaceous. Peak metamorphism was reached during the Turonian in early Late Cretaceous time. The second orogenic stage during the Paleogene is characterized by the closure of the Alpine Tethys between the Adriatic plate and Europe in respond to northward African motion (Schmid et al., 2004). An overview of the tectonic classification for the several Alpine domains is displayed in figure 2 below (by Schmid et al., 2004).

2.1.1 Cretaceous (Eo-Alpine) orogeny

Prior to the Cretaceous orogenic phase is the opening of the Alpine Tethys Oceanic domains. This Oceanic domain includes the Piedmont-Liguria Ocean, also known as the Alpine Tethys, and the Valais ocean. The Piedmont Liguria Ocean separates Europe from the Apulian plate, and later on during the Cretaceous the Valais Ocean opens between Iberia and Europe (fig. 3). The opening of these oceans is kinematically linked to the opening of the Atlantic Ocean and started during the Middle Jurassic (Schmid et al., 2004).

Cretaceous orogeny started during the Valanginian in the Early Cretaceous and was ongoing till Late Cretaceous time. A SE directed subduction zone was formed related to the closure of the Meliata Ocean. Spreading of the Meliata Ocean started already in Triassic time, coeval with the opening of the Neotethys Ocean (Schmid et al., 2008). The Meliata Ocean was located east of Apulia and was closing in a westwards direction forming the SE directed subduction zone (fig. 3 and fig. 4). Associated to this subduction zone is W- to NW- directed nappe stacking with the Upper Austroalpine nappes forming an orogenic wedge which grew continuously during the Cretaceous (Schuster, 1998). Peak metamorphism, with UHP conditions in the Slovenian part of the Austoalpine unit, was reached during the Turonian in early Late Cretaceous time. After the closure of the Meliata Ocean during Cretaceous time, Apulia behaved as one block (Schmid et al., 2004).

After the orogenic event, which started in the Early Cretaceous, a phase of Late Cretaceous extension took place. In eastern Switzerland the extension affected the higher tectonic levels with normal faulting and at deeper levels with folding (Froitzheim et al., 1994). Further eastward in Austria, major subsidence in the central Alpine Gosau basins took place, which cause is still under discussion**.** Wagreich (1993) suggests a model involving subduction erosion, which is explained as a mechanism whereby subduction of the swell (or ridge) leads to subcrustal tectonic erosion (STE) and rapid subsidence and tilting. Froitzheim et al. (1997) relates the basin formation to slab roll back, whereas Willingshofer et al. (1999) relates the subsidence of the central Alpine Gosau basins to the collapse of a very weak thickened continental crust.

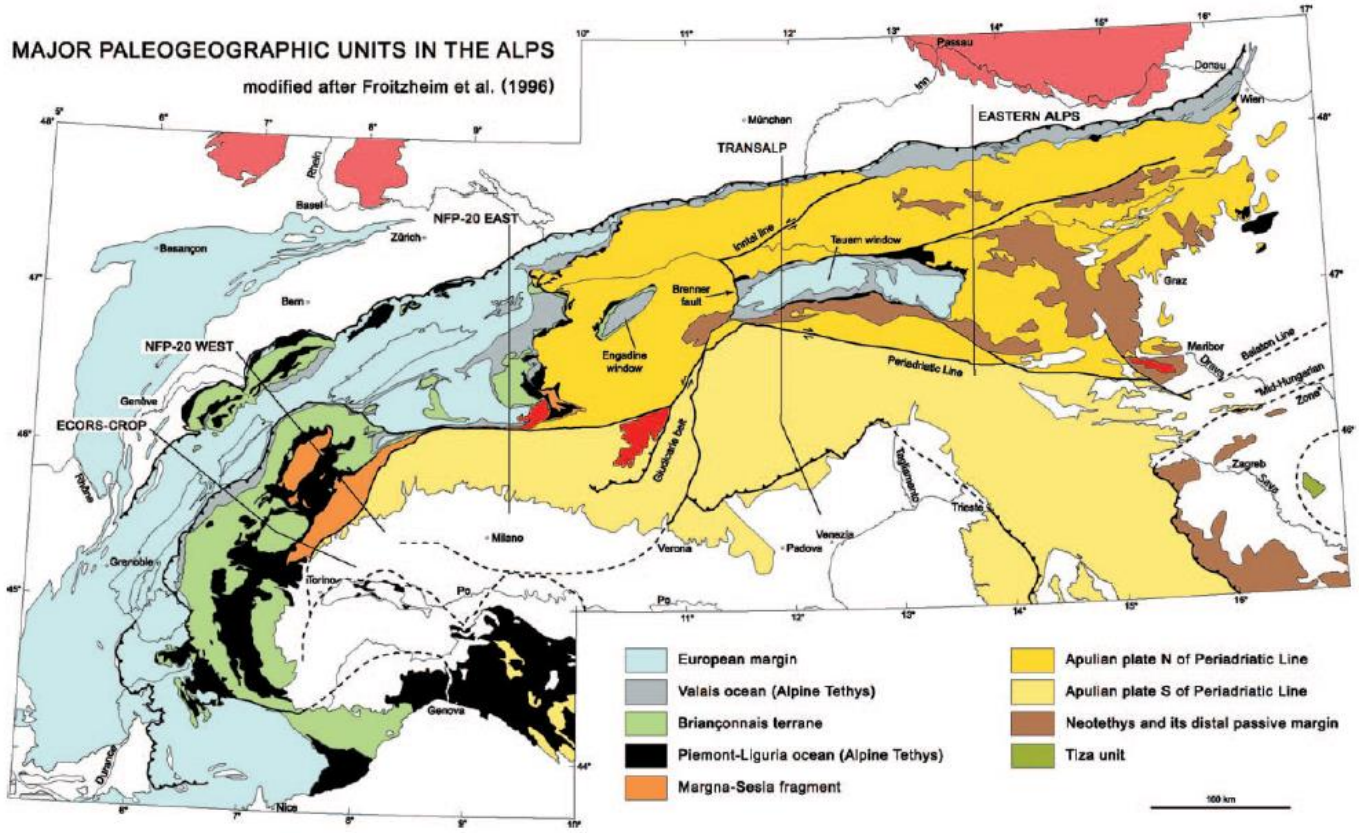

***Figure 2**. Map of the major paleographic and tectonic units in the Alps (Schmid et al., 2004).*

2.1.2 Paleogene orogeny

The Paleogene Alpine orogeny is related to the closure of the Alpine Tethys due to the ongoing northward movement of Africa. During this orogeny the European plate subducts beneath the Adriatic micro-continent in S-SE direction. During Late Cretaceous time (~85Ma) the closure of the Alpine Tethys starts and a subduction zone was formed. Closure of this ocean marks the beginning of the second Alpine orogenic phase. The actual Paleogene collision however, started during the Early Eocene around 50-53 Ma and around 45 Ma the continental units from Europe enter the subduction zone (Schmid et al., 2013). Subduction was ongoing until at least Early Oligocene time, as indicated by eclogites of the European margin, which are now exposed in the Tauern window.

The processes described above resulted in the formation of the Penninic, Subpenninic and Helvetic nappes. The Penninic nappes thrusted northwards onto the foreland during the final stages of the collisional event, which led to the detachment of the sediments from their underlying strata. These sediments would later form the Helvetic nappes. The Eocene- Oligocene continental collision and associated nappe stacking is followed by a phase of post-collisional shortening due to the ongoing N-S convergent movement. This stage involves back thrusting of the Central Alps over the Southern Alps, along the Insubric line (Schmid et al.,1989).

2.1.3 Neogene to recent

As mentioned above, during Oligocene to Miocene time the ongoing N-S convergent motion in the Eastern Alps was mainly expressed by the formation of conjugate strike-slip faults. Most of the dextral strike-slip deformation took place in branches parallel to the Periadriatic fault (E-W oriented), such as the Simplon ductile shear zone and the Rhone-Simplon Line (Steck 1984, 1990). Sinistral displacement took place along the Giudicarie Line (fig. 2), accommodating the northward motion of the Southern Alps coeval with eastward extrusion of the Eastern Alps (Castellarin et al., 1993). The lateral extrusion probably started from the Oligocene – Miocene boundary onwards, and had its main phase of movement in late Early and early Middle Miocene (Ratschbacher et al., 1991).

The lateral tectonic extrusion in the Eastern Alps is defined as a combination of the following tectonic processes; 1) An overall northerly compression (Apulia against Eurasia), 2) a strong foreland (Bohemian massif), 3) lack of constraint along a lateral boundary (Carpathian region) and 4) a previously thickened, gravitationally unstable, thermally weakened crust (Eastern Alpine orogenic belt) (Ratschbacher, 1991).

The large scale orogeny parallel extension of the Austroalpine units was responsible for the formation of the so called Penninic windows; the Engadine, Rechnitz and Tauern window. A rapid drop in temperature recorded in Penninic contents of the Rechnitz window indicates a exhumation age of 17Ma (Tari, 1996). The Tauern window, which is the largest of Penninic windows located in the center of the Eastern Alps, provides a glimpse into the sequence of the Nappes. It shows that the Austroalpine nappes lie on top of the Penninic nappes. The Penninic nappes consist of units of the distal European margin as well as oceanic pieces of the Alpine Tethys. The overlying Austroalpine nappes consist of relics of the southern margin of Piedmont-Liguria Ocean.

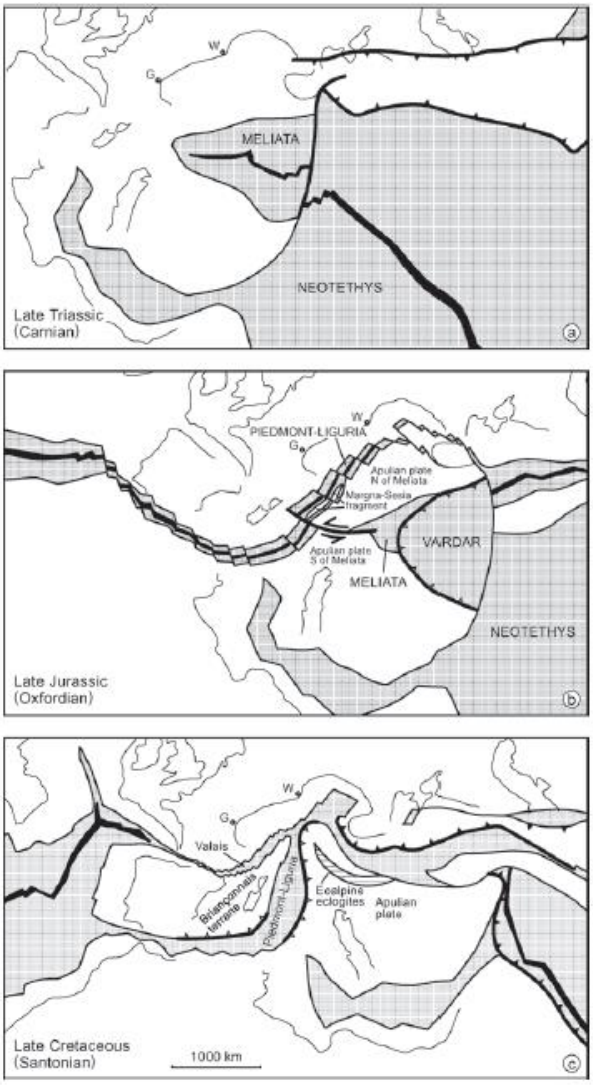

Figure 3*. Large-scale paleogeographic reconstruction illustrating the development of the oceanic domains in; A) Late Triassic, B) Late Jurassic and C) Late Cretaceous time. Modified by Schmid et al., 2004.*

After the early Miocene, a stage of post-collisional shortening affected the Southern Alps and influenced especially the deep structure of the Alps. A second phase

of post-collisional shortening involves back thrusting of the Central Alps over the Southern Alps, along the Insubric line (Schmid et al.,1989). After the Late Oligocene, the Periadriatic line formed due to post-collisional deformation, which is induced by dextral transpression between the Adriatic microplate and the European plate. In the Western Alps this resulted in foreland thrusting and thereby substantial uplift and backthrusting. Whereas in the Eastern Alps this dextral movement is mainly expressed by lateral escape along conjugate strike slip faults with minor vertical movement (Schmid, 1989). Also associated to this strike-slip deformation are Miocene age normal faults, such as the Simplon, the Brenner or Katschberg normal faults (Mancktelow 1990, 1992). The Brenner Fault represents the low angle detachment fault which is linked to the unroofing of the western Tauern window, which also involved enhanced footwall erosion and simultaneous upright antiformal folding. This combination indicates orogen parallel extension during continued N-S Alpine convergence (Fügenschuh et al., 1997).

Schmid et al., (1996) proposes that it was this phase that led to the greatest amount of post-Adamello shortening by frontal thrusting onto the Molasse foreland basin and to the foreland thrust wedge of the Southern Alps. The foredeep sediments in the frontal Southern Alps were mainly deposited during the Neogene and ended in the latest Messinian. Stratigraphic and structural data documents active compressional deformation during the Pliocene and Pleistocene (Venzo, 1977; Castellarin and Cantelli 2000; Bertelli et al. 2003).

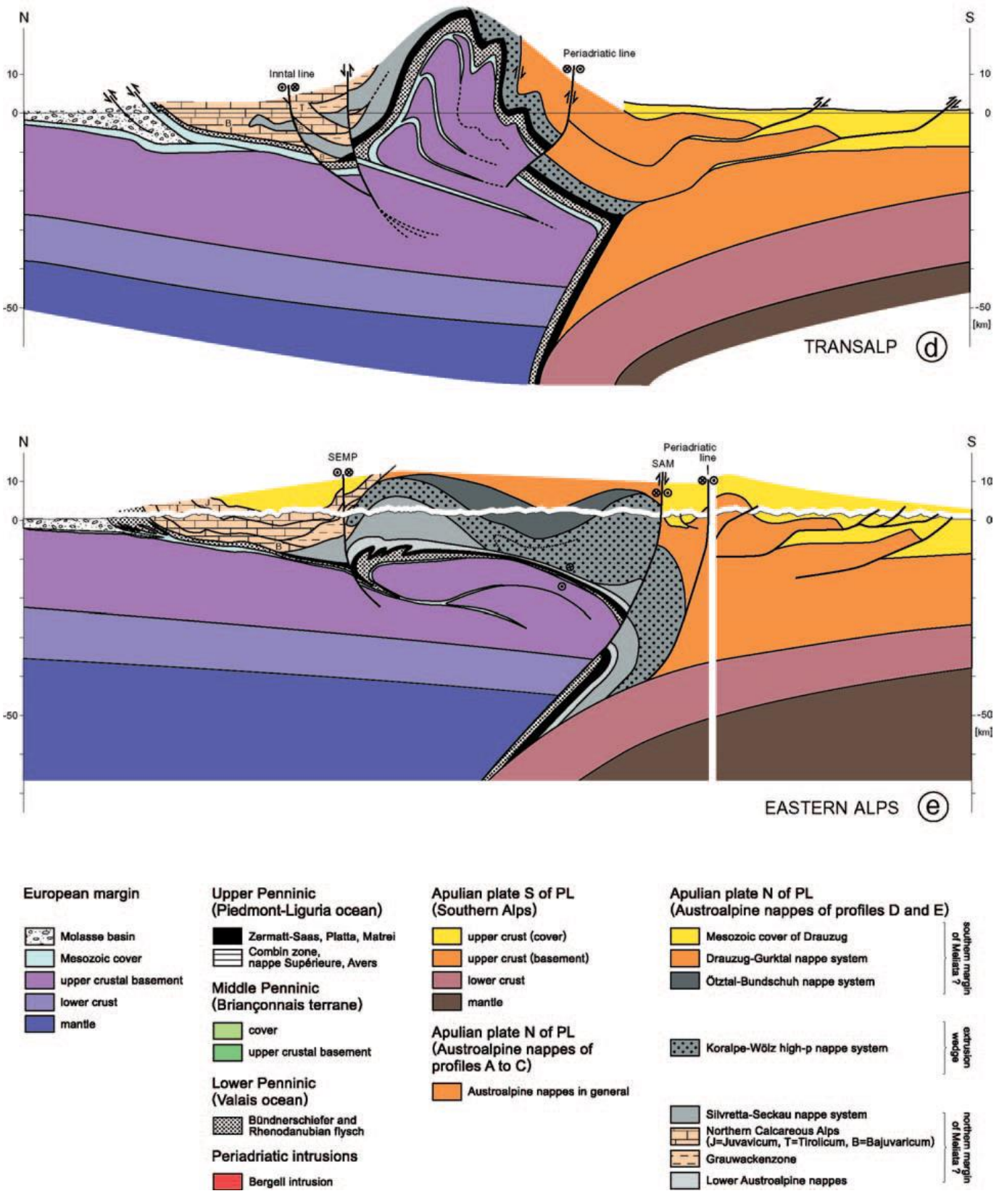

Figure 4. *The **TRANSALP transect** and the **EASTERN ALPS transect.** These cross-sections provide an overall architecture of the Western and Eastern Alps and their forelands. The sections are largely based on recent geophysical-geological transects. For the TRANSALP transect is the geometry of the Moho at a depth of >60 km still poorly constrained by reflection seismic data, while no reflection seismic information is available at all in the case of the EASTERN ALPS transect (Schmidt et al., 2004).*

2.2 The Southern Alps

The Friuli Alps are located in the Southern Alps, east of the Dolomites and west of the external Dinarides. As the Southern Alps are part of the larger Alpine system, they as well are formed by Dinaric deformation during the Paleogene and Alpine deformation during Neogene times. The various segments of the Periadriatic Line, from west to east, the Canavese, Insubric, Giudicarie, Pustertal and Gailtal lines mark the western and northern boundary of the Southern Alps (e.g. Schmid et al.,1989).

The Southern Alps are widely described as a dominantly south-verging fold-and-thrust belt developed at the margin of the Adriatic micro-plate (fig. 5) (e.g. Castelarin et al. 1992; Schönborn 1992, 1999). Adria is a stable continental crustal block according to multiple different paleogeographic and palinspastic interpretations (D'Argenio et al., 1980; e.g., Vai 1977; Stamfi and Mosar 1999). The thrust belt formed during the Miocene and overprints most of the Late Cretaceous and early Paleogene structures (Ratschbacher et al., 1991).

The present day geometry of the fold-and-thrust belt is the result of; 1) rifting phases during Permian and Triassic times (Doglioni, 1987), 2) basin infill and formation of carbonate platforms, 3) from Jurassic ongoing convergent movement between Adria and Europe (the direction of the convergent movement varied significantly over time), 4) the shape of the indenting Adriatic microplate (Schönborn, 1999).

A distinction exists between the western and eastern part of the Southern Alps, based on the deformation history (Schönborn, 1999). The Eastern Southern Alps are defined as the area east of the N Giudicarie Line (Castellarin & Cantelli, 2000), whereas the various segments of the Periadriatic Line, from west to east, the Canavese, Insubric, Giudicarie, Pustertal and Gailtal lines mark the western and northern boundary of the Southern Alps (e.g. Schmid et al. 1989). The western area is marked by a late Cretaceous compressional phase followed by Oligocene to Late Miocene strike-slip faults and major middle Miocene (Burdigalian to Serravallian) thrusting. The eastern part of the Southern Alps is affected by SW vergent thrusts, associated to the most external Dinarides during Paleocene and Eocene times (Cousin, 1981; Doglioni 1987), and from the Late Miocene onward by SSE vergent thrusting, associated to a phase of Alpine deformation (fig. 5). Seismicity data of the area records ongoing deformation (e.g., Andersen and Jackson, 1987), which is expressed at the surface mainly as dextral strike-slip faults.

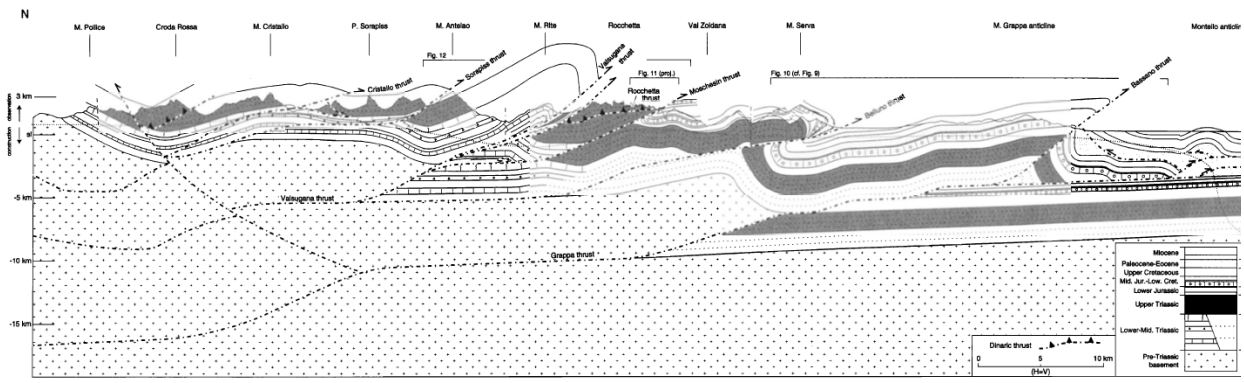

Figure 5. *Cross-section through the eastern part of the Southern Alps (Schönborn, 1999). The south vergent fold-and-thrust belt formed due to N-S convergence and involves three thrust systems (from N to S); Marmolada-Sorapiss, Valsugana and the Grappa system. Due to rheological differences within the stratigraphic sequence a classical ramp-flat tectonic style developed. The deep rooted thrusts caused uplift of the basement which resulted in the significant elevation of the upper Triassic sequences in the area.*

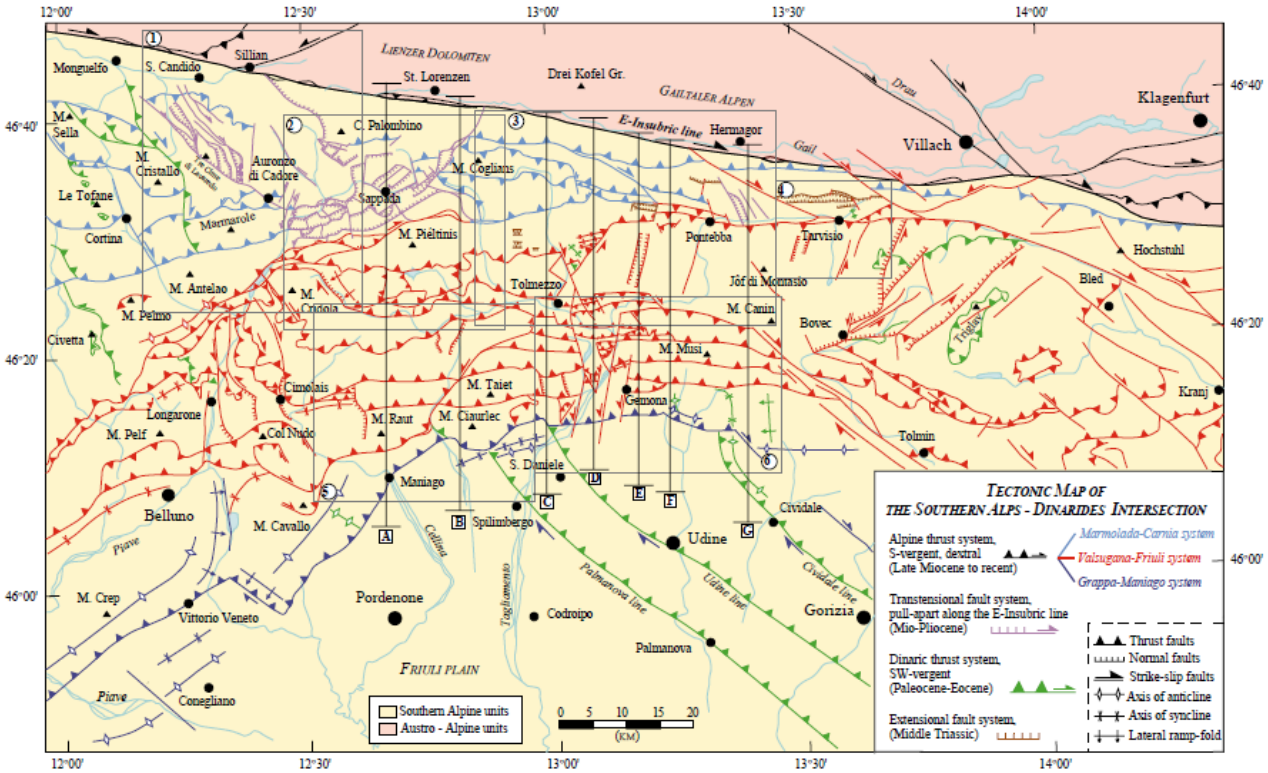

Figure 6. *Simplified tectonic map of the eastern part of the Southern Alps. In green the SW vergent Dinaric thrust system and in blue and red the several Alpine thrust systems (S vergent). Based on mapping of Nussbaum (2002) and previous mapping of Castellarin (1981), Bigi et al. (1992), and Schönborn (1999).*

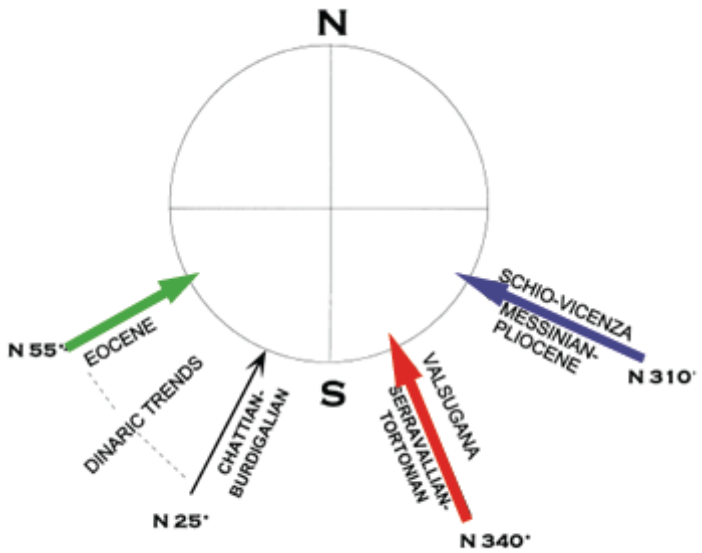

Figure 7. *Projection of the present azimuthal direction of the main structural systems in the Eastern-Southern Alps (adjusted after Castellarin et al., 1998b). The colored arrows are linked to the thrust-systems presented in the tectonic map above (fig. 7) and in the deformation summary below. The direction of of the map correspond with a Dinaric orientation of 55° and with at least two distinct Alpine orietations of 340° and 310°.*

The SSE verging thrust belt developed mainly during a Neogene phase of contraction and oblique inversion of the earlier Mesozoic passive margin of Adria (e.g. Bertonni et al. 1993). Displacement of crystalline basement is also associated to this Neogene thrusting phase (Doglinoni & Bsellini 1987; Doglinoi 1990; Schönborn 1999; Transalp Working Groep 2002). The current setting of the thrust belt is considered to be the result of the, from North to South, in sequence development of three major thrust systems; the Marmolada-Sorapiss, Valsugana and the Grappa system (fig. 5). There is wide agreement on the existence of these three major thrust systems, although they are often differently named in the various research reports.

2.2.1 The Dinaric phase

The external Dinarides

The external Dinarides are bound to the eastern side of the southeastern Alps and occupies the northeastern part of the Adriatic micro-plate. The main formations are Mesozoic to Tertiary shallow-marine and carbonate platform deposits. The External Dinarides are part of the Alpine Orogenic system and are widely described as a fold-and-thrust belt with generally SW-vergent structures. The External Dinarids are considered to be the highly deformed upper crust of Adria formed during NE subduction (Reference). The different variations of the geological evolution of the NE part of the Adriatic region indicates the complexity of its history (Pamić et al., 1998 and references therein). The main Dinaric thrusting took place during the Paleogene or the Miocene (Schmid et al., 2008 and references therein). Associated to this thrusting is a major detachment horizon that was activated during Paleogene compression within the Upper Jurassic – Lower Cretaceous succession (Biancone Formation), the formations on top contain thin-skinned type of structures which root in the detachment below. Multiplication of the tectonostratigraphic units took place and accommodates a large amount of shortening in the upper crust. The formations below the décollement are not affected by the Paleogene compression but show traces from a pre-orogenic extensional phase. Reflection seismic data indicates a reversely up-thrown of the crystalline basement segment (Prelogovic et al., 1995a), formed during a late-orogenic thick-skinned phase associated to the collision of the Dinaridic and the Adriatic domain, which is also related to the still active wrenching in the area (Korbar, 2009).

Dinaric deformation in the Southern Alps

Dinaric deformation started in the Southern Alps started the Paleocene and extended westwards towards the central Dolomites, which records several Dinaric thrust faults which doubled the Dolomia Principale Fm. (Doglioni, 1987). Kinematic indicators strongly suggests a SW directed system (fig. 6 and fig. 7), while the apparent direction of transport appears to be west due to large scale rotation of blocks initiated by strike-slip deformation of Alpine age (Doglioni, 1985, 1987).

Overall, the Dinaric structures cannot be linked to a continuous and consistent fault system, as is often the case with the Alpine thrust systems. Many of the Dinaric faults were dismembered by southward thrusting during the Alpine contractional event. However the Paleogene-Neogene Dinaric structures are characterized by three geometries; cross-cutting thrusts, superposed folds and Dinaric thrusts cross-cut by Alpine normal faults (Nussbaum, 2002).

The Dinaric WSW to SW vergent thrusts are cut-off and dismembered by the younger Alpine thrusts, however the structures contain evidence for two former décollement horizons associated to the Dinaric thrusting (Nussbaum, 2002). The evaporitic layers of the Bellerophon Formation and the Biancone layer, one of the lower horizons of the Cretaceous limestones. Most of the Dinaric deformation concentrated around these detachment horizons, especially around the Bellerophon décollement and is the main cause for the flat-ramp tectonic style of the most northern part of the external Dinarides (Nussbaum, 2002). The Dinaric small scale folds (SW-vergent) in the Bellerophon formation are refolded by large scale (dm to m) SSE-vergent folds and are cross-cut by transpressional thrust faults associated to Alpine deformation. The absence of metamorphism

along 250 km of exposed rock across Dinaric strike supports the idea of a low critical taper and thus a thin-skinned style of deformation (Nussbaum, 2002).

2.2.2 The Alpine phase

The interference between Dinaric and Alpine structures occurs dominantly in the eastern Southern Alps, however the structures formed by the interference are also visible in the central Southern Alps (Bernoulli et al., 1992; Schönborn, 1992a, 1994; Bertotti et al., 1993). During Middle Triassic and Early Jurassic time, rifting caused normal faulting in the sequences of the passive margin. The formation of these normal faults was prior to the spreading of the Halstatt-Meliata ocean in the east and the Alpine Tethys in the west. Later on during the Neogene compressional phase, the normal faults acted as natural weaknesses and were reactivated by thrusts faults. The Neogene shortening, with a maximum principal stress axis of NNW (fig. 7 and fig. 8) (Doglioni & Bosellini 1987; Castellarin & Cantelli 2000), reactivated the steep N to NNE striking normal faults with a sinistral strike-slip component (Zampieri et al. 2003; Massironi et al. 2006). This resulted in the in general E-W oriented, straight, Alpine thrusts. The Maniago thrust however, the main frontal thrust of the Alpine system, is curved (fig. 6). The reason for the bend of this fault is suspected to be the shape of the Jurassic-Cretaceous Friuli platform boundary. This example may well illustrate the strong influence of the depositional sequences and it shapes, on the tectonic structures.

The southern Alps can be subdivided further into several transverse zones, such zones form along old faults originating from previous tectonic events (such as the Middle Triassic - Early Jurassic rifting), or paleogeographic boundaries such as the margins of a rigid carbonate platform (Thomas, 1990). These paleo-faults are not easily recognizable in the field, abrupt thickness variation of the covering sediments, or when fault reactivation results in brecciation of rocks, are the most common indication for a buried paleo-fault. However reactivation usually creates a new network of faults parallel to the paleo-fault (Gillcrist et al., 1987). The nature of the fault reactivation is depended from the orientation between the paleo-fault and the new main compressional stresses (Morris et al., 1996). In general the following relationships are found between subsequent compression and paleogeographic boundaries and paleo-faults; thrust faults are formed when the paleographic boundary is perpendicular to the direction of shortening, when the compression is oblique to the paleo-structure, strike-slip faults are usually formed, for example the Dinaric sinistral transverse faults which are parallel to the northwestern boundary of the Friuli platform. Due to these transverse zones, the orientation of the deformation structures can be deflected compared to the main N-S alpine transport direction. To constrain the timing of deformation, the youngest sediments below the thrust fault must be dated. The foredeep sediments in the frontal Eastern Southern Alps were mainly deposited during the Neogene and ended in the latest Messinian. The Miocene sediments of the foreland deposits indicate the onset of thrusting in the eastern part of the Southern Alps during the late Miocene (Tortonian). Stratigraphic and structural data documents active compressional deformation during the Pliocene and Pleistocene (Venzo, 1977; Castellarin and Cantelli 2000; Bertelli et al. 2003), and the uplift of Quaternary terraces (Benedetti et al., 1995) and the continuous seismicity in the Friuli area indicate the ongoing deformation. Late extensional deformation, associated to uplifting of the orogenic wedge, is clearly documented in the Eastern Southern Alps by minor normal faulting, subsequent to the main compressional phases (see overview below, after Castellarin and Cantelli, 2000).

In summary, the following major deformation phases are distinguished in the Eastern Southern Alps (after Castellarin and Cantelli, 2000). The azimuthal direction of the phases is shown in figure 8 on the following page.

N-S compression, Pre-Adamello phases

During the Late Cretaceous–Early Eocene this deformation phase produced ENE striking thrusts, related to the eo-Alpine pre-collisional convergence. However, Pre-Adamello structures have not been recognized east of the South-Giudicarie line.

NE-SW compression, Dinaric Eocene phase

During the Eocene a prominent SW vergent, NW trending thrusts system formed. These structures are considered to be a continuation of the external Dinarides. The Dinaric phases would later on be drastically affected by the Alpine compressions (especially the Valugana phase).

NNE-SSW compression, Insubric – Helvetic or "Gonfolite" phase

Mainly during the Chattian to Burdigalian, this early post-collisional phase produced SW-NW (WNW-ESE) trending thrusts, which affected mostly the subsurface (po-plain).

NNW-SSE (N-S) compression, Valsugana phases

Serravallian to Tortonian ENE-WSW (E-W) trending thrusts related to the neo-Alpine post-collisional deformation. This phase is strongly developed throughout the whole Southern Alps, although in the east the structures are most prominent.

N-S to NE-SW compression, Adriatic phases

Late post-collisional Messinian to Pliocene NE trending thrusts related to the neo-Alpine deformation. Alternations between N-S and NW-SE compressions cannot be excluded for the Friuli area.

Figure 8.

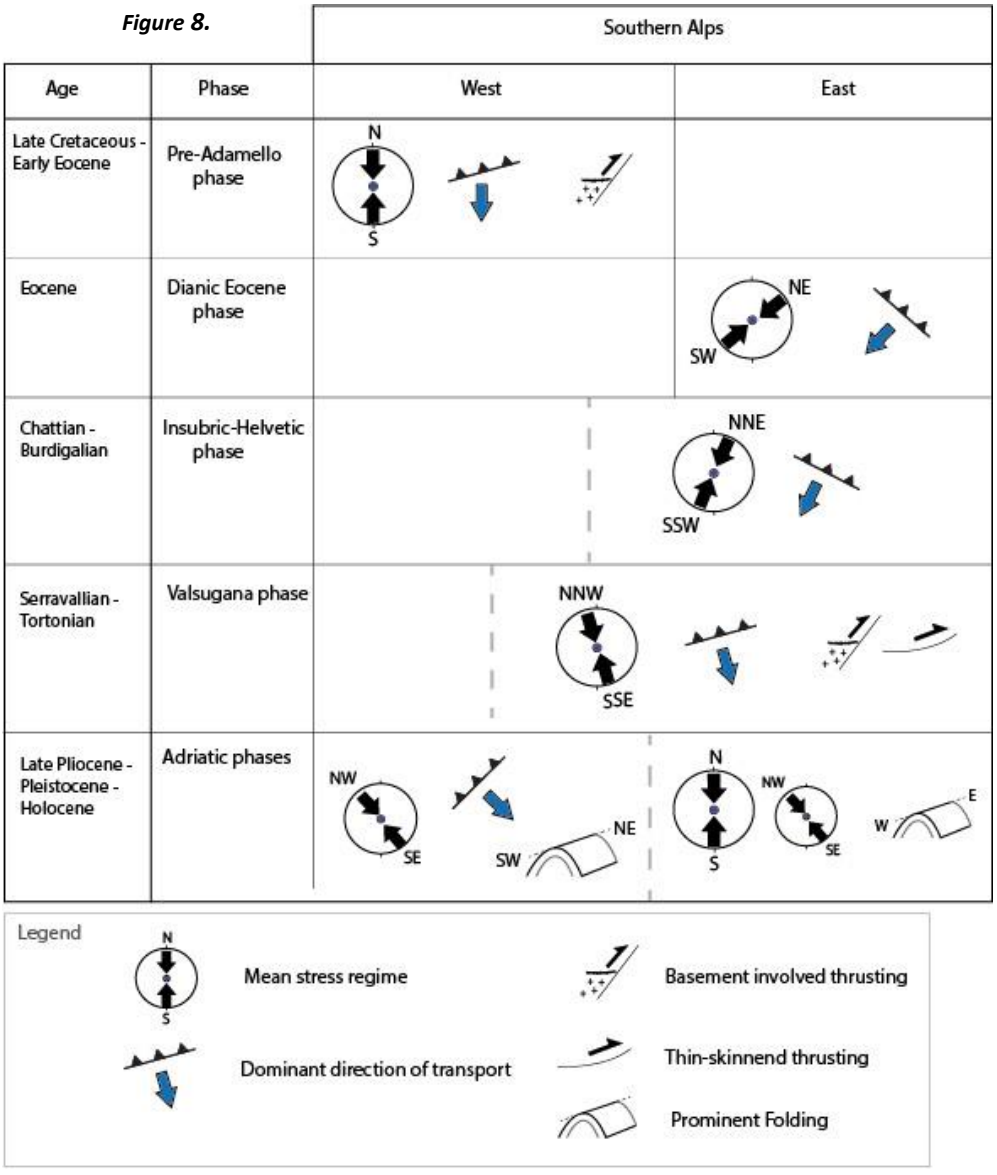

Figure 8. *An overview of the type of deformation structures and the azimuthal directions of the different stress regimes in the Eastern and/or Western Southern Alps through time (after Castellarin & Cantelli, 2000).*

3.Methodology

In order to obtain kinematic and geometric constrains for the reconstruction of a detailed 54 km long N-S cross-section through the Friuli Alps, a 3-week field work has been conducted in the Friuli region in north-eastern Italy. During this fieldwork structural data has been collected, focusing on distinguishing Dinaric from Alpine structures. By taking systematic measurements from the structural features in the area like; bedding planes, foliation/cleavage planes, fault planes, fold axes and the various shear structures, and determining their relative timing and mutual relationship, an overview of the distinct deformation phases could be obtained.

The combination of the obtained deformational evolution (D1-D5) and the constructed N-S cross-section, constrained by the very same field data, enabled us to make some statements about the tectonic styles of the Dinaric and Alpine deformation phases in the Friuli Alps. To test the validity of the cross-section and to obtain a proper estimate of the amount of shortening since Eocene/Miocene time in this area, balancing of the cross-section have been conducted by the use of the software "MOVE" (Move 2015, Midland Valley Exploration) for 2D/3D kinematic modelling.

The restoration and testing of the validity of the cross-section occur simultaneously, since geometric problems are detected during the restoration workflow, when area and line length balance issues and mismatches come to light. The amount of correction needed to correct such issues and mismatches determines the validity of the section. At the end of the reconstruction, the amount of shortening can be obtained by comparing the restored, i.e. the undeformed, section with the present deformed section.

The two main modules that have been used during the restoration are *unfolding by flexural slip* and the *movement of horizons along faults*. The methodology for the flexural slip unfolding algorithm, as carried out during the reconstruction, concerns the following steps; the separation of the section in different fault blocks, after which each fault block can be unfolded by the flexural slip algorithm. By manually placing the blocks back together, after which correction for gaps and overlapping horizons have to be carried out. By re-folding the adjusted fault blocks to their original state, the validity structure is tested.

After the unfolding of the individual fault blocks, the fault blocks are moved in the opposite direction as the sense of displacement. The reconstruction of the displaced horizons along the faults, starts with the youngest structure and ends oldest. The most common and continuous horizon is chosen as a marker bed, in this case the Dürrenstein Formation.

The corrected and balanced cross-section can then be compared to the cross-section, which provides matter for discussion on the kinematics, geometries, mechanics and the estimation of the total shortening. The comparison will also provide valuable insights on the deformation styles that took place in the Friuli area (thin-skinned versus thick-skinned tectonics).

4. Lithology and Tectonostratigraphic evolution

In this chapter the tectonostratigraphic evolution and a lithological description of the different sedimentological formations of the eastern Southern Alps is provided. The presented information on, tectonic events, depositional environment, layer thicknesses and the occurrence of the formations is based on both information from literature and the newly obtained field observations. For the lithological description, the geological map of Friuli Alps *(Carte Geologica del Friuli Venezia Giulia, 1:15000. By Carulli, 2006)* is used as the main source of information in addition to own field observations. This geological map can be found in appendix B.

4.1 Variscan basement

Below the sedimentary succession of the Eastern Southern Alps lies the Variscan basement. We rely on the brief description of the Variscan Basement by Nussbaum (2002), since we have not examined the basement during the field studies.

The basement consists of all rocks that have been deformed by the Variscan deformation and of the syn-orogenic sediments on top of the folded basement. The Variscan deformation includes two phases, a ductile event under greenschist facies conditions (Tmax: 300-450°), and a second event under sub-greenschist conditions (Tmax: 260-300°C). After the deformation and metamorphism of the basement, wrench faulting created pull apart-basins in which the Late-Variscan molasse was deposited till Late-Carboniferous times.

The Late- to Post-Variscan sequence consists of two distinct cycles, separated by major intra-Permian block-faulting (Krainer, 1992). The block-faulting is indicated by reworked material of the lower cycle sequences occurring within the sediments of the second cycle. The lower cycle consists of Late Carboniferous-Early Permian sediments and volcanic deposits. The deposits of the second cycle are more widely distributed and not restricted to discrete basins. The second cycle sediments include the shallow marine sequences of the Val Gardena Formation, which merges into the evaporitic and carbonate sequences of the Bellerophon Formation.

4.2 The sedimentary succession of the Eastern Southern Alps

The sedimentary succession of the Eastern part of the Southern Alps starts with the late to post-Variscan sequence which consists of two cycles of sedimentation as described earlier. The stratigraphic sequence of the second cycle, starts with the continental to shallow marine sediments of the Val Gardena Formation.

4.2.1 Middle-Permian – Middle-Triassic

The **Val Gardena Formation** was deposited during a strong syn-sedimentary tectonic setting, associated to the strong block faulting, resulting in abrupt thickness variations between 0 and 500 m. The sediments consist of alluvial fan deposits which pass locally into lower flood plain and sabkha deposits. Val Gardena sediments are not encountered during the fieldwork and are therefore not described in detail. The Val Gardena is largely exposed in the North-western part of the area, as indicated by the geological map, and is the most wide spread basement unit in the area. On top of the Val Gardena Formation lies the **Bellerophon Formation** which consist mainly of shallow marine, evaporitic and carbonate sediments deposited under lagoonal and carbonate platform conditions. The cm-dm thick beds of marls and siltstones are intercalated with thinly layered (dm) brown/dark grey dolomites and limestones, and at the bottom of the formation saccharoidal laminated gypsum with on top dm-m thick sequence of black marls (fig. 9A and B). The laminated gypsum is the first weak horizon in the stratigraphy which makes it an ideal décollement for both Dinaric and Alpine thrust deformation. The Bellerophon Formation is 250-300m thick and is exposed in the northern part of the area, especially in the north western part, where it represents the transition zone between the younger post-Permian formations which are overlain by the older Variscan basement.

During the Permian-Triassic transition a major climatic shift changes the depositional environment significantly, resulting in the unconformable deposition of the shallow shelf to subtidal, tidal flat and mudflat sediments of the **Werfen Formation** on top of the Val Gardena and Bellerophon Formations (Krainer, 1993). The Lower-Triassic Werfen Formation consists of various lithologies including cm-dm thick oolitic limestone beds intercalated with marls, yellow well bedded limestone and dolostones as well as grey and light brown laminated micritic limestones. The total thickness of the Werfen Formation is 600 -700m (Nussbaum, 2002) and is largely exposed in the north western part of the area, covering a large surface area, south of the basement (mainly Val Gardena Formation) units in the North.

During the Middle-Triassic, the Southern Alps was characterized by a platform/basin system as result of a phase of rifting related to the opening of the Meliata Ocean. Several fast growing carbonate platforms, separated by deep lagoons, were formed and the dolostone and limestone sequences of the **Serla** and **Schlern Formations** were deposited (e.g., Leonardi,1967, Bosellini 1984, Buser,1987). However, the Schlern and del Serla carbonates do not dominate the landscape like the Upper-Triassic Formations, they still occur as quite massive bodies. The sequences of the Dolomia del Serla Formation consists of both poorly and well bedded whitish dolostones and dolomitic limestones, often vuggy and/or brecciated (fig. 9C). The geological map indicates an interruption of the carbonate build-up for both the eastern and the western part of the Friuli area, by a basinal sequence lying directly on top of the Serla Formation. On top of the eroded basinal depostis, the massive, well bedded, light grey dolostones and dolomitic limestones of the Schlern Formation were deposited (fig. 9D). The total thickness of the Serla and Schlern exceeds 1000m. The extend of the platform carbonates of the Schlern is interrupted by deep water and tuffaceous sediments of the **Buchenstein Formation**. The Buchenstein Formation represents the third of in total three Middle-Triassic magmatic events, related to the rifting of the future Halstatt-Meliatta ocean (Stampfli et al., 1991). The first, Late Anisian of age, is indicated by ignimbrites and volcanic clasts. The second event, during the early Ladinian is known as the Riofreddo Volcanics, which is related to an explosive hydromagmatic activity (Gianolla, 1992). The Buchenstein Formation consist of basinal tuffitic sediments and 0,5-2 cm thick dark grey limestone beds intercalated with sandy layers and black shales of late Ladinian age (fig. 9E & F). The Buchenstein Formation can be found at the surface mainly in the (north) eastern part of the area, no outcrops are encountered or indicated by the geological map west of the Tagliamento river.

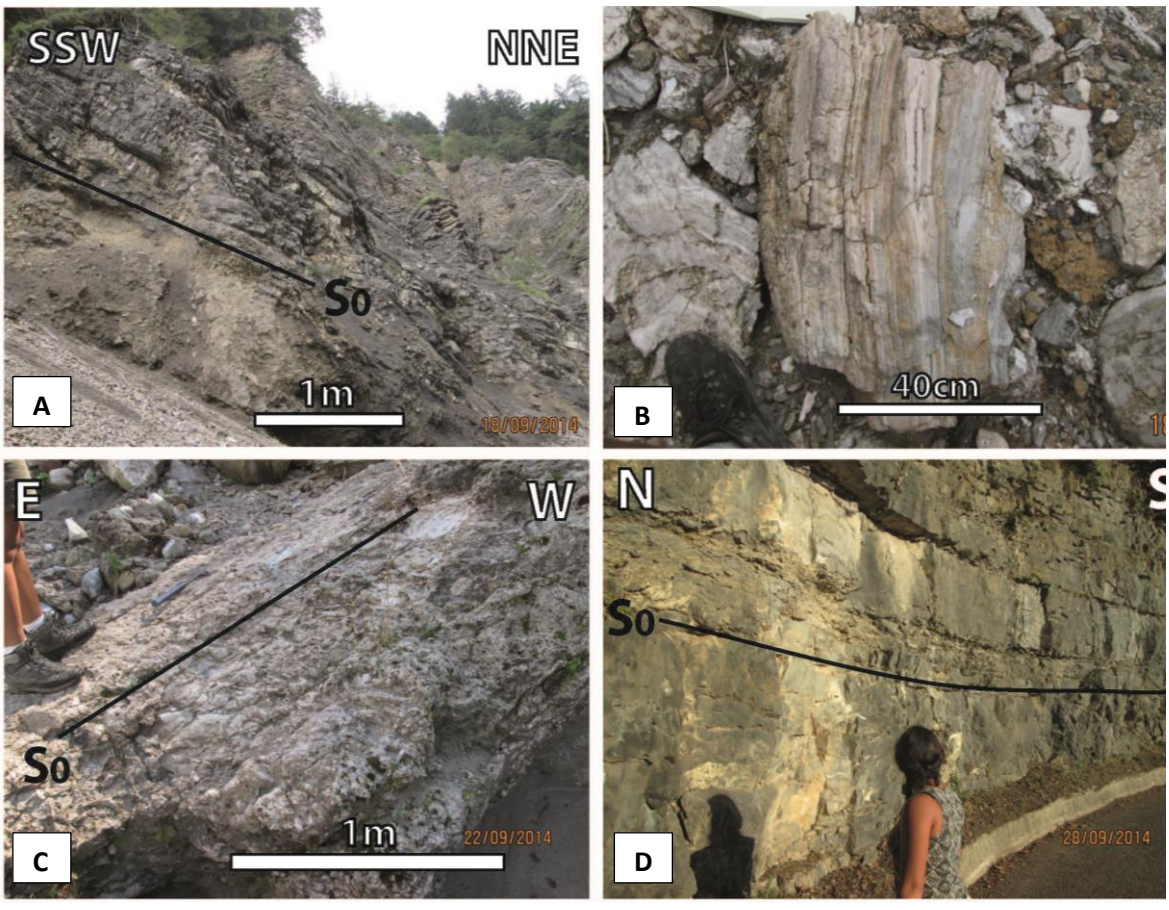

Figure 9. A) *Outcrop of the top part of the Bellerophon Formation (stop 11.6); dm thick limestone beds alternating with beds of dark grey/brownish marls.* ***B)*** *Outcrop of the lower part of the Bellerophon (stop 11.7); loose block of the Bellerophon evaporate sequence; laminated, saccharoidal gypsum, generally intercalated with black/brownish marls.* ***C)*** *Poorly bedded, vuggy dolostone of the del Serla Formation (stop 15.2).* ***D)*** *Well-bedded dolostone sequence of the Schlern Formation (stop 21.7).* ***E)*** *Steep, cm-thick, folded limestone and tuffaceous beds of the Buchenstein Formation in the Eastern part of the area (Stop 2.3).* ***F)*** *Green volcanic, tuffaceous body of rock within the Buchenstein Formation, contains a mm fine lamination representing the succession of different types of ash flow (stop 17.6).*

4.2.2 Upper-Triassic

The lower Upper –Triassic formations consist of the Val Degano and Dürrenstein Formations. The **Val Degano Formation** is characterized by abrupt thickness variations, indicating the syntectonic depositional conditions due to the Middle-Triassic rifting phase. The Val Degano Formation is the lowermost formation of the Upper-Triassic and consists mainly of dark grey limestone beds alternating with cm-dm beds of marls with green tuffaceous sandstone and occasionally coal lenses at the base (fig. 10B). The Val Degano sequences are mainly exposed in the northern fold-and-thrust belt along with sequences of the Dürrenstein Formation. The **Dürrenstein Formation** is an overall shallowing-upward sequence, deposited mainly on a carbonate ramp (Preto & Hinnov, 2003). However, clastic sediments indicate periods of floodplain and mixed clastic-carbonate platform conditions besides the pure carbonate ramp conditions. The sequences consist of well stratified dolomitic limestone and dolostones, but is characterized by its violet sandstones which makes it a non-typical carbonate platform sequence (fig. 10A). The Dürrenstein is exposed in the northern part of the area where it overlies the Val Degano formation, but is also deposited later in time, as interrupting layer in the carbonate platform deposits of the Dolomia Principale sequence (stratigraphic column fig 13). The Dürrenstein indicates a major shift in growth modus after de deposition of the fast growing Middle-Triassic platform formations, the Serla and Schlern Formation.
In late Carnian time, the shift in growth modus
The relatively soft, dm-thick beds of dolostone and/or nodular limestones interbedded with cm-dm thick beds of marls of the **Raibl Formation** lie stratigraphically in between the rigid carbonates of the Middle-Triassic (Schlern & Serla) and the massive carbonate bodies of the Upper-Triassic formations (Dolomia Principale & Dachstein) (fig. 10C). Therefore, the Raibl Formation is considered to be the second major décollement horizon in the stratigraphy of the Friuli Alps. The Raibl Formation is mainly exposed in the Eastern part of the research area and does not occur at the surface west of the Tagliamento river. The thickness of the Raibl formation in the Eastern part of the area is ~500m and thins out towards the west.

During the Norian a large scale peritidal platform formed, creating carbonate bodies of 1000-1700m thick of the **Dolomia Principale Formation**. The Dolomia Principale mainly consists of light grey and brown dolostones, generally well stratified in cm-m thick beds. However, the Dolomia Principale also appear as poorly bedded, massive dolostone bodies, and is locally heavily brecciated. These thick carbonate bodies were able to form due to a high sedimentation rate and thermal subsidence as response to the Middle-Triassic rifting. In between the carbonate platforms, locally basins formed and deep marine sediments were deposited. The last in the series of Triassic Carbonate Platform formations is the **Dachstein Formation**. The limestones of the Dachstein Formation are deposited under similar carbonate ramp conditions as the Dolomia Principle. The Dachstein Formation occurs as light grey micritic limestone, mostly in dm-m thick beds. The Dachstein is in some cases

hard to distinguish of the Dolomia Principale Formation, however in general the Dachstein limestones are but less dolomitized and the rock weathers light grey. The age of the Dachstein Formation is not very well constraint and is estimated on late Norian, Rhaetian or early Hettangian (Feist-burkhardt, Götz, & Szulc et al., 2005).

Figure 10. A) *Dürrenstein sandstone (stop 21.3).* ***B)*** *Val Degano sequence of dark grey limestones intercalated with cm-dm thick beds of marls (stop 20.3).* ***C)*** *An outcrop of the Raibl Formation in the eastern part of the area, typical alternation of dm thick limestone beds and marls (stop 10.4).* ***D)*** *A Closer view of a typical Raibl sequence of dm thick beds of limestone and marls. Most of the deformation is localized within the softer marly beds (stop 10.4).* ***E)*** *Typical massive body of m-thick dolostone beds of the Dolomia Principale Formation (stop 8.10).* ***F)*** *dm thick limestone beds of the Dachstein Formation (stop 18.3).*

4.2.3 Jurassic

The Early-Jurassic is characterized by extensional faulting and subsidence initiated by the opening of the Alpine Tethys in the West. In early Liassic time this lead to the breakup of the Upper-Triassic carbonate platform in two parts, the Trento high in the west and the Friuli platform in the east, separated by the Belluno basin. The Trento high drowned during the late Liassic, resulting in the deposition of basinal sediments. The Friuli platform on the other hand, remained under shallow-water conditions the entire Mesozoic (Schönborn, 1999). The Belluno basin was filled with debris material and at the end of the Middle-Triassic it was no longer a deep trough and the Upper-Jurassic slope and shallow marine sequences of the the Vajont, Polcenigo, Fonzaso and Biancone Formation were deposited.

The Calcari Grigi del Friuli, Chiampomano, Soverzene and Igne Formation were deposited, and later from Middle-Triassic till Early-Cretaceous time, the Vajont, Polcenigo, Fonzaso and Biancone Formation. The Upper-Jurassic Formations represent the interplay between event (storm and debris-flow deposits) and background sedimentation (ongoing sedimentation in a slope/shallow-marine environment in between the storm and mass flow sedimentation). In the Belluno basin, the **Chiampomano Formation** and the **Soverzene Formation** lie on top of the Dolomia Principale (Schönborn, 1999) and consist mainly of dm thick beds of organic rich limestones and dolostones, calcareous turbidites and slump structures (fig. 11A & B). Sequences of the Chiampomano Formation are especially well exposed in the center of the area, just north of the Tagliamento river.

On top of the Soverzene Formation lies the **Igne Formation**, which is a transition layer between peritidal and basinal conditions. Subsequent to the dm thick limestone and dolostone beds, interbedded with black shales and marly limestones of the Igne Formation, is the deposition of the thick Oolitic limestones and turbidites of the **Vajont Formation**, which is largely responsible for the in-fill of the Belluno basin (Schönborn, 1999). There is evidence from the field to assume that the Upper-Jurassic formations act as a third décollement horizon in the stratigraphy of the Friuli Alps for thrust deformation. On top of the Vajont limestones lie the fossil rich limestones of the **Calcari di Polcenigo,** which were deposited under carbonate platform conditions and consists of homogeneous light grey, generally fossil rich, limestone bodies. The Polcenigo outcrops are quite massive and exhibit little internal structure apart from some occasionally encountered non-penetrative fracture cleavage (fig. 11C).

The last phases of the Upper-Jurassic is characterized by the background sediments, the chert rich and nodular limestones of the **Fonzaso Formation**., followed by the **Biancone Formation** and on top the **Soccher Formation** consisting of grey micritic limestones with dark grey silica rich nodules. The Fonzaso Formation includes dm - thick beds of micritic limestones, beds of fossil rich limestone with reddisch silica rich nodules. The Biancone Formation consist of dm-thick bed of micritic limestone, grey/greenish and reddish nodular limestone beds and bioclastic calcirudites (fig. 11D). In the field it turned out that it is difficult to distinguish these formations from one another.

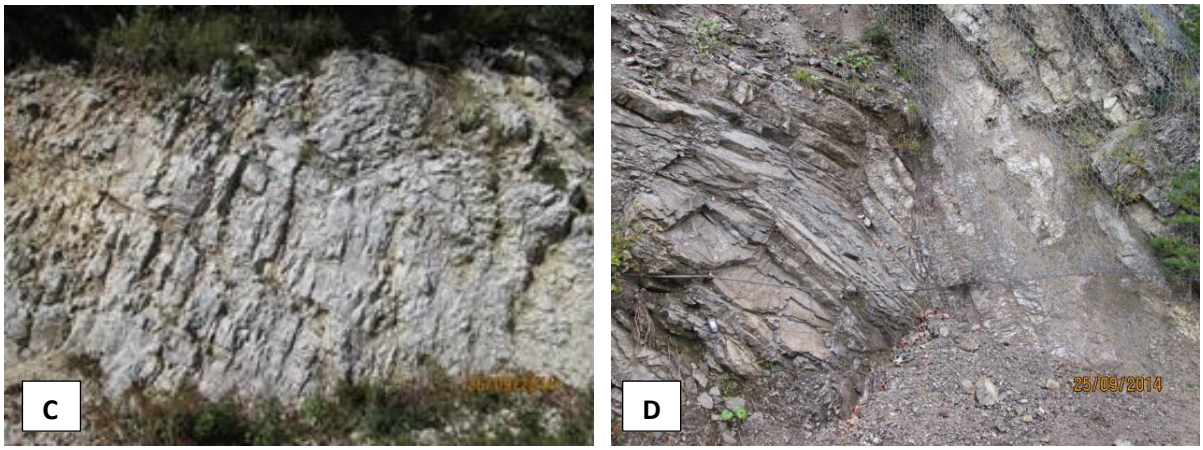

***Figure 11**. **A)** Sequence of cm-dm thick limestone beds of the Chiampomano Formation (stop 13.2). **B)** Laminated limestone bed, containing thin blackish layers of chert (stop 13.2). **C)** Light grey limestone body of the Polcenigo Formation. Occasionally the rock exhibits fracture planes, which appear non-consistent after measuring. **D)** Biancone sequence, dm thick limestone beds (stop 13.1).*

4.2.4 Cretaceous

At the end of the Late-Jurassic a barrier reef was built on the Friuli Platform, which lead during the Cretaceous to the deposition of bioclastic limestones deposited under protected shallow water conditions (reefs). During Late Cretaceous time, between ~90 till ~80 Ma the reef building stopped and aerial erosion affected the Cretaceous sequences, the exact timing however is unknown. This resulted during the Cenozoic in the unconformable deposition of the Paleocene-Eocene flysch deposits on top of the Cretaceous Formations. The **Upper-Cretaceous Limestone** (17c) is dominantly present in the southern part of the area with its characteristic massive white/light grey bioclastic limestone bodies, which determine the appearance of the landscape (fig. 12A). The rigid bioclastic limestone bodies are occasionally interbedded with cm-dm thick beds of micritic limestone. A smooth sectional view was provided in a local limestone quarry (fig. 12B), it revealed several transitions from fossil-rich horizons to more mudstone type of rock, within the seemingly homogenous limestone bodies. The total thickness of the Cretaceous sequence reach up to 1200m.

4.2.5 Cenozoic

The Cenozoic sedimentation is characterized by flysch and molasses deposits, from the late Paleocene till middle Eocene time the flysch was deposited and the main molasses sequence is deposited during the Oligocene (Nussbaum, 2002). The **Eocene flysch** deposits are associated to the external Dinarides and cover the Friuli platform from the east. The flysch is deposited transgressively on the fossil rich limestones of the Cretaceous. The Paleogene, or **Eocene flysch** consist of cm-dm thick beds of limestone intercalated with cm-m thick beds of marls. The marls are usually dark grey or brown colored, but also occur light brown/yellowish colored. Occasionally sequences of marls intercalated thin limestone beds, lay adjacent to thick carbonate beds and/or sandstones and siltstones. Apart from the typical flysch sequences, the alternating marls and limestone beds, the Eocene flysch also consist of conglomerates and turbiditic sediments. The, in general fining upward conglomerates, are often very poorly sorted and contain clasts from 1- 20 cm in size, which suggests they were deposited during debris-flow events. The turbiditic deposits usually consist of finer grained, fining upward conglomerates with clasts varying in size from mm - 5cm scale. The Eocene flysch has been recognized in the field as the fourth and youngest décollement horizon in the Friuli Alps stratigraphy (stratigraphic column fig. 14).

The deposition of the **molasse** sediments in the Dinaric foredeep basin (Veneto basin) and the internal basin (Sava basin in Slovenia) started during the Late Oligocene and continued until the Early Miocene. The **Oligocene molasse** is mainly exposed as conglomerates and mega-breccia's (fig. 12E & F). But also occurs as sandstones and siltstones, green glauconitic sandstones with pectinids and shales with mollusks and corals. The conglomerates are mainly poorly sorted, polymictic with 1-30 cm in size, well rounded pebbles. From the early Miocene onward, the Veneto basin was filled by an eastward thickening sandy and marly sequence. From Middle Miocene time onwards the area became part of the northward thickening, Alpine foredeep. The middle Miocene marly sediments indicate deposition with basinal conditions. The Upper-Miocene sequences are

characterized by continental and fluvial sediments, which indicate Alpine uplift since the middle Miocene (Amato *et al.*, 1977). The late Miocene deposits mainly consist of conglomerates and mega-breccia's, which are believed to be a product of the uplifting Alpine mountains. From the late Miocene onward till the Quarternary, the Friuli plain is affected by the deposition of fluvial deposits (Amato *et al.*, 1977).

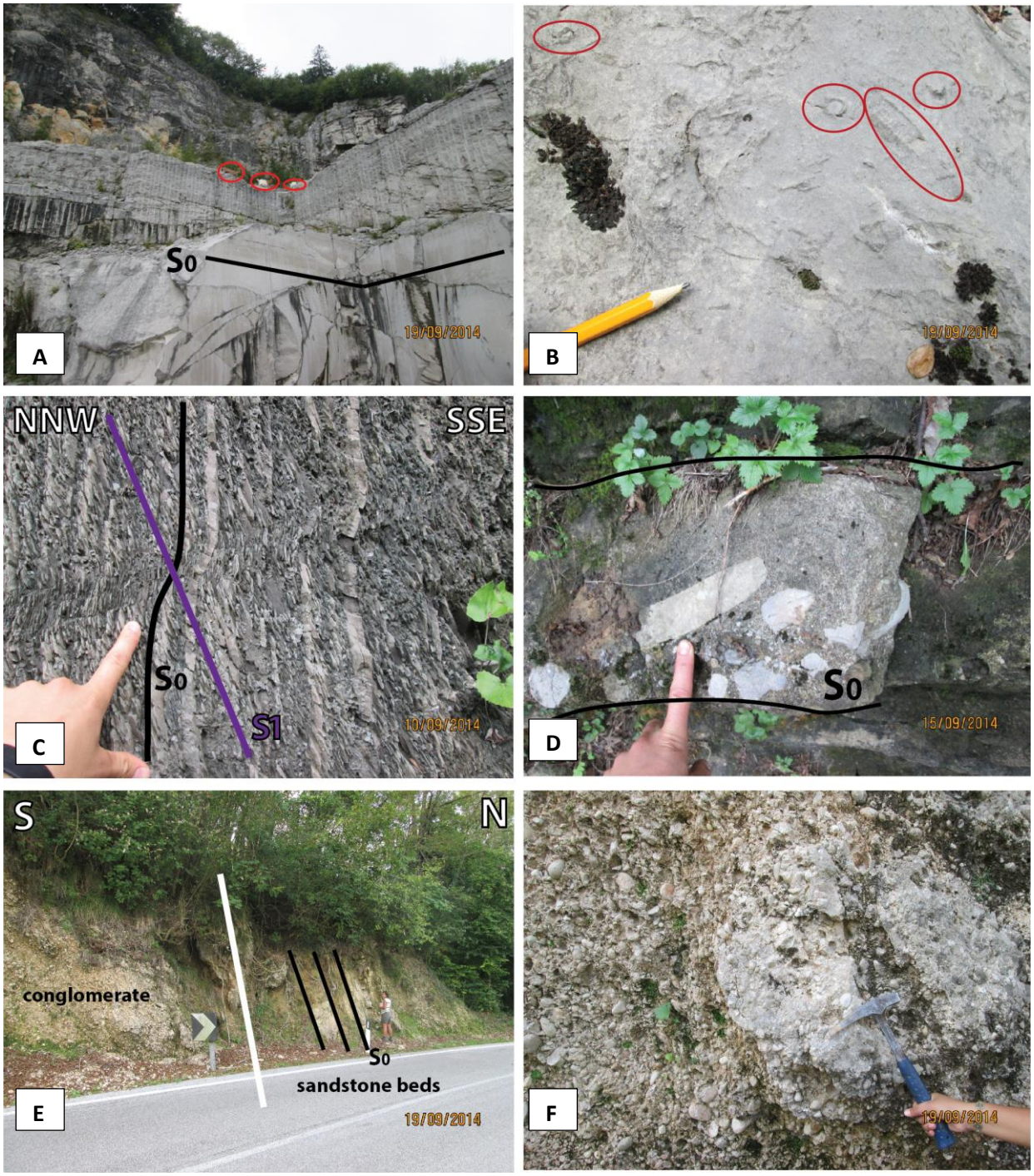

Figure 12. ***A)*** *Upper-Cretaceous limestone exposed in a quarry west of Clauzetto, goats in the middle of the picture for scale (stop 12.9).* ***B)*** *Upper-Cretaceous fossil-rich limestone, circle-shaped bioclasts are interpreted as rudists (stop 12.6).* ***C)*** *Eocene Flysch outcrop in the Eastern part of the area (stop 3.3), shows a typical flysch sequence, the alternation of calcareous beds with dark colored marls.* ***D)*** *A sequence of the Eocene Flysch in the Eastern part of the area, just west of the town of Micottis (stop 8.8). This outcrop exposes poorly sorted, fining upward, m-thick beds of polymitic conglomerates interbedded with dm-m thick limestone beds. These debris-slow conglomerates show a wide ranch in clast size, from mm-scale up to 20cm* ***E)*** *A ~25m thick Molasse sequence exposed in the western part of the area. The sequence consists mainly of polymitic conglomerate with a wide variety in clast size 1 – 30 cm, but also exposes steep oriented sandstone beds (stop 12.5).* ***F)*** *Close-up of the molasses conglomerate (stop 12.5).*

4.3 Tectono-stratigraphic column of the Friuli Alps

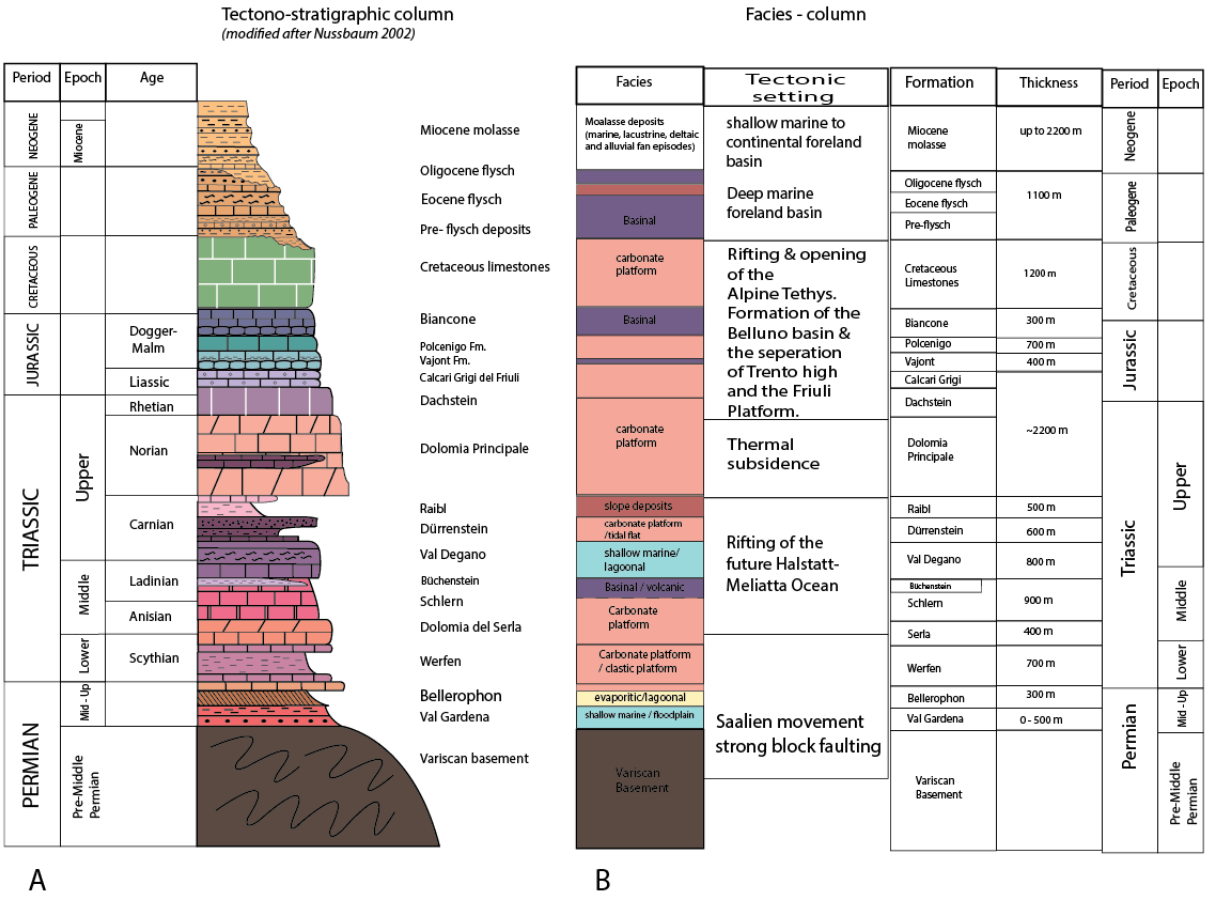

Figure 13. A) *Tectono-stratigraphic column of the sedimentary cover of the Friuli Alps.* ***B)*** *The Facies-column is a translation of the formations in Tectono-stratigraphic column into facies-groups column. The tectonic setting responsible for the particular depositional environment is indicated as well as the thickness.*

The above figure provides a clear view of the tectono-stratigraphic sequence of the Friuli Alps, which is characterized by its alternation of basinal/slope deposits with rigid carbonate-platform bodies (Lower Triassic, Upper-Triassic and Cretaceous) as described in the previous chapter.

The sequence of the tectono-stratigraphic column above is largely based on new field-observations, the absolute dating of the formations however has been determined by correlation with previous studies (Nussbaum, 2002) on the tectono-stratigraphic sequence of the eastern Southern Alps.

4.3 Facies map

Since it is one of the main goals of this study to investigate the influence of the paleo-geographical evolution of the Friuli Alps on its tectonic evolution, the wide variety of occurring formations is grouped into six facies-units.

The facies map consist of 6 facies-units, these units are composed of the formations described in the previous paragraph. All formations which were formed in the same depositional environment are now clustered in one group, a so called facies-unit. For example, all the typical carbonate platform formations, the Schlern, del Serla, Dolomia Principale, Dachstein Formation and Upper-Cretaceous Limestone are now housed together in the

Carbonate platform facies-unit. The same principle is applied for the other formations, which resulted in the following six main facies-units.

1) Cenozoic sediments
2) Carbonate platform
3) Slope deposits
4) Shallow marine
5) Basinal deposits
6) Basement

The subdivision in facies units also provides a classification of relative strength. The m-thick beds of dolostone and limestone of the Carbonte platform-unit and the dm-thick limestone beds of the shallow marine-unite for instance, are relatively stronger than the shaley, marly, tuffaceous and thinly layered limestone beds of the Basinal-unit. It is this contrast in relative strength between the facies units that is expected to be of great influence on the deformation style of the area.

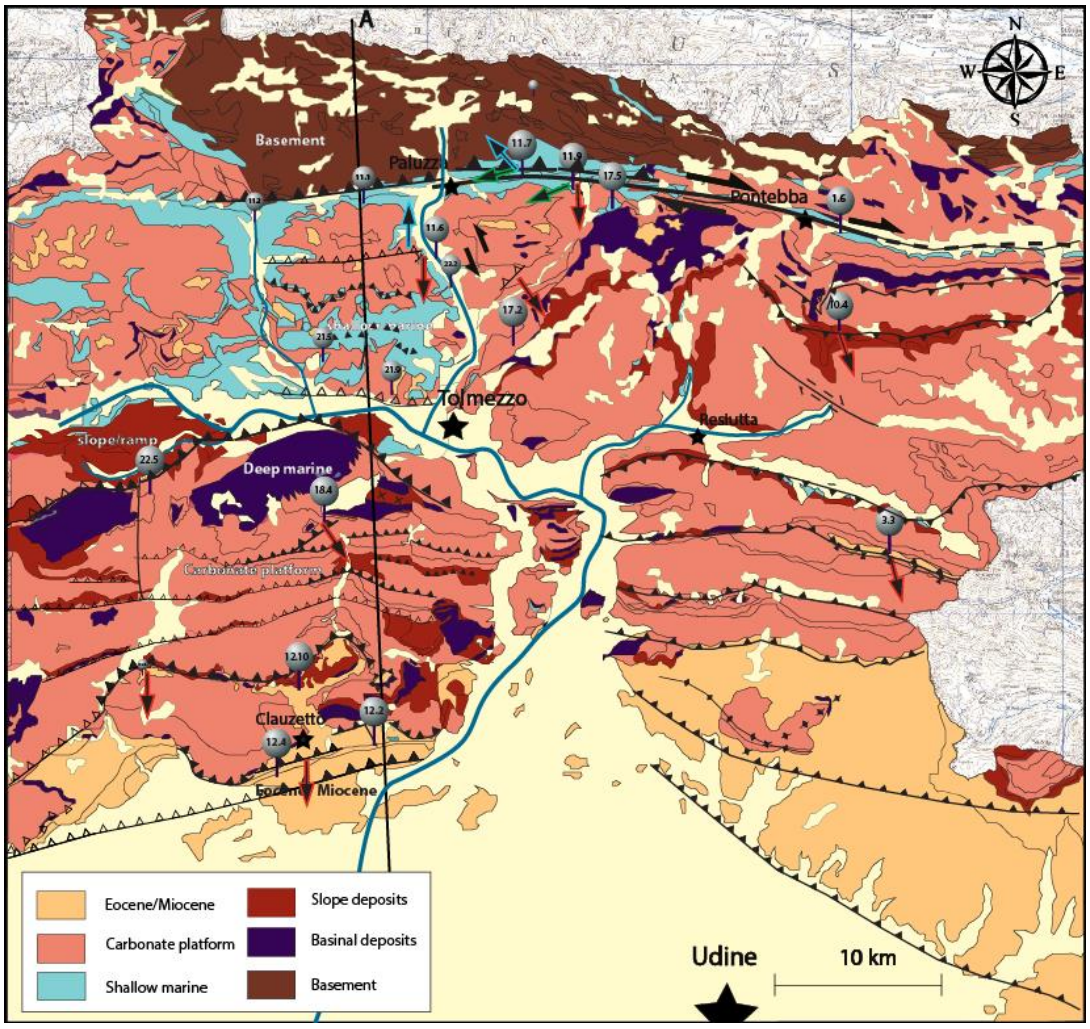

Figure 14 *Facies-map modified after the Geological map of the Friuli Venezia Giulia (edited after Giovanni Battista Carulli et al., 2006). The Facies-map displays the 6 main sedimentary facies-units which are formed out of clusters of the geological units. The colours of the facies-units correspond to the colours used in the facies cross-section in chapter 6.4 (fig. 16).*

The facies-map clearly shows the dominant occurrence of the carbonate platform sequences which cover up to 60% of the research area. Basement rock is only exposed in the northern part of the area. The Eocene and Miocene sequences are mainly exposed in the south, where they represent the infill of the foreland basin.

It is worth mentioning that there appears to be a link between the different facies boundaries and large deformational structural in the area. In general is the transition of carbonate platform into slope or basinal deposits facies, marked by a large south vergent fault structures (fig. 14).

5. Field results

A structural analysis has been carried out in the Friuli region, where data is collected from Tarcento in the South, to the Austrian border in the north (figure 15). During this field study a total of 141 outcrops were visited in the various facies-units described earlier. The data distribution is rather narrow and is concentred within two elongated rectangle areas, this with regard to the compiling of two cross-sections through the area. The field results presented below originate mainly from the western part of the research area, since that is the focus of this report.

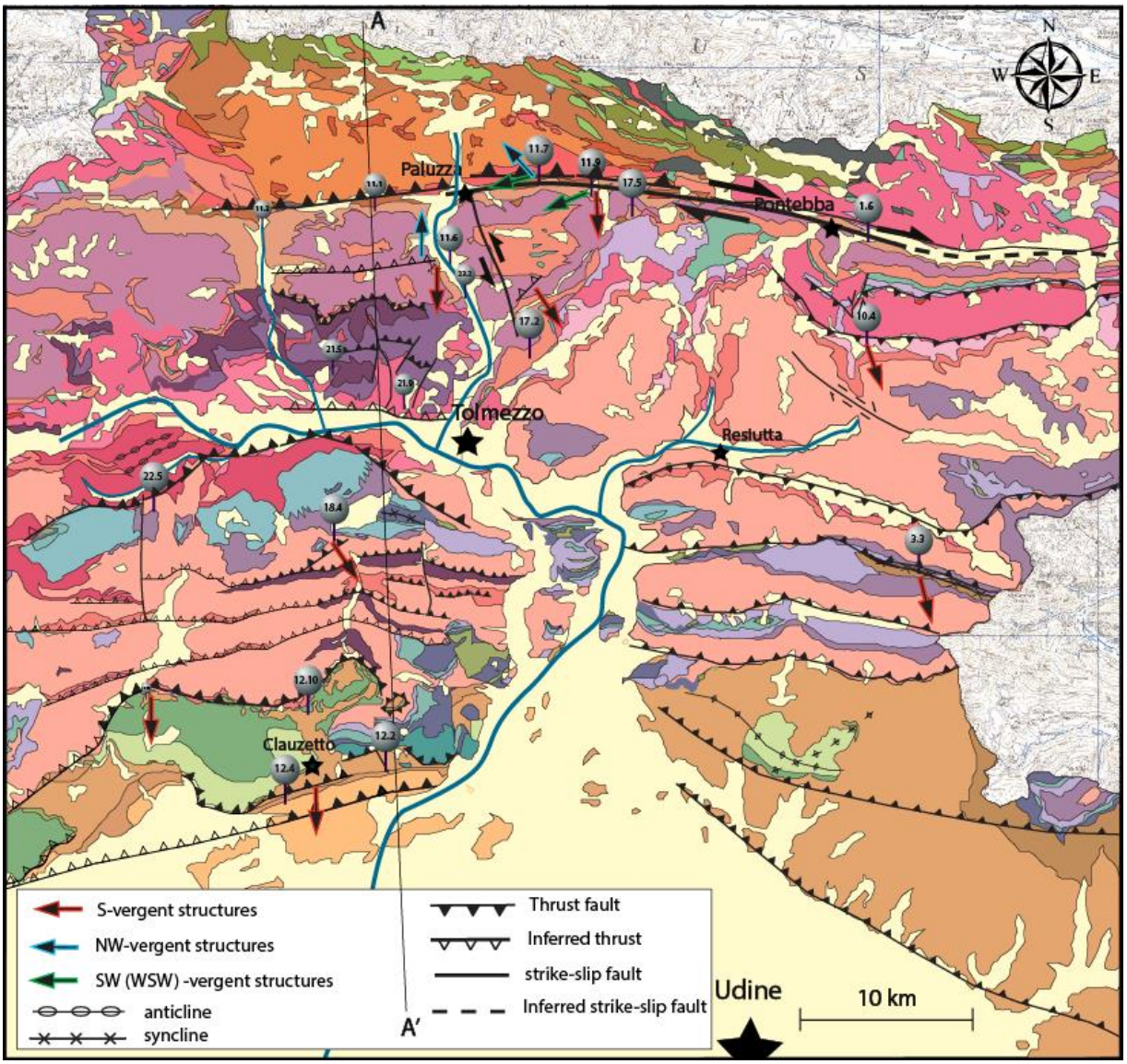

***Figure 15**. Geological map of the Friuli area. This map gives an overview of the large scale geological structures and key outcrops in the western part of the research area. The colors of the structures corresponds with the structures in the cross-sections of chapter 7.*

5.1 Main structures

The nature of the deformation structures found in the area is strongly related to the competence differences within the formations and between the different formations. The sequences of the rigid carbonate platform-unit clearly contains the least evidence for internal deformation, in contrast to the relatively softer sediments of the Eocene flysch and the basinal and slope deposit-units, which show evidence for strong internal deformation.

It is not surprising that the strongest internal deformation was found in the Bellerophon and the Raibl Formation, these sequences are described in literature as the main décollement horizons in the Eastern Southern Alps (Nussbaum, 2000; Schöborn, 1991). However, as the following chapter will indicate, two more décollement horizons have been recognized in the basinal sequences of the Eocene Flysch and the slope/basinal deposits of the Upper-Jurassic to Lower-Cretaceous Biancone Formation. Furthermore, deformation structures unrelated to decollement layers will also be presented in this chapter.

5.1.1 Planar structures, S_0 and S_1

The penetrative structural element in the area is the bedding plane foliation which is bidirectional oriented. The bedding planes, or S_0 planes, dominantly dip with low to medium angles towards the N (NNW) and the S (SSE), indicating that the area is predominantly affected by an overall N-S directed contractional deformation (fig. 16A, B). Besides the primary S_0 planes is the area also affected by a secondary planar cleavage, a S_1 foliation. The appearance of the S_1 foliation strongly depends on the lithology. For instance, in the marly sequences of the Raibl Formation the S_1 is defined by pervasive foliation planes, while in the more rigid carbonate platform sequences, the S_1 occurs as less distinct cleavage planes. The stereographic projection shows one main orientation of steeply NNW dipping S_1 planes, which indicates folding around an ENE-WSW trending axis (fig 17). This cluster of ENE-WSW oriented S_1 planes is in accordance with the E-W plunging folds (fig. 17B).

5.1.2 Folds

Tilting and folding of the bedding occurs throughout the whole area on a large scale and is visible in nearly all formations. The tilted bedding, forming hectometre scale syn- and anticlinal structures, is linked to large scale thrust deformation and emerges most clearly in the rigid carbonate formations due to the little internal deformation in these sequences. Folding at smaller scale, cm-m sized structures, is primarily observed in the less competent formations as the; Bellerophon, Werfen, Raibl, Buchenstein, Biancone Formation and in the Eocene Flysch. The common observation of bedding parallel striations, indicates flexural slip as an important folding mechanism in the area. The refolded of pre-existing fold structures observed in the field (Bellerophon Formation, fig. 16D), as well as the stereographic projection of the fold axes from the area, indicate multiple phases of folding. The dominant orientation however is that of shallow east and westward plunging folds, indicating N-S compressional deformation (fig. 16C).

5.1.3 Faults

Thrusting is observed from cm scale to complete fault zones up to 30 meters wide. A large part of these thrusts strike E-W to NE-SW and show top to the south movement. The large thrust faults are indicated by large scale breccia zones which mainly appear as a sub-horizontal band (up to 30 m thick) containing fault rock material as cataclastic rock and fault gouge. These fault zones appear to be restricted to carbonate platform formations, as they are mainly encountered in the Dolomia Principale Formation. These observations are of great importance for this study, however they do not emerge as well as they should by the stereographic projections, this due to the lack of measurable planes and slip indicators in such brecciated zones.

Small scale normal faulting is encountered in all units and the majority of the faults cross-cuts most of the other structures, indicating that they belong to a relatively young deformation phase.

Strike-slip deformation is observed on a large (20m) and small scale (cm) throughout the whole area and affects all units. In the north-eastern part of the area, the strike-slip faults are mainly E-W oriented and display a dextral sense of movement (fig. 18D). In the Western part of the area, the majority of the strike-slip planes is NNW-SSE oriented and shows both dextral and sinistral displacement (fig. 18C).

5.1.4 Shearing

Both continuous (ductile) and discontinuous (brittle) shear structures are encountered in the area. A ductile response to shear-stresses is limited to sequences of the Bellerophon and in a lesser extent the Raibl Formation, this due to the specific rheological response of these relatively soft lithologies (gypsum and marls, respectively). The direction of shearing varies from non-coaxial top NNW to top SW shearing to coaxial NE-SW extensional shearing. Semi-brittle shearing is mainly E-W oriented and shows an overall movement towards the east.

The lower Bellerophon gypsum contains a pervasive mylonitic foliation and lineation which is generally heavily folded, and which clearly indicates that at least two phases of folding have affected the mylonite (fig. 19). Sigma-clasts in the mylonite indicate top NW non-coaxial shearing. S-C' shear bands found in the limestone beds of the upper Bellerophon Formation, indicate top N shearing, while continuous shearing exposed by an offset marker (vein) at a different location indicates top SW (WSW) shearing. Non-coaxial shearing is also indicated by boudins in the limestone beds, and localized shear in the relatively soft marly layers, of the Raibl Formation.

Semi-brittle shearing is also encountered in both the Bellerophon and the Raibl Formation. The Bellerophon in the north-eastern part of the study area, indicates E-W semi-brittle displacement, which is probably related to a relatively late phase of E-W oriented strike-slip deformation with a predominantly dextral displacement.

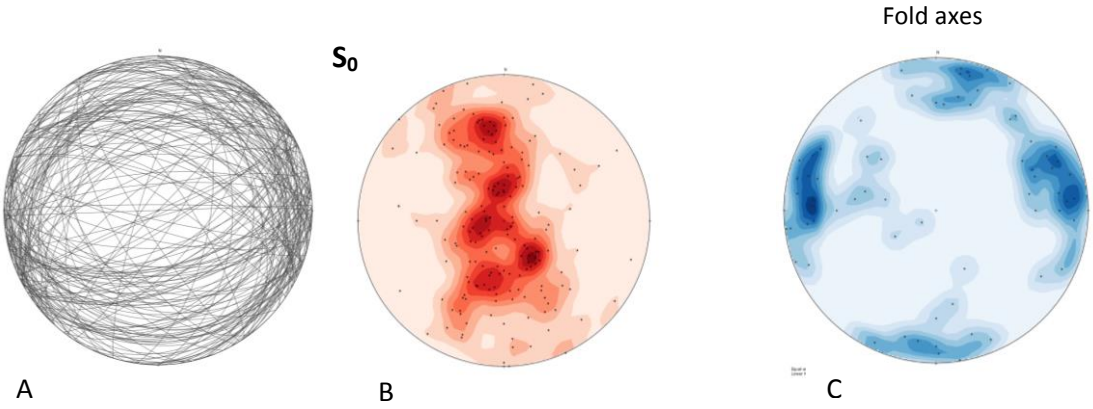

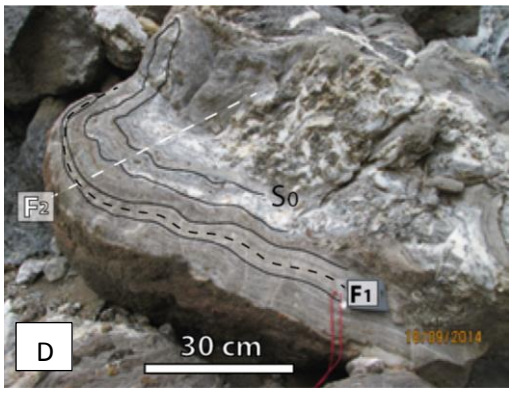

Figure 16. A) *Lower hemisphere Schmidt net projection of the S_0 planes measured in the eastern and western part of the area (n=183).* ***B)*** *Schmidt net projection of the poles of the S_0 planes measured in the Eastern and Western part of the research area. A N-S belt of moderate to steep orientated poles can be recognized, indicating low –medium angle dipping foliations towards the N (NNW) and the S (SSE).* ***C)*** *All fold axes, of the western and eastern part of the research area. Two main clusters are shown. E-W oriented fold axes, and N (NNE)-S oriented. A minor third cluster can be recognized with NE – SW plunging fold axes (n=69).* ***D)*** *A hand piece of the heavily folded mylonite of the evaporitic sequence of the Bellerophon Formation, indicating at least two generations of folds within the mylonite, orientation unknown (stop 11.7).*

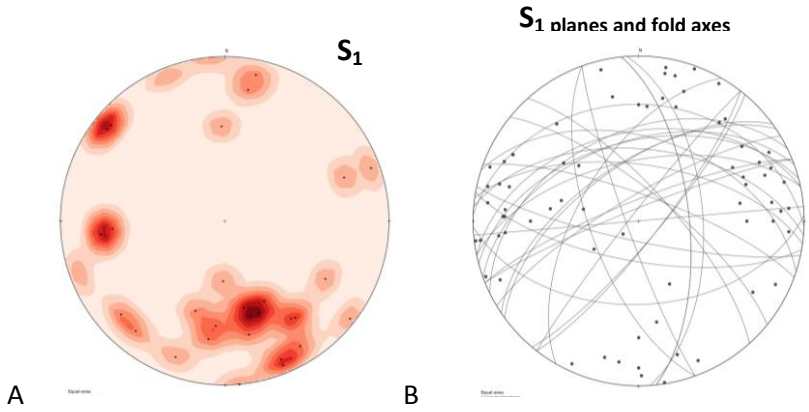

***Figure 17**. **A)** Schmidt net projection of the poles of the S_1 planes of the Eastern and Western area (n=30). A main cluster of E-W striking foliation planes can be recognized, with a majority dipping to the NNW. Two smaller cluster of NW-SE and NE-SW oriented planes can be recognized as well. **B)** Projection of all S_1 planes and all fold axes, the main clusters of E-W oriented S_1 planes correspond to the E-W plunging fold axes.*

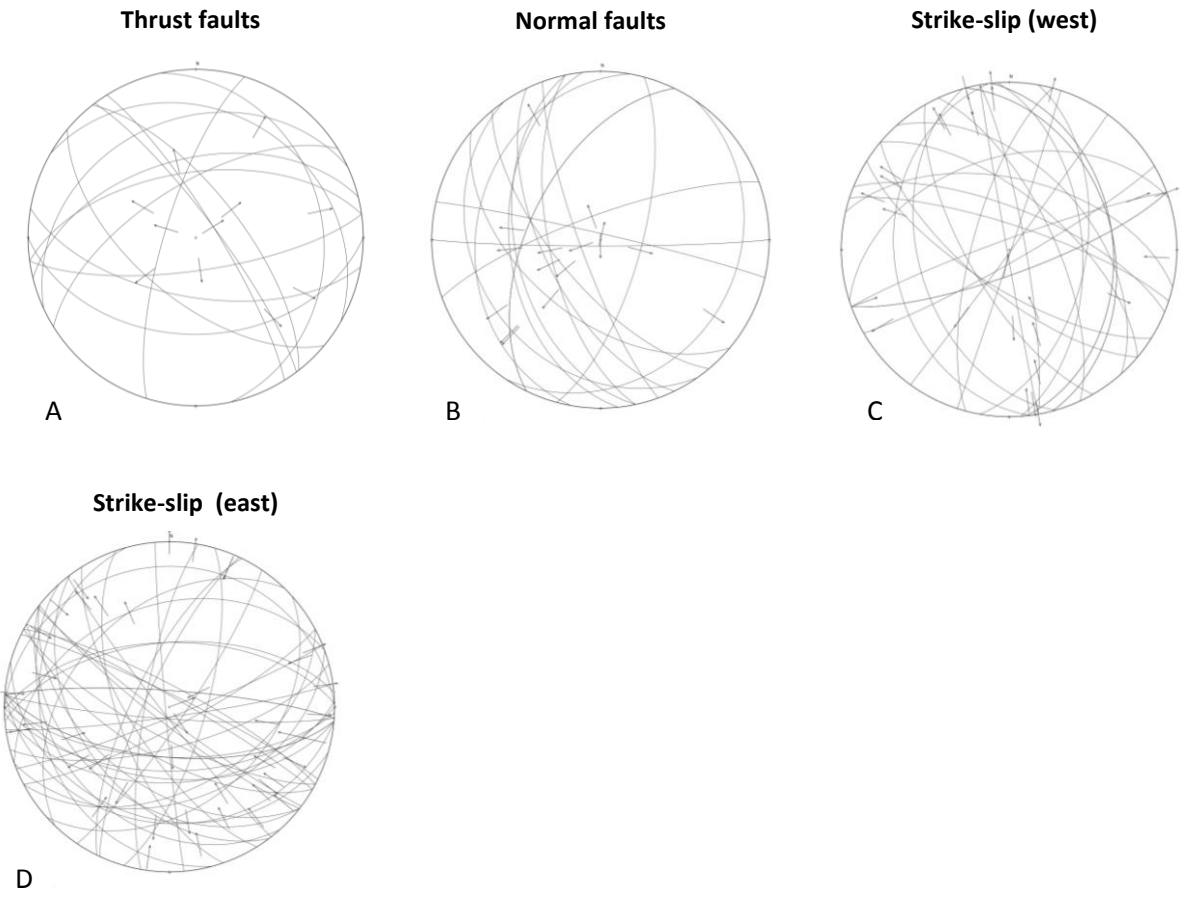

***Figure 18**. Schmidt net projections of the measured fault planes in the area. **A)** Measured thrust planes in the western area (n=13). This stereographic projection does not give a realistic representation of all the thrusts encountered in the field. **B)** The measured normal fault planes in the western area (n=16). The dominant orientation is NNW-SSE and the majority of the planes dips towards the west. **C)** Strike-slip planes in the western area (n=27). Predominantly NNW-SSE striking planes which dip both to the east and west. **D)** Strike-slip planes in the eastern part of the area (n=44), which appears to be more affected by a ENE-WSW striking Fault system than the strike-slip planes measured in the western part of the area and are therefore predominantly E-W to ENE-WSW oriented.*

5.2 Deformation phases

In this chapter the examined deformation features are grouped in phases and presented in chronologic order, starting with the oldest deformation phase D1, and ending with the youngest phase D5. The stereographic projection of the stress regimes found by fault data analysis in WinTensor, is added to the corresponding phases. The relative age of the phases is based on the structural and cross-cutting relationships which will be further discussed in this chapter. Figure 36, at the end of this chapter, provides a table with an overview of the five deformation phases that have been distinguished in the different formations in the area.

D1 – Normal faulting (NE-SW extension)

The D1 involves NE-SW oriented normal faults on cm-m scale and indicates a NE-SW extensional regime.

The oldest deformation phase is of extensional nature and is expressed in the field by cm – m scale normal faults. These normal faults of a small scale horst-and-graben structure in the Werfen Formation appears to have been formed before tilting of the bedding (fig. 19a).

The drag folds, associated to the faults in the Val Degano Formation, of figure 20b indicate normal displacement, however the marker horizon suggest reverse displacement. Therefore, the structure is interpreted as a reversed normal fault, reactivated during a subsequent phase of shortening. The amount of kinematic indicators on the fault planes itself, is very limited, which means that the proposed orientation of the extension, in NE – SW, is based on the orientations of the fault planes (NW – SE) and the orientation of the associated drag folds of the maker beds (fig. 20c).

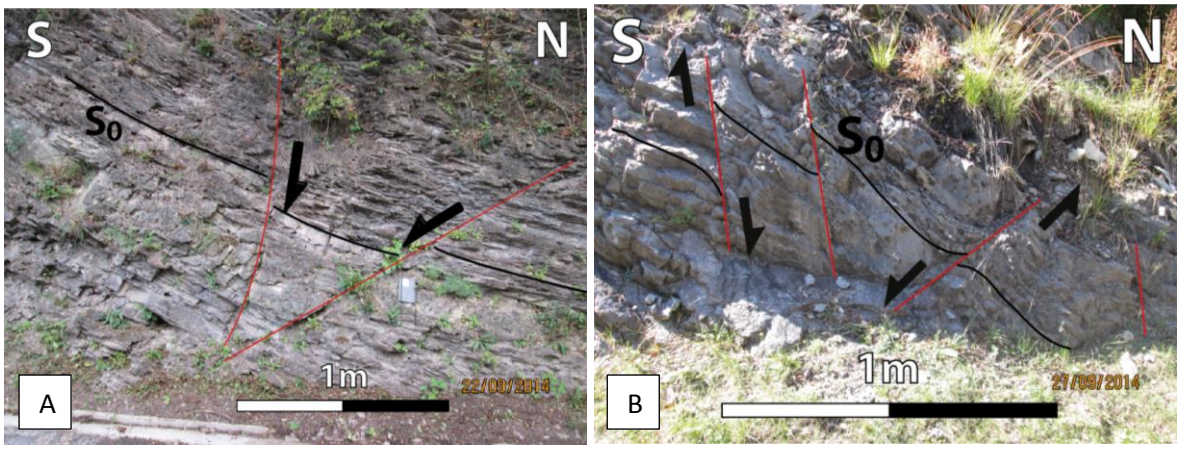

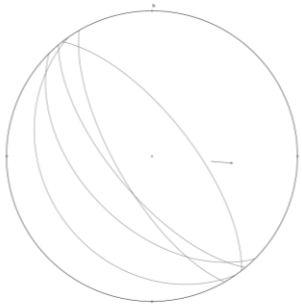

C

Figure 20. A*) Tilted normal faults in the red shales of the Werfen Formation (Stop 15.7).* ***B)*** *Reactivated normal faults in the Val Degano Formation (stop 20.3).* ***C)*** *Equal area projection of the tilted normal faults in the Werfen and Val Degano Formation.*

Besides the brittle response of the Val Degano and Werfen formation, also the Raibl Formation exhibits extensional structures. The high competence contrast between the limestone beds and the marls make the Raibl Formation very prone for boudinage structures to form. The boudinaged structures give the limestone beds of the Raibl a typical nodular appearance. The boudins and pinch and swell structures in the limestone beds, found at stop 10.1 and 10.4 in the Raibl Formation, indicate NE-SW directed coaxial shearing (fig. 21A & B). Because boudins usually form in the ductile regime, where the rock can deform by means of plastic

deformation mechanisms, thus at a depth from 10-15 km or lower (respectively the middle and lower crust), it is likely that these relatively ductile structures, the NE-SW boudins, are formed early in the deformational history.

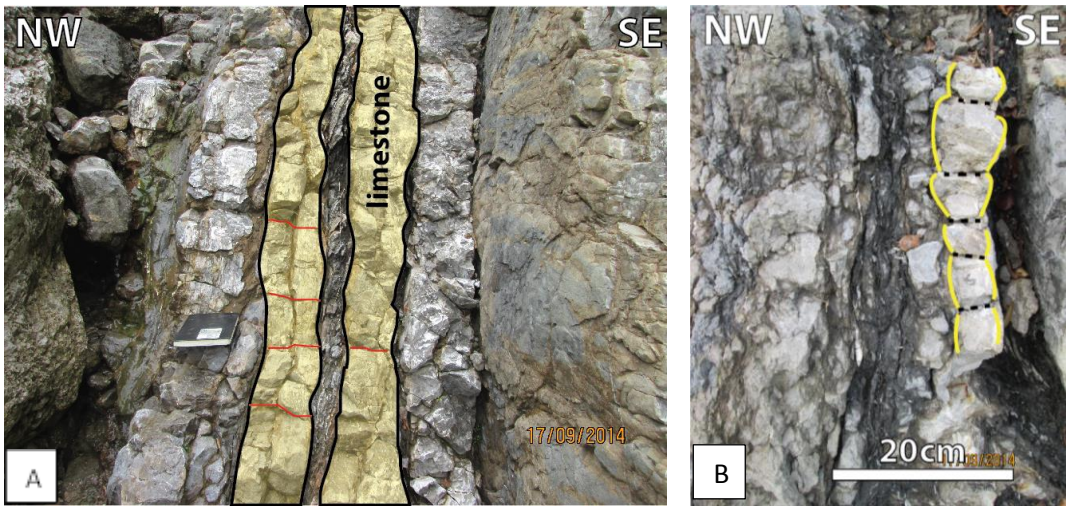

Figure 21 A) *Pinch and swell structures of limestone beds (yellow) interbedded with marls in the Raibl Formation (stop 10.1). The contrast between the less competent marls and the more competent limestone beds, causes the formation of a pinch and swell structure which are frequently separated by small fractures perpendicular to the bedding plane.* ***B)*** *Similar boudinage structures have been found in another Raibl outcrop (stop 10.4) not far from stop 10.1.*

D2 – NE-SW to E-W shortening

The orientation of the D2 deformation phase varies from N-S to NW-SE and is represented by various contractional structures, indicating a former NE-SW to E-W directed stress regime. The scale of the NW-SE oriented structures, both folds and thrusts, is generally small (dm – m), no large scale (hectometer) faulting or folding have been encountered.

The D2 is mainly recognized in the field by SW to WSW-vergent thrusts, top SW kinkbands and N-S plunging folds (fig. 22, 23 and 24). But also by a pervasive conjugate fault set, which is visible throughout the complete outcrop of the green volcanic rocks of the Middle-Triassic Riofreddo Formation, indicating SW-NE compressional deformation (fig. 23A & B).

Besides the top WNW to NW ductile shearing observed in the lower Bellerophon gypsum, is also top to the SW shearing portrayed within the upper Bellerophon limestones, confirming the overall westward (SW-WNW) shear motion during the D2 deformation (fig. 23E) and by asymmetric shear structures in the marly layers of the Raibl Formation. The marls situated in between the previously formed limestone boudins (D1 structures), are folded and indicate top SW layer parallel shearing (fig. 23D). Considering the high susceptibility of the Bellerophon evaporitic sequence, and the relatively soft marls of the Raibl Formation, reactivation and overprinting structures are very likely to form.

The Eocene flysch in the south of the research area shows evidence for NE – SW directed layer parallel slip. The consistent NE – SW oriented striae on the bedding plane of the flysch sequence of stop 12.4, in the Western part of the area correlates with the D2 NE-SW directed shortening(fig. 23C).

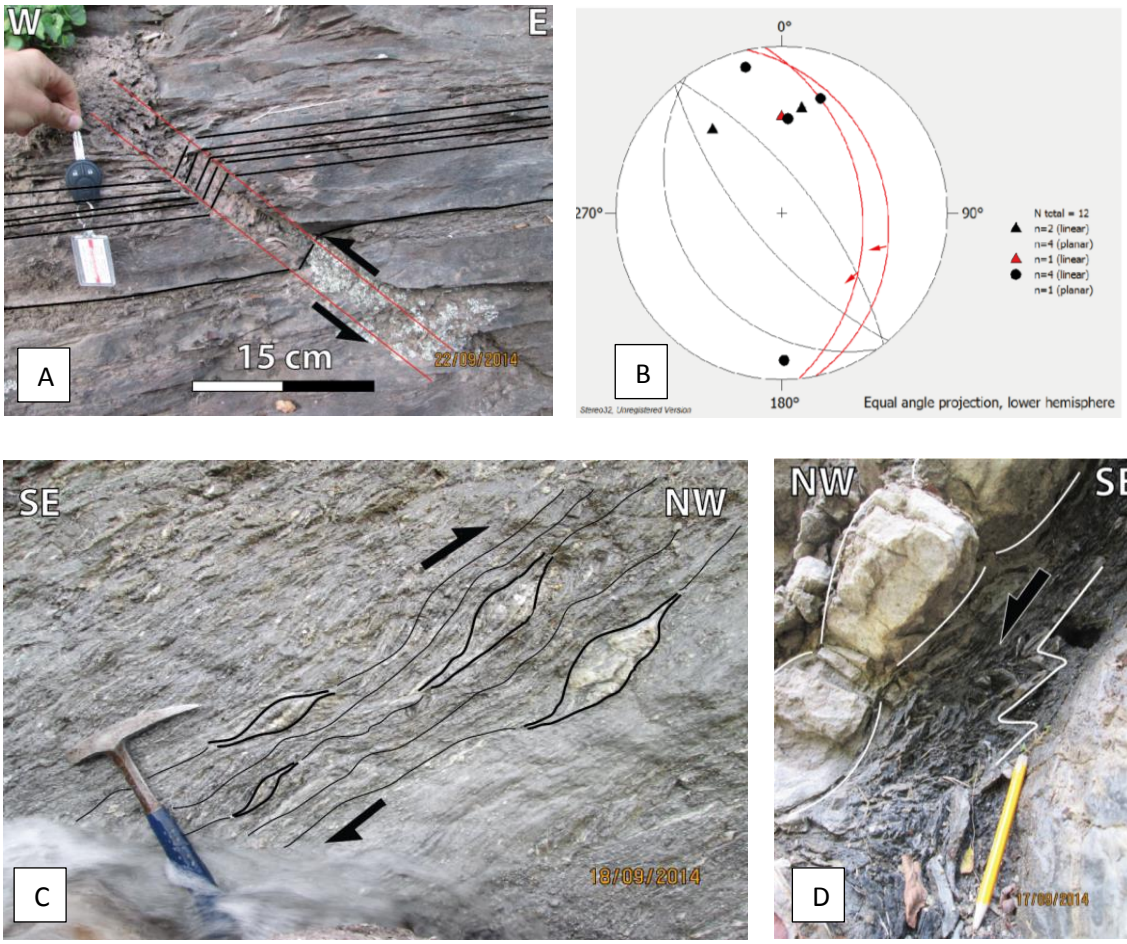

***Figure 22**. **A)** Red shales of the Werfen Formation contain shallow N (and S) plunging fold axes and top SW-WSW kink folds (red). The black great circles represent normal faults of the D1 phase exposed in the Werfen Formation of stop 15.7). **B)** Schmidt net projection of the WSW-vergent kinkbands (red great circels), N-S plunging fold axes (black dots), S0 planes (black great circles) and the axes of two drag-folds (black triangles). **C)** Mylonitized gypsum of the lower Bellerophon sequence containing sigma-clasts indicating top WNW to NW shearing (stop 11.7). **D)** Non-coaxial layer-parallel top SW shearing indicated by the asymmetric fold structures in the marly beds situated in between the previously formed limestone boudins of the Raibl Formation (stop 10.1).*

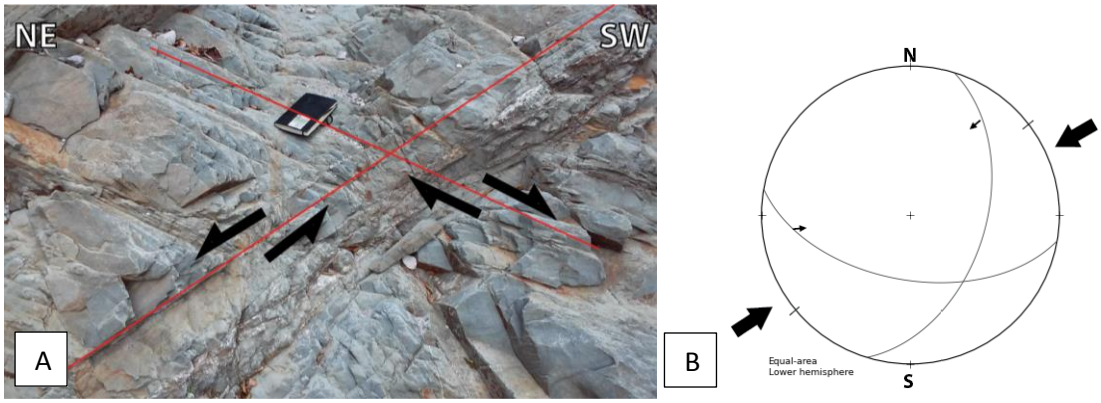

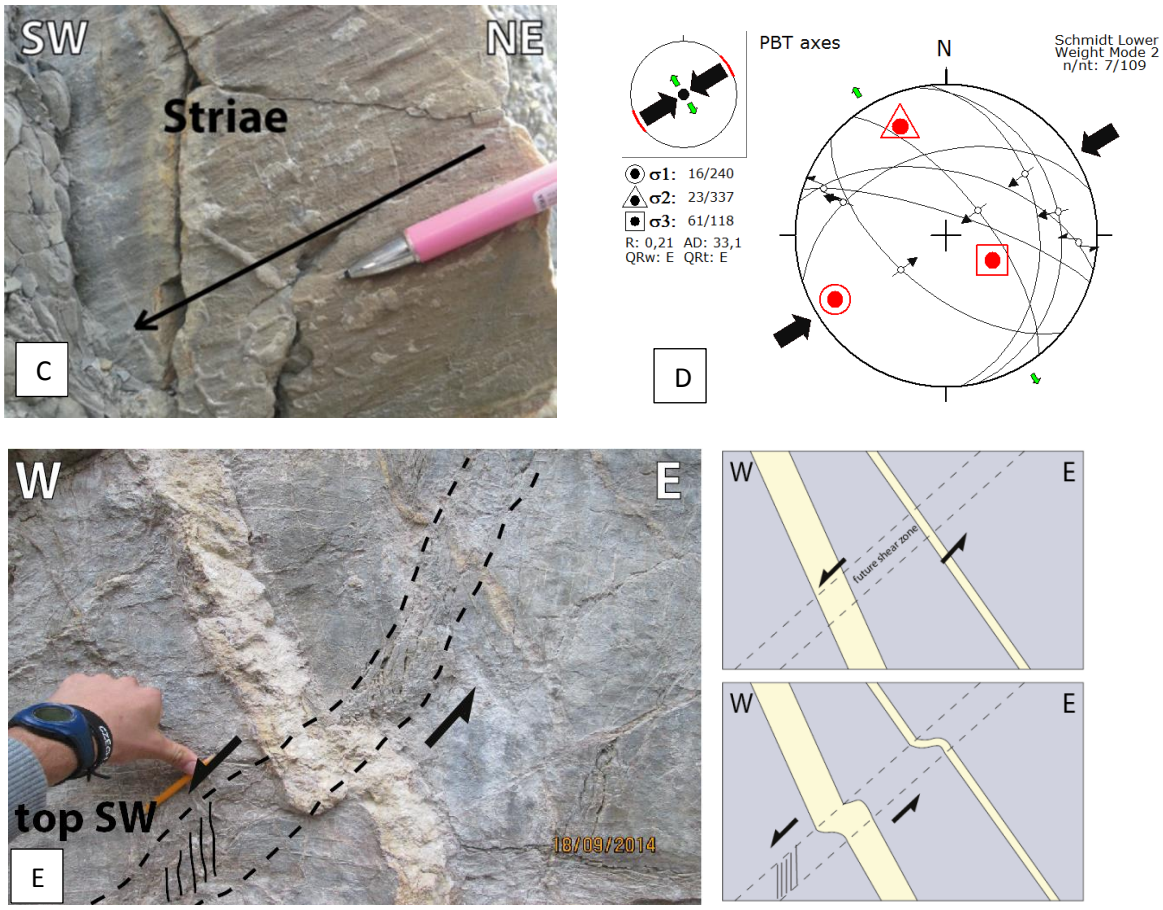

Figure 23. A) *Conjugate faults have affected the whole outcrop of the Middle-Triassic green volcanic rocks of the Riofreddo Formation at stop 17.6 .**B)** Lower hemisphere Schmidt net projection of the conjugate fault set in the Riofreddo volcanics, indicating NE-SW compression. The two orientations of the planes of the conjugate fault set was very consistent throughout the whole outcrop and are therefore represented by just two great circles. **C)** The near vertical bedding planes Eocene Flysch (stop 12.4) contain consistent SW – NE oriented striae, indicating layer parallel slip in SW – NE direction. **D)** Proposed stress axes derived from PBT cluster analysis in WinTensor. Indicating SW-NE compression. **E)** A pre-existing vein in the upper Bellerophon breccia acts as a marker for semi-brittle shearing, the drag structure indicates a normal shear sense top to the SW (WSW) (stop 11.9).*

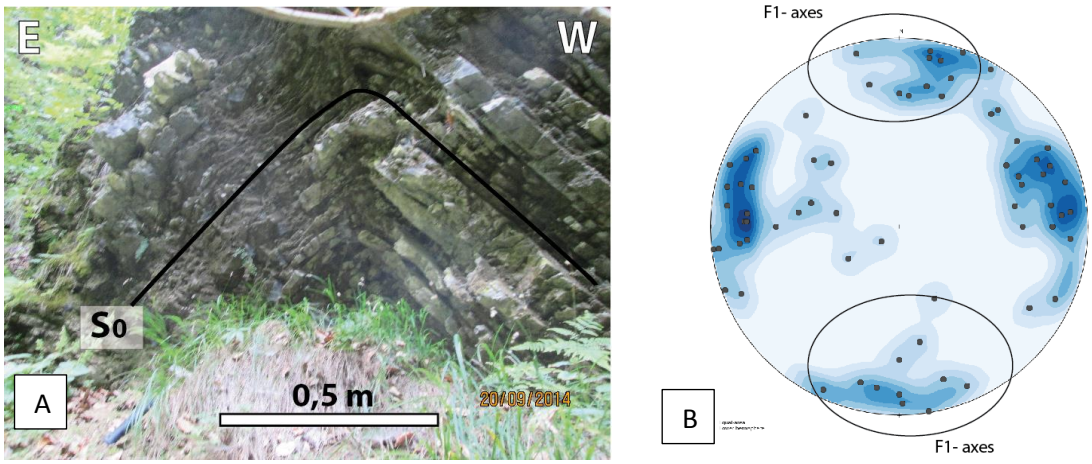

Figure 24. A) *N –S plunging, m-scale chevron folds in the Chiampomano formation (stop 13.3). **B)** Schmidt net projection of the, north and south plunging F1 fold axes.*

D3 – N-S shortening

The D3 phase has been most decisive for the present appearance of the landscape and is expressed by many convergent structures as; thrust faults from cm – hectometre scale, F2 folds, S_1 foliation, shear- and kinkbands and layer parallel slip. The orientation and the kinematic indicators of the structures suggest a N-S (to NNW-SSE) contractional stress regime, with a dominant southward direction of transport.

D3 - Thrusting and shearing

The most pronounced D3 structures are S-vergent thrust faults. The southward thrusting is observed in the area by the development of significant brecciated zones at the base of the faults and by the duplication of formations. The large scale cataclastic fault zones exclusively occur at the base of the carbonate platform formations (Schlern, Dolomia Principale and Cretaceous Limestone). In the northern part of the area, a north dipping limestone sequence of the Bellerophon Formation is duplicated. In the centre of the research area, the overall north dipping dolostones of the Dolomia Principale Formation are exposed for kilometers long and are at least three times interrupted by a large fault zone, strongly suggesting duplication in southward direction (fig. 25a). The large scale fault zones mainly appear as sub-horizontal bands, containing fault rock material such as cataclastic rock and fault gouge (fig. 25b). These cataclastic bands are usually several meters up to 30m wide (fig. 25b).

Apart from these brecciated zones, the thrusting is also documented by the superposition of older formations on top of, often intensely deformed, younger formations. For example, in the eastern part of the area the dolostone sequences of the Schlern Formation overlie the sub-vertical oriented bedding planes of the Raibl Formation, which are intensely folded and exhibit small scale thrusts and discontinuous shear structures, indicating an overall southward movement (fig. 25 C & D). Apart from the brittle shear structures found in the Raibl Formation, continuous shearing is observed in the Bellerophon Formation of stop 11.9, which exposes a sub-horizontal top-S shear zone (fig. 26 E & F). The limestones of the Bellerophon also indicate top to the north ductile shearing, which is exactly opposite of the dominant direction of movement. However, it is not unusual to find locally opposite (conjugate) directed shear within a generally south vergent system.

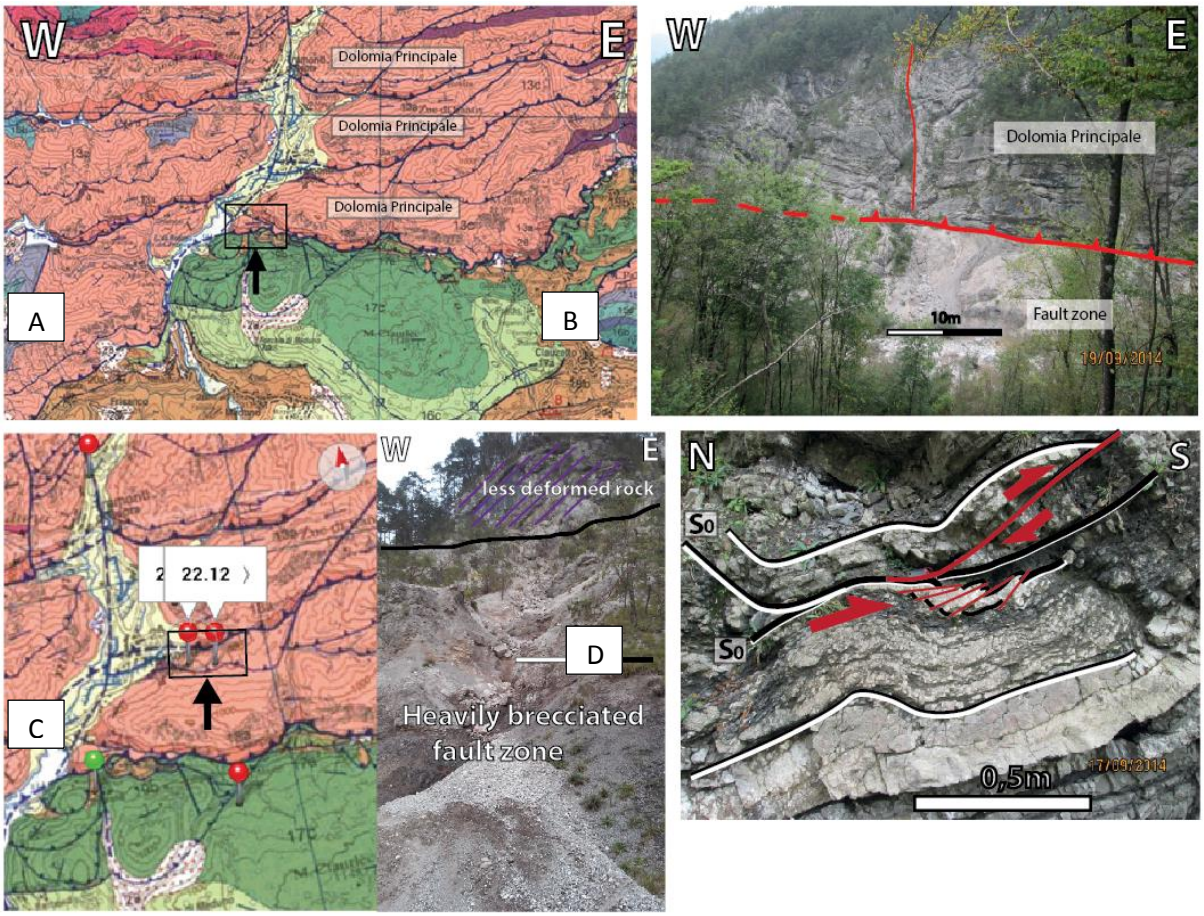

Figure 25. A) *Viewpoint of the photograph (23b) is indicated by the arrow on the geological map, looking towards a major S-vergent thrust fault which is responsible for the placement of the Dolomia Principale on top of the Cretaceous and Flysch formations. This thrust is but one of the s-vergent thrust faults that have duplicated the Dolomia Principale.* ***B)*** *Field photograph of a large sub-horizontal fault zone representing a large scale thrust fault in the Southern part of the area, containing fault breccia and gouge.* ***C)*** *Field photograph of another large sub-horizontal fault zone, representing a large thrust.* ***D)*** *Meter scale S-vergent thrust faults in the limestone beds of the Raibl Formation (stop 10.4).*

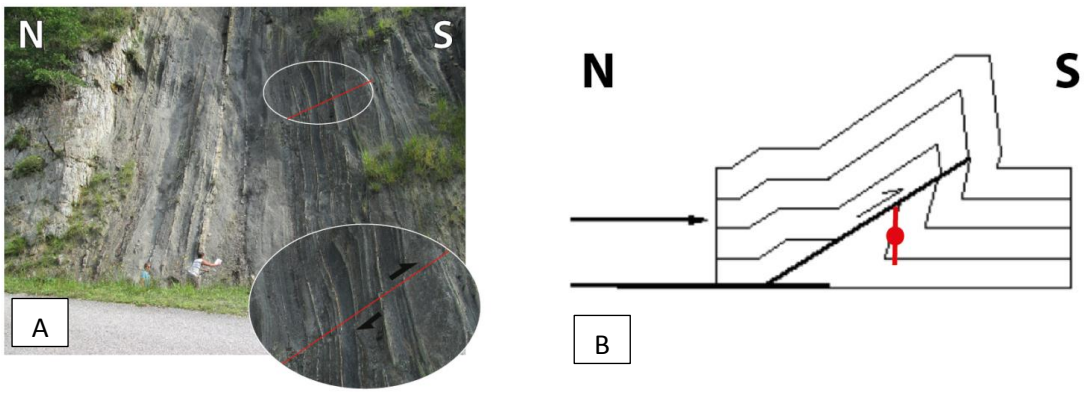

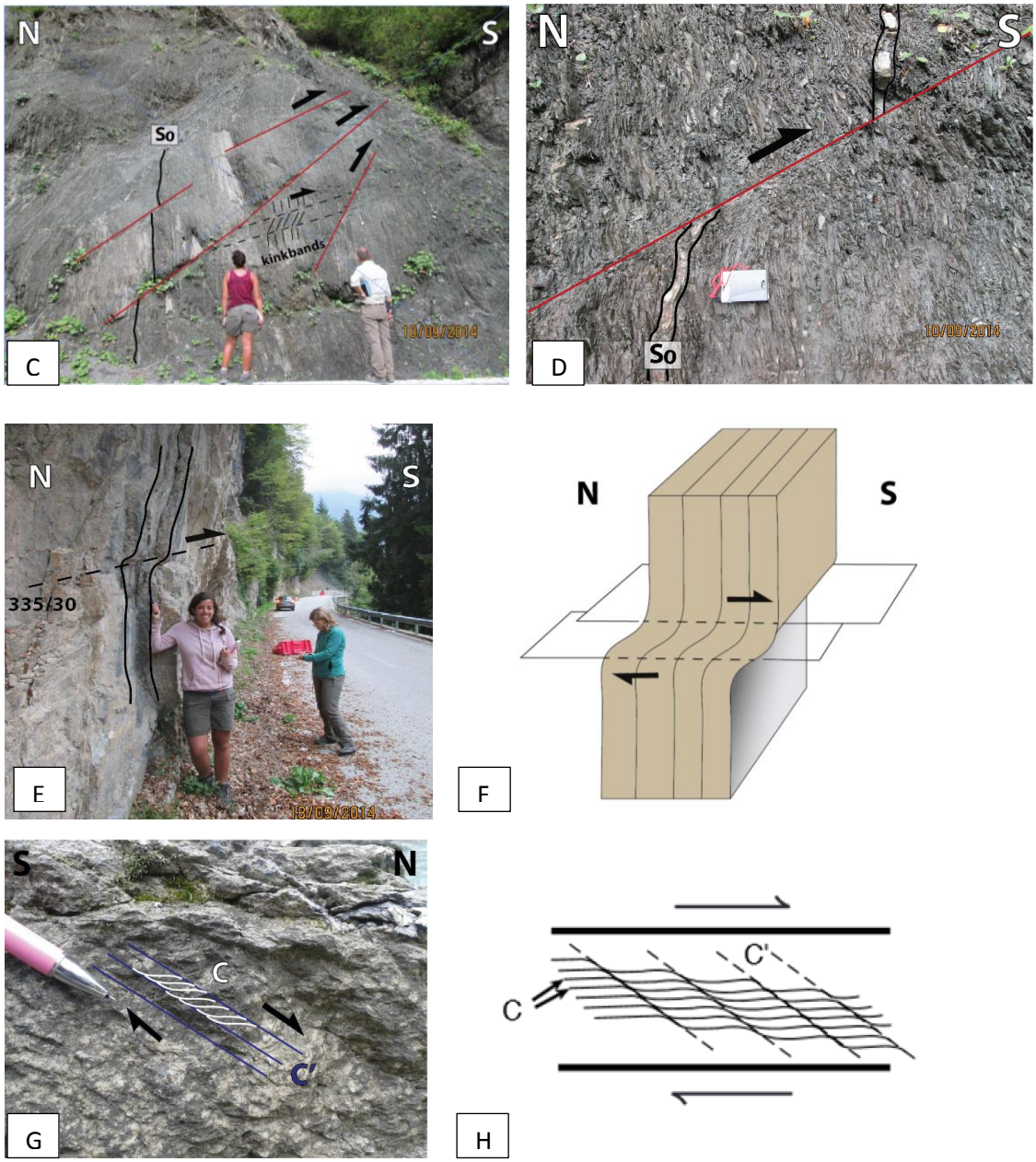

Figure 26. A) *Vertical bedding planes in the foreland flysch in the western part of the area, the flysch contains small scale S-vergent thrusts reflecting the larger scale southward movement (stop 12.4).* ***B)*** *The steep bedding of the flysch is interpreted as part of the footwall syncline of one of the large S-vergent frontal thrusts.****C)*** *South vergent thrusts and kinkbands in the sub-vertical to vertical bedding planes of the flysch in the eastern part of the area.* ***D)*** *Close-up of a thrust fault in the flysch, a displacement of 40cm is measured.* ***E)*** *The vertical to sub-vertical layers of the Bellerophon Formation are affected by a sub-horizontal shear zone, indicating a thrust shear sense top to the S (stop 11.9).* ***F)*** *Schematic illustration of the interpreted sub-horizontal shear zone.* ***G)*** *C-C' shear bands, indicating top N shearing in the Bellerophon (stop 11.6).* ***H)*** *Schematic illustration of the field relation shown in figure 26g.*

D3 – Folding and S1 foliation

Associated to these S-vergent thrusts are the northward and southward dipping bedding planes, which are part of large syn- and anticlinal structures. Small scale thrust faults within the western flysch sequence itself reflect the large scale direction of movement towards the South as well (fig. 26B). The top SSE thrusts (m scale) and top SSE kinkbands encountered in the flysch in the eastern part of the area, are also in accordance with the overall top to the South movement of the D3 phase.

At a smaller scale the N – S shortening is indicated by E – W oriented dm –m scale folds. These F2 folds are often asymmetric chevron folds, where the longer and shorter limb relation generally indicates a southward direction of movement (fig. 29b). Although not all F2 folds are asymmetric, the overall east and westwards and predominantly shallow plunging fold axes still indicate sub horizontal N –S directed shortening.

The Buchtenstein Formation contains, both in the eastern and the western part of the area very steep E-W plunging folds, mainly asymmetric dm-m scale folds indicating top S shortening (fig. 27). The majority of the Buchtenstein Formation bedding planes, as well as the F2 fold axes, show a sub-vertical to vertical dip/plunge. The F2 folds are linked to an S_1 axial plane foliation, which appears in the less competent rocks as a penetrative planar fabric and in the more rigid sequences as a spaced fracture cleavage. Overall is the S_1 represented by moderate N to NNW dipping planes (fig. 29).

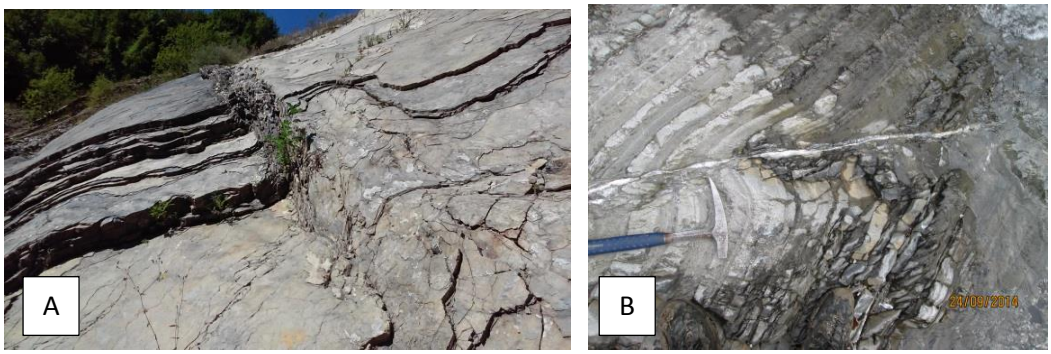

Figure 27. A) *Steep, folded limestone beds of the Buchenstein Formation in the Eastern part of the area (Stop 2.3). The asymmetric nature of these east plunging folds (or maybe drag folds) indicate top South movement.* ***B)*** *Steep, folded beds of the Buchenstein Formation in the western part of the area (stop 17.5). The predominantly eastward plunging fold axes*

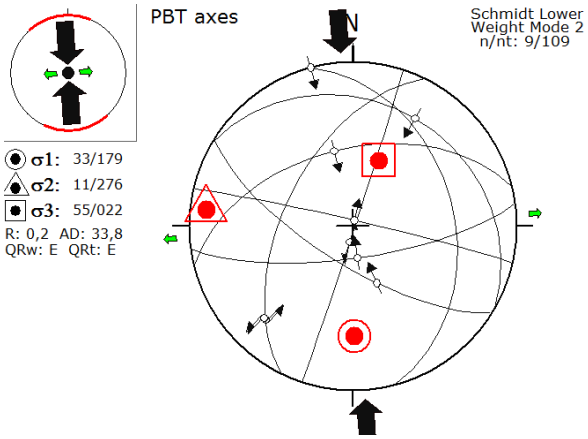

Figure 28*. Stress analysis by WinTensor indicating a N-S contractional regime. Fault sets from thrusts from multiple outcrops, mainly in the Dolomia Principale Formation (n=9).*

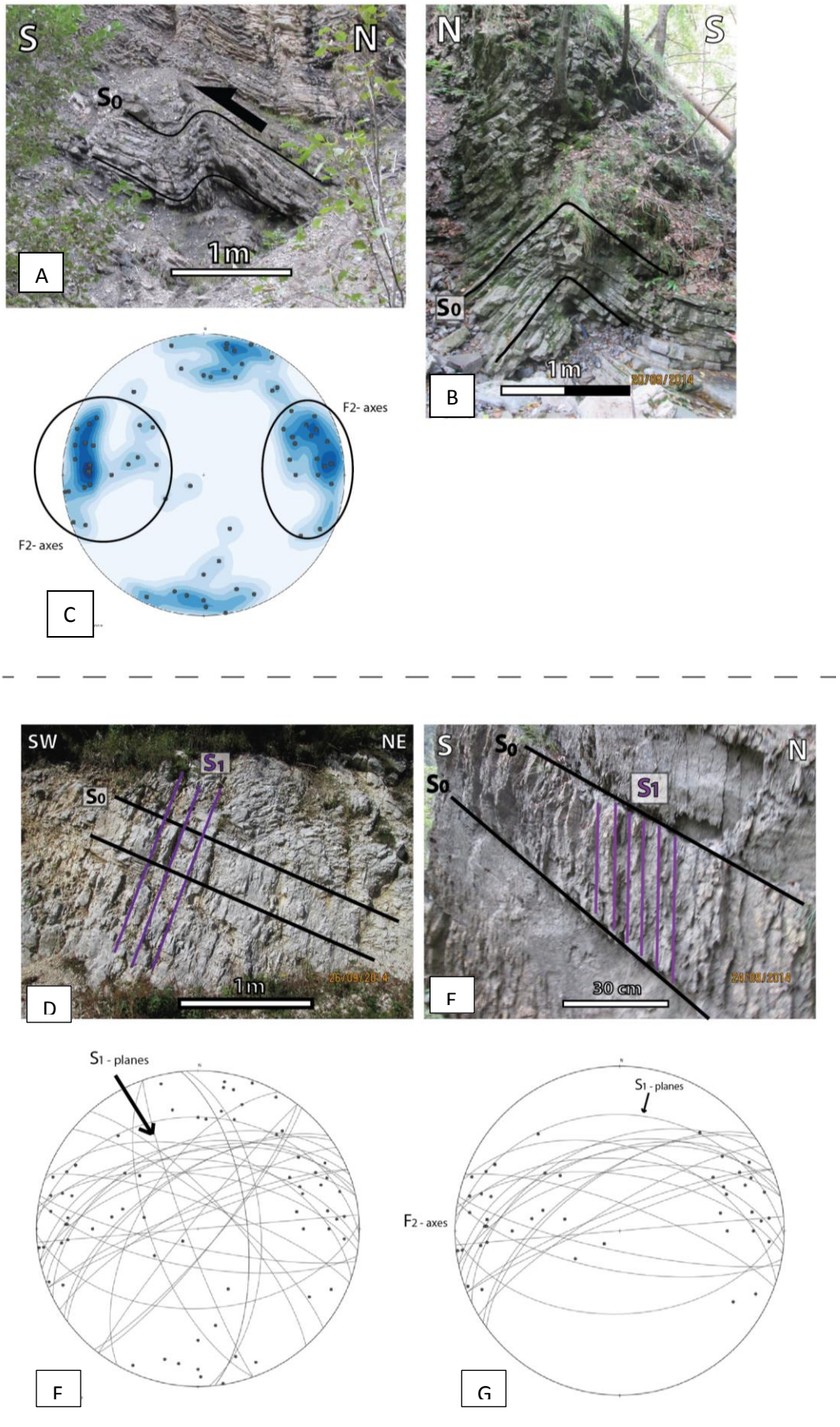

Figure 29. A) *Asymmetric meter scale S-vergent folds in the limestone beds of the upper Bellerophon sequence (stop 11.6).* ***B)*** *E-W plunging meter scale Chevron folds in the Upper-Jurassic Biancone Formation (stop 13.2).* ***C)*** *The E and W plunging*

F2 fold axes indicated by the black circles. ***D)*** *S1 planes in the Valdegaon limestone, represented by a spaced fracture cleavage.* ***E)*** *S1 planes in the Buchtenstein marls, represented by a very pervasive planar foliation.* ***F)*** *Stereographic projection of all the fold axes, the F2 cluster is indicated by the black circle.* ***G)*** *Stereographic projection of the relationship between the S1 planes and the F2 fold axes. The E-W dipping F2 folds plot nicely on the E-W oriented S1 main cluster.*

D4 – NW-SE shortening (Thrusting & Folding)

The D4 phase is the third shortening phase encountered in the area, and is mainly expressed by SE-vergent thrusts and NE-SW oriented open folds (F3). The NE-SW striking thrust faults are encountered from dm scale up to several meters (fig. 30). The number of NE-SW oriented thrusts, however, is relatively low compared to the amount of D3 thrusts (the E-W striking faults). The D4 structures indicate a NW-SE compressional regime.

The majority of the NE-SW oriented open folds plunges under a low angle towards the NE (fig. 30D). In the Biancone Formation (stop 13.2), F3 structures have refolded the F2 folds (fig. 30C). The refolding of the F2 folds is the main indication for the relative timing of the deformation events and sets the NW-SE shortening phase later in time. The F3 folds are especially well exposed in the Upper-Jurassic and Lower-Cretaceous slope/basinal deposits (fig. 30C), and to a lesser extent in the upper Bellerophon Formation (fig. 30B). The D4 structures are also well exposed in the upper part of the Bellerophon formation. Near the town of Dierico, just south of Paularo, a steep SE dipping Bellorophon sequence is exposed. The open folds in the dark limestones and marls of the Bellerophon are folded along a NE – SW oriented axis with an overall shallow plunge towards the NE.

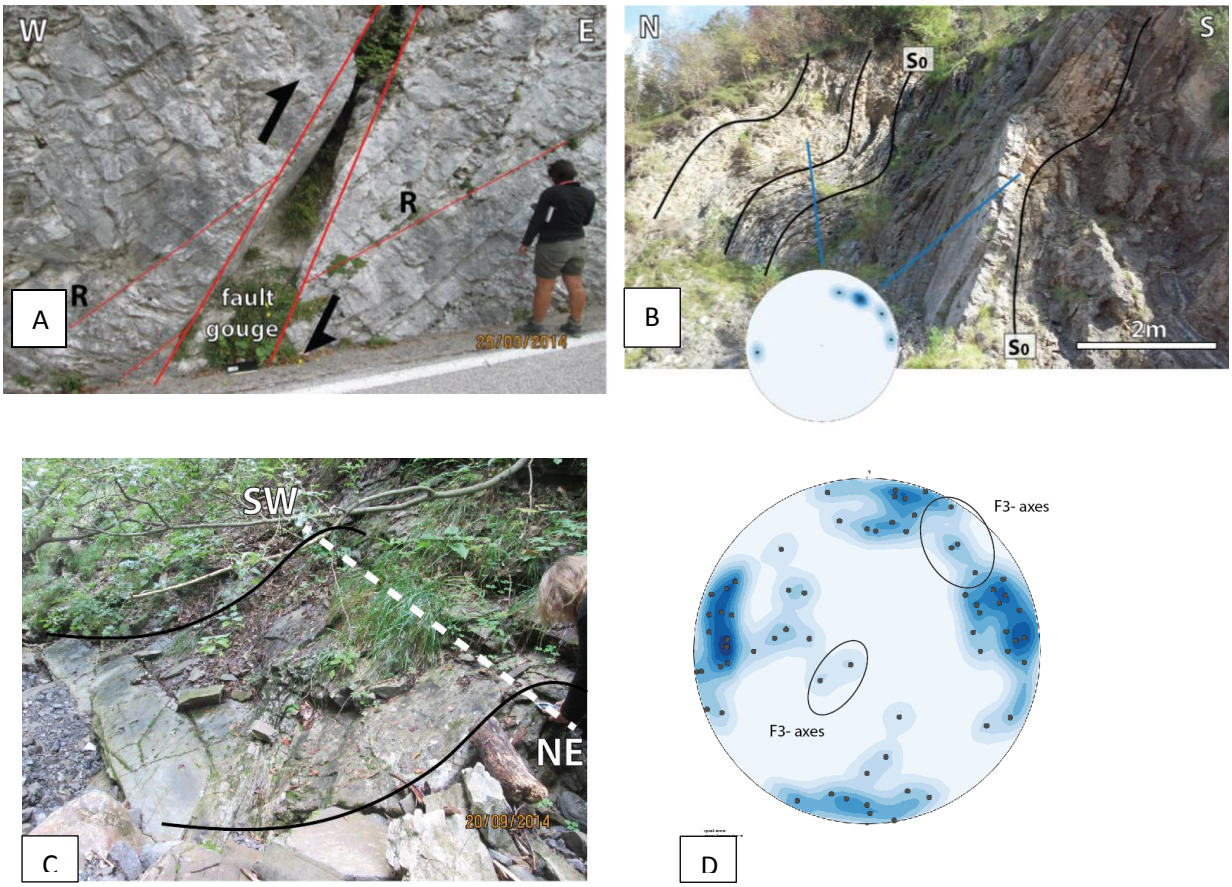

Figure 30*.* ***A)*** *Large thrust fault in dolostones of the Dolomia Principale (stop 18.4). Kinematic indicators, slickensides and Riedel shears, indicate top to the SE thrusting.* ***B)*** *NE-SW oriented m –scale folds in the upper Bellerophon Formation, the stereographic projection shows the associated fold axes (stop 23.2).* ***C)*** *NE - SW oriented open F3 folds have refolded the F2 chevron type folds (stop 13.2).* ***D)*** *Schmidt net projection of the NE-SW plunging F3 fold axes.*

D5 –Transpressional phase with strike-slip (NNW-SSE) & normal faulting (NNW-SSE)

This relatively late deformation phase is indicated by strike-slip faults on various scales and, in general small scale, normal faults. Sub-vertical to vertical fault zones with high angle fault planes represent the large scale strike-slip deformation in the area (fig 32 C,D). A weak N-S to NNW-SSE preferred orientation is observed for the strike-slip planes, which show equally sinistral and dextral displacement. Apart from these N-S to NNW-SSE oriented strike-slip faults, which have been encountered throughout the whole area, exhibits the northern part of the area evidence for a large scale E-W oriented dextral strike-slip zone. Some of the larger strike-slip zones contain the earlier discussed mirror plane surfaces (fig. 32B). Apart from the association of these planes to severe strike-slip deformation, no other distinct trend, regarding the spatial or orientational distribution e.g., have been found.

Considering the mutual orientation of the strike-slip deformation and the normal faulting, and the similar relative timing of these fault structures (both occur late in the deformational evolution), these structures have been housed in one transpressional regime.

Strike-slip faults are often encountered in faultzones which are indicated by the geological map as large thrust faults. The measured fault planes indeed indicate strike-slip deformation while the superposition of the formations and the tilted bedding indicates S-vergent thrusting, such observations are often encountered in the thrust sequence of the Dolomia Principale (fig. 32A). This strongly suggests the reactivation of pre-existing thrust faults as strike-slip during this youngest phase of deformation.

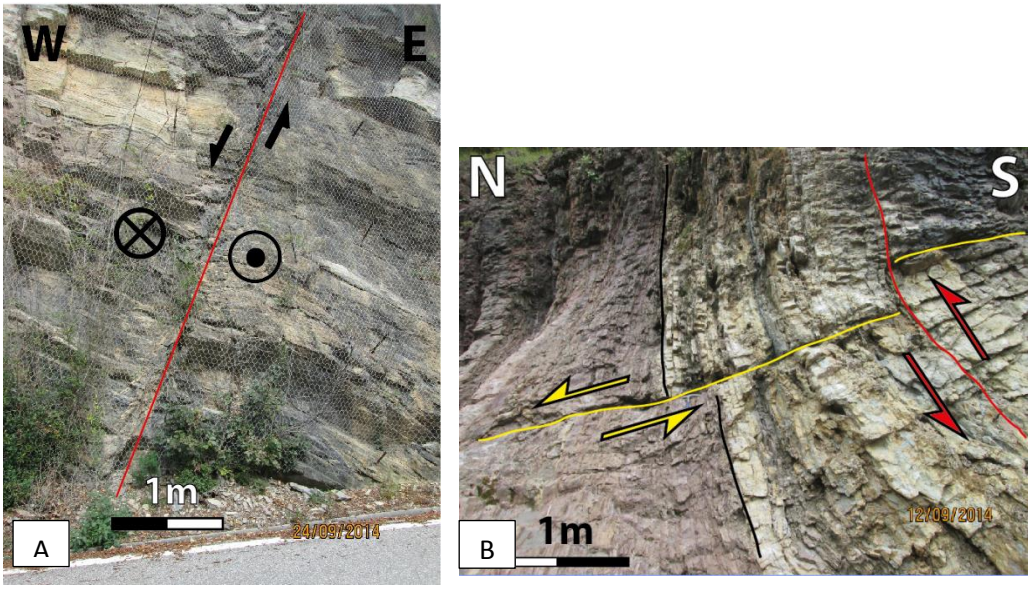

Figure 31. A) *Large scale sinistral strike-slip with normal component (stop 17.2).* ***B)*** *The relative timing between the normal faults and the strike-slip deformation is indicated, a NW-SE oriented normal fault that is displaced by an E-W strike-slip fault.*

The D5 strike-slip faults occur in almost all units and cross-cut all other structures, hence the interpretation as the youngest deformation phase. Strike-slip deformation is observed at cm scale, but there is also evidence for large scale displacement along strike-slip faults. Two kilometers NW of Tolmezzo a massive dolostone sequence of the Schlern Formation is located, at a lateral distance of maximal 200 meters, right next to sandstones of the Dürrenstein formation. The Schlern Formation lies stratigraphically below the Dürrenstein Formation but is exposed due to southward thrusting and southward dipping bedding planes. The thrust however is cut by a strike-slip fault, causes the Schlern sequences to be situated laterally right next to the Dürrenstein sandstones (fig. 32 F).

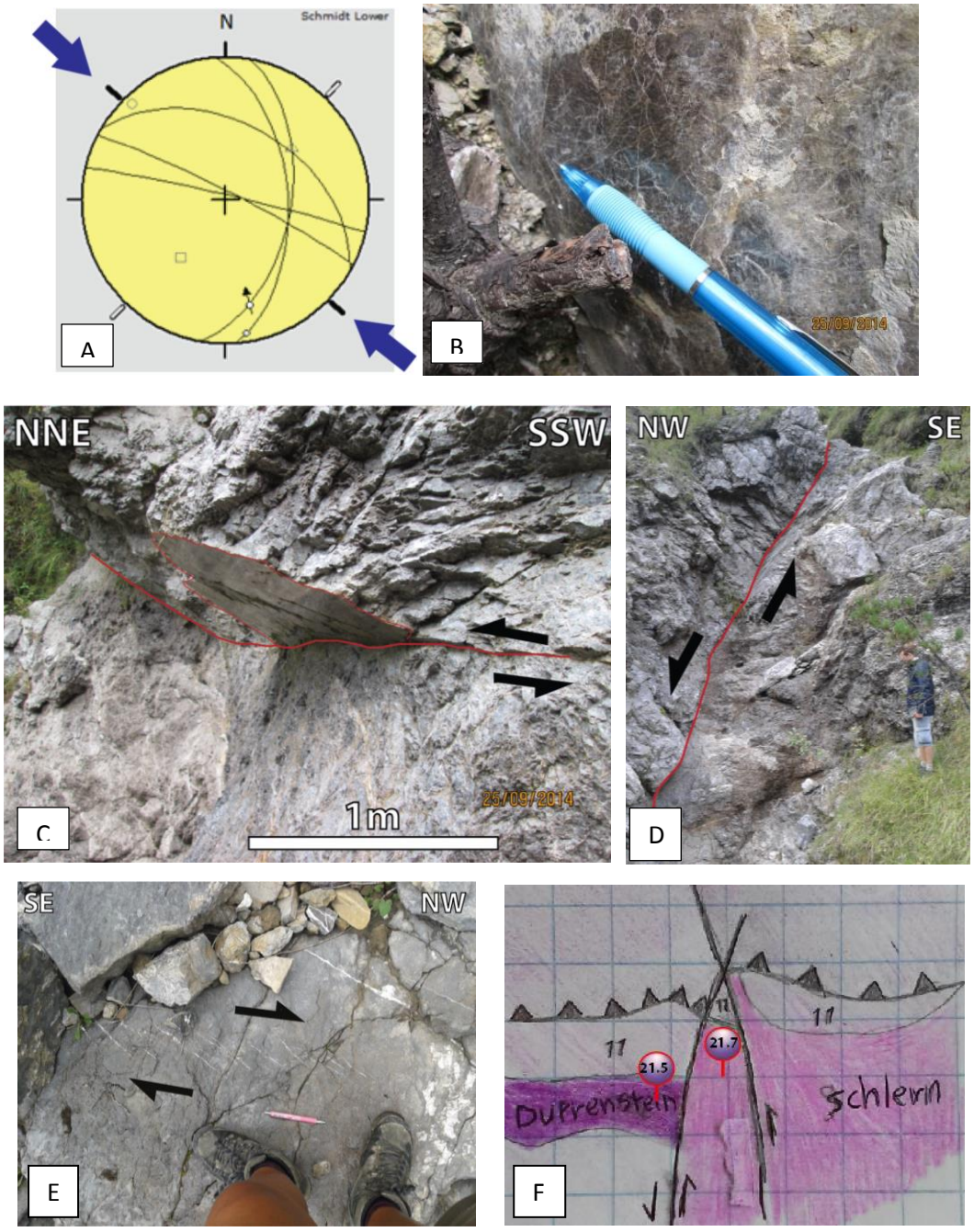

Figure 32. A) *Lower hemisphere Schmidt net projection of strike-slip planes measured in a fault zone which is indicated by the geological map as a large SW-vergent thrust fault which is responsible for the displacement of the Dolomia Principale dolostones on top of the Dachstein sequences (stop 18.1). The planes indicate NW-SE compression.* ***B)*** *Mirror plane encountered in this strike-slip zone.* ***C)*** *Mirror plane encountered in a 30m scale strike-slip zone in the dolostones of the Dolomia Principale Formation (stop 18.6). The strike-slip motion is not consistent with the geological map, which indicates a large northward dipping thrust at this location.* ***D)*** *A field photograph indicating the scale of the strike-slip fault zone. Figure 45.* ***E)*** *En-echelon tension gashes in the upper Bellerophon limestones, indicating NW – SE striking dextral shearing (stop 11.6).* ***F)*** *NNW-SSE striking strike-slip faults cuts through an older S-vergent thrust fault.*

D5 - E-W strike-slip shear

Apart from the overall NNW-SSE striking D5 strike-slip faults, exhibits the northern region of the Friuli area evidence for E-W oriented strike-slip deformation. The limestone beds of the Upper Bellerophon Formation in the north-eastern part of the area, indicate dextral shearing along a large E-W oriented strike-slip zone (fig.

33C). The strike-slip deformation is exposed along the river bank, Southeast of Pontebba. The dextral shear is indicated by displaced calcite veins, large scale drag folding and en-echelon tension gashes and stylolite's (fig. 33A). These type of shear structures indicate shearing under semi-brittle conditions. Beside the Bellerophon Formation also in the Raibl formation (stop 10.4) an E-W strike-slip shear zone has been encountered (fig. 33B). The more abundant NNW-SSE oriented strike-slip faults, previously discussed, have been interpreted as R'-shear structures as part of the larger dextral E-W strike-slip regime (fig. 33C).

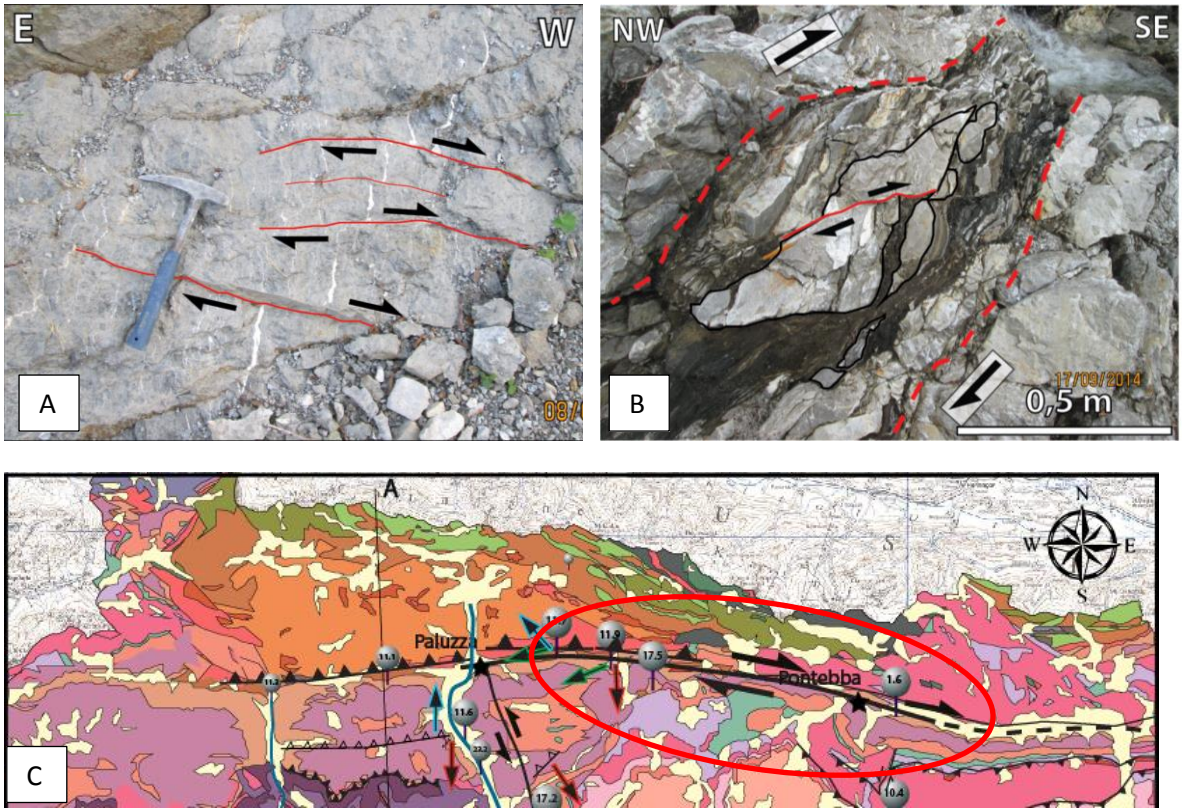

Figure 33. ***A)*** *E-W oriented, dextral strike-slip faults in the Bellerophon Formation in the north-eastern part of the area (stop 1.6), the offset is indicated by displaced veins.* ***B)*** *Asymmetric boundins separated by shear fractures in the Raibl Formation (stop 10.4). The limestone beds form the separated boundins while the less competent marls, which are more prone to flow, wrap around the boudins. The shearing associated to this structures indicates non-coaxial top to the E strike-slip shearing.* ***C)*** *The northern part of the geological map is shown in order to indicate the large E-W dextral strike-slip fault in the area.*

D5 - Normal faulting

Associated to the strike-slip deformation are D5 small scale normal faults, visible in nearly all units. The normal faults usually occur along a NW-SE to NNW-SSE strike and the majority dips towards the WSW and forms occasionally dm-m scale half-graben structures (fig. 34B). The majority of the D5 fault plane angles are within the conventional range of 40-70 degrees which indicates, in contrast to the D1 normal faulting phase, that this phase of normal faulting occurred after tilting of the bedding. The normal faults occur in almost all formations and cut through the older deformation structures. Figure 34B illustrates a D5 normal fault cutting through the mylonitized gypsum of the lower Bellerophon Formation (stop 11.7)

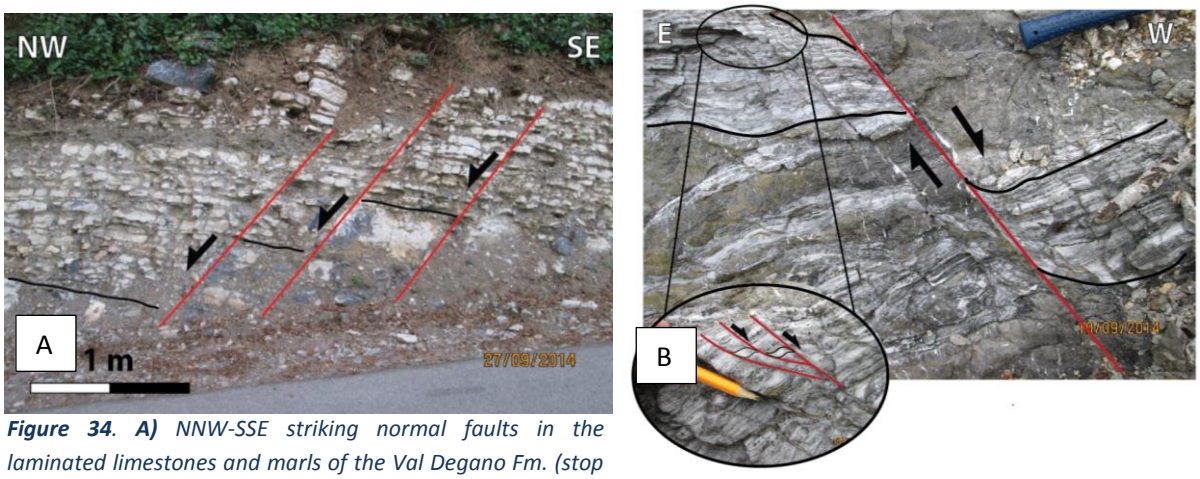

***Figure 34**. **A)** NNW-SSE striking normal faults in the laminated limestones and marls of the Val Degano Fm. (stop 20.9). **B)** The mylonitic gypsum of the Bellerophon formation is cut by a NNW-SSE trending normal fault (stop 11.7). Associated to the main fault plane, are smaller semi-brittle discrete shear planes, which also clearly overprint the older mylonitic foliation.*

Stress analysis by WinTensor, of the complete normal fault sets, indicates a WSW-ENE extensional regime (fig. 35). The orientation of the strike-slip faults indicates a NW-SE compressional regime. As the schematic illustration below shows fit both structures within one transpressional regime (fig. 36 A, B and C). Due to NW-SE compression, NNW-SSE strike-slip faults from which create a pull-apart effect creating a WSW-ENE to SW-NE directed extensional regime related to the formation of syn-D5 normal faults.

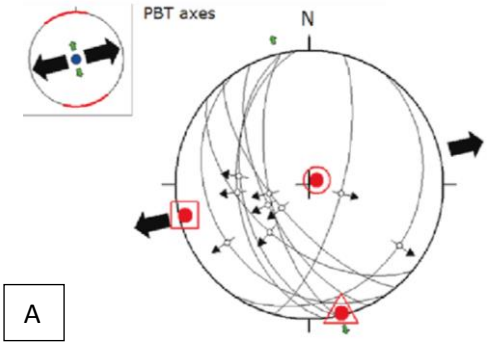

***Figure 35. A)** Stress analysis by WinTensor indicating an ENE-WSW extensional regime, presented in a lower hemisphere Schmidt net projection. Fault sets (n=9) from multiple different outcrops in the Val Degano Formation, Bellerophon and Werfen Formation. **B)** Rose diagram projection of the strike-slip faults. **C)** Rose diagram projection of the normal faults. Both structures fit into the same stress regime (a NNW-SSE to NW-SE compressional and ENE-WSW to NE-SW extensional regime).*

Strike-slip fault slip directions

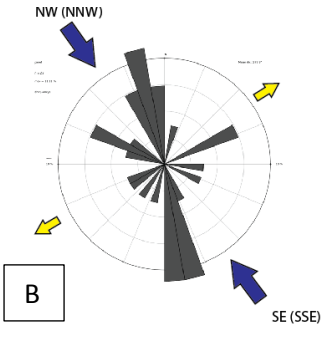

Normal fault slip directions

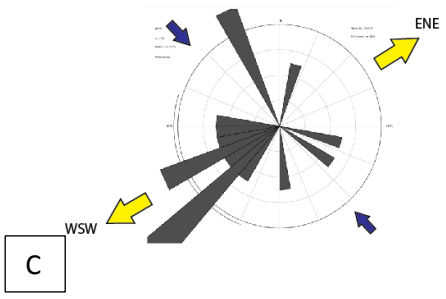

Figure 36. Overview of the Deformation phases D1 - D5

Deformation phase	Stress Tensor (WinTensor)	characteristics	Formations encountered in
D1 NE-SW Extension		Tilted normal faults (NW-SE oriented) NW-SE boudinage (Raibl)	Werfen Fm. Val Degano Raibl
D2 NE-SW Compression (ENE-WSW)	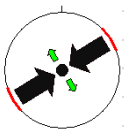	SW (WSW)- vergent thrusts ENE-WSW oriented open-tight folds (dm-m scale) top SW-WNW ductile shearing NE-SW oriented tension gashes	Middle-Triassic vulcanics Werfen Fm. Bellerophon Fm.
D3 N-S Compression (NNW-SSE)	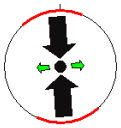	SSE-vergent thrusts (m -hm scale) S-vergent folds (dm-m scale) E-W oriented syn- and anticlines (hm scale) S1 foliation N-S oriented tension gashes SSE-vegent kinkbands (cm-dm scale)	Eocene Flysch Champmano Fm Dolomia Principale Raibl Fm. Buchenstein Fm. Werfen Fm. Bellerophon Fm.
D4 NW-SE Compression	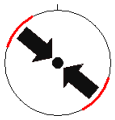	NE - SW oriented open folds (m scale) top NW shearing	Champmano Fm Dolomia Principale Bellerophon
D5 NW-SE Compression ESE-WNW Extension	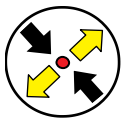	NNW - SSE normal faults (dm-m scale) strike-slip fauliting (dm-hm scale) (thrusts reactivated by strike-slip deformation)	All formations

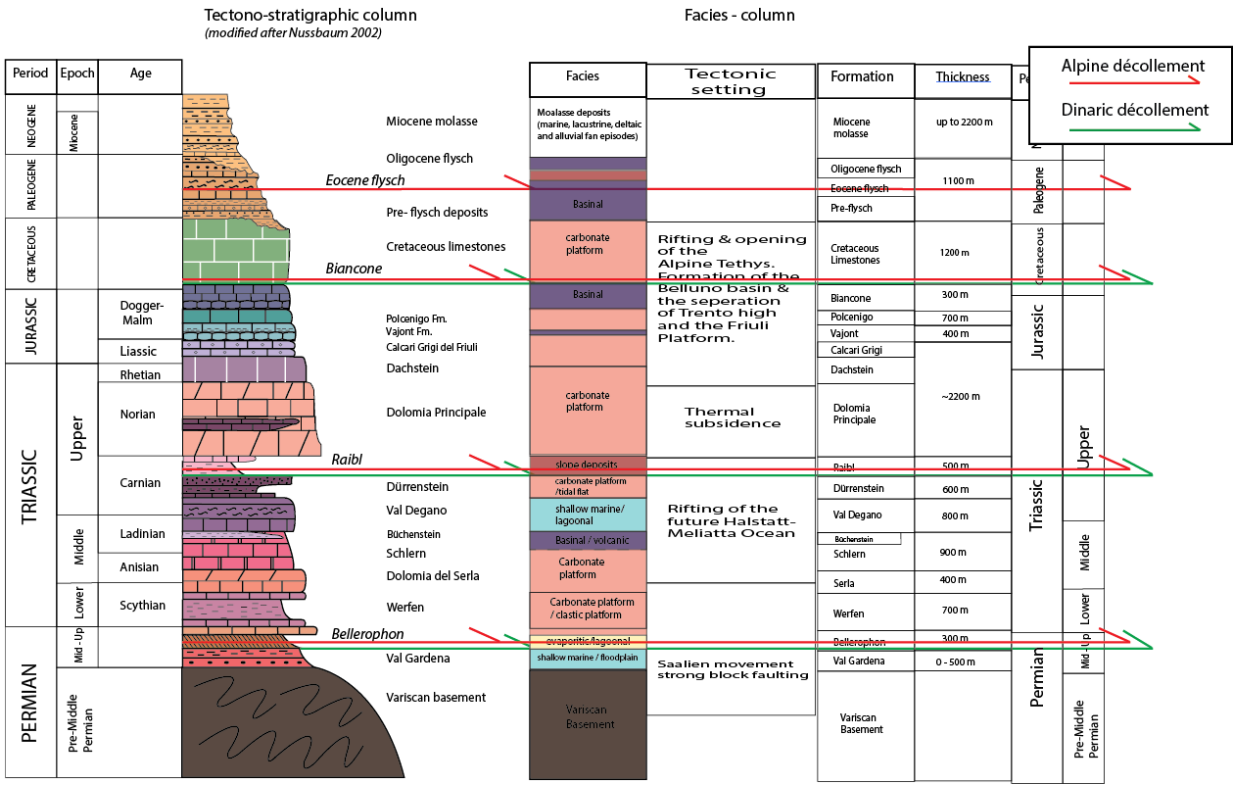

Figure 37. *Tectono-stratigraphic column (modified after Nussbaum 2002). The main décollement levels in the Friuli Alps, Bellerophon, Raibl, Biancone and the Eocene flysch deposits, are indicated by the green, yellow and orange arrows. The table on the right indicates the tectonic events during the deposition of the different formations.*

5.3 Cross-sections

As previously emphasized by Nussbaum (2002), is the kinematic approach an essential tool and probably the best method for the construction of a balanced cross-section through the Friuli Alps since there is no deep seismic data to constrain the structure of the deep subsurface. Therefore, extrapolation of the interpreted surface geology, which has been examined during the field study, is required to infer the deeper structure of the Friuli fold and thrust belt. By means of the into depth extrapolated field data, two cross-sectional models have been constructed. The N-S transect spans the entire orogenic system, from the more internal parts in the North till the foreland deposits in the South (the location of the A-A' transect is shown on the geological map of figure 15 in the previous chapter).

Usually the section line is chosen to be parallel to the direction of main transportation, which would mean a N-S line for studying the overall S-directed transport associated to Alpine phases of shortening in the area, and a NE-SW transect for the overall WSW to SW directed transport during Dinaric phases. During this study, the main focus lies with the kinematic evolution of the Alpine system which led to the choice for a N-S transect. However the influence of the Dinaric system cannot be ignored.

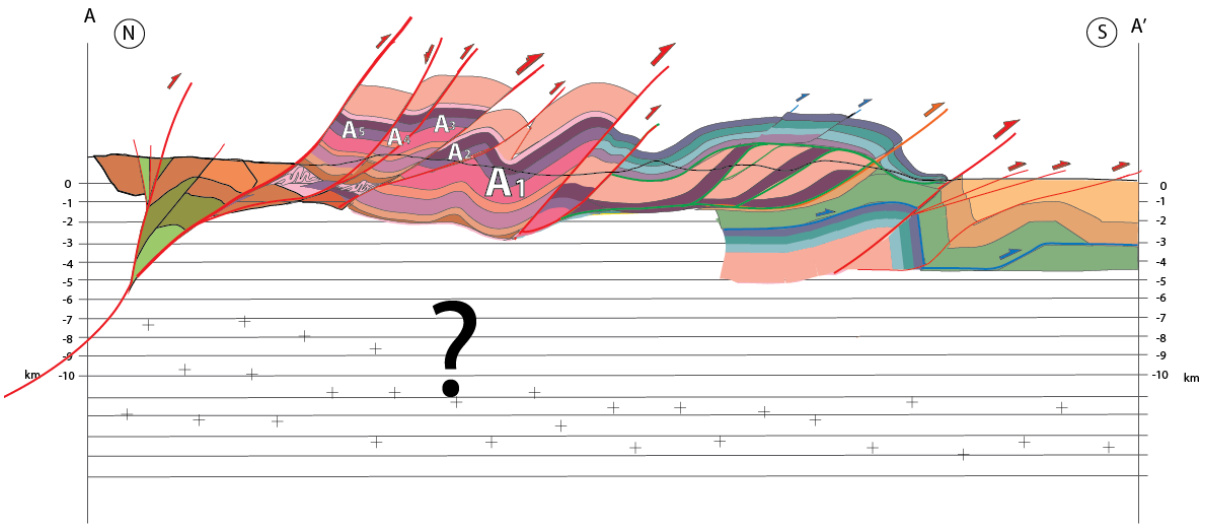

Figure 38. *The above cross-section illustrates the interpretation of the (sub)surface geology based on field observations. The geometry of the deep structures is unknown due to the lack of borehole information or reflections seismic data in the Friuli Alps. The location of the transect is shown on the geological map of figure 15 in the previous chapter.*

Figure 38 shows the sectional view of the surface geology which is constructed by use of field observations. The geometry of the deep structure of the Friuli Alps can only be accessed by into-depth extrapolation of the deformation mechanisms indicated by the geometries at the surface.

The surface geology clearly indicates a dominant S-vergent deformational evolution of the sedimentary sequence, wherein at least two distinct phases with different deformational styles can be distinguished. First a phase with a dominant thin-skinned character with ramp-flat style of faulting along multiple décollement levels within the stratigraphic sequence, and subsequent a phase of dominant thick-skinned thrusting, involving the displacement of former décollements and basement material. The full correlation between field data and the structures reflected by the cross-sections will be discussed in section 2 of chapter 6 (*Chronological overview of the deformational evolution; Links between new field data, cross-sections and previous work*), after the section has been balanced in MOVE which will be addressed in chapter 5.

"Maximum" and "Minimum" shortening models

Since it is one of the main aims of this research to determine the amount of shortening in the Friuli Alps since the Miocene, two different cross-sections are presented involving different interpretations of the deeper subsurface, leading to different amounts of shortening. The maximal shortening model involves a flat-ramp-flat style of faulting with basically one basal décollement in the Bellerophon evaporites. The minimal shortening model involves more basement thrusting, leading to a smaller amount of shortening (fig 39 and fig. 40). Based on the field observations, the maximal shortening model is favored and will therefore be further discussed during the next chapters of this report.

Maximum shortening model

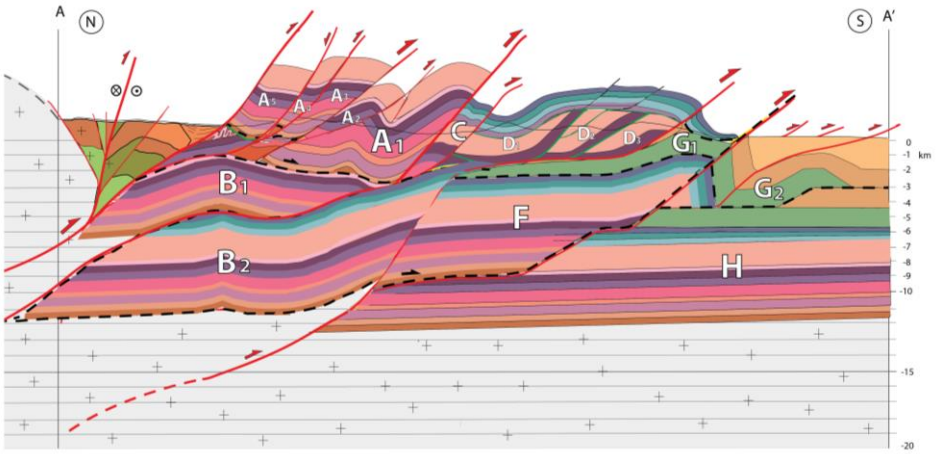

Figure 39. *Interpretation of the N-S profile using a template of predominantly thin-skinned tectonics.*

In the maximum shortening model a template of predominantly thin-skinned tectonics have been used. The choice for a thin-skinned infill of the deeper structure involves the following characteristics;

- Longer décollements with great amounts of horizontal, southward, transport of thrust sheets
- Less basement material involved during thrusting
- Estimated shortening ~45 km

Minimum shortening model

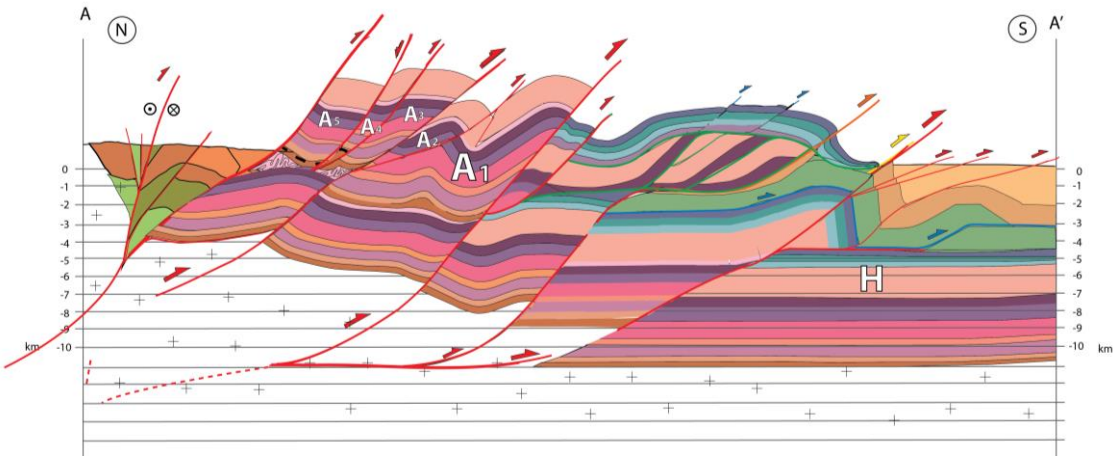

Figure 40. *Interpretation of the N-S profile using a template of predominantly thick-skinned tectonics.*

In the minimum shortening model a template of predominantly thick-skinned tectonics have been used. The choice for a thick-skinned infill of the deeper structure involves the following characteristics;

- More basement involved thrusting, with more vertical displacement
- Shorter décollements with less southward transport
- Estimated shortening ~20 km

5.4 Restoring and balancing the cross-sections in MOVE

MOVE 2015 software is used in order to restore and balance the interpreted cross-sections. After the images of the by hand constructed cross-sections were digitized in the working section of MOVE, restoration and balancing could be executed (fig. 41).

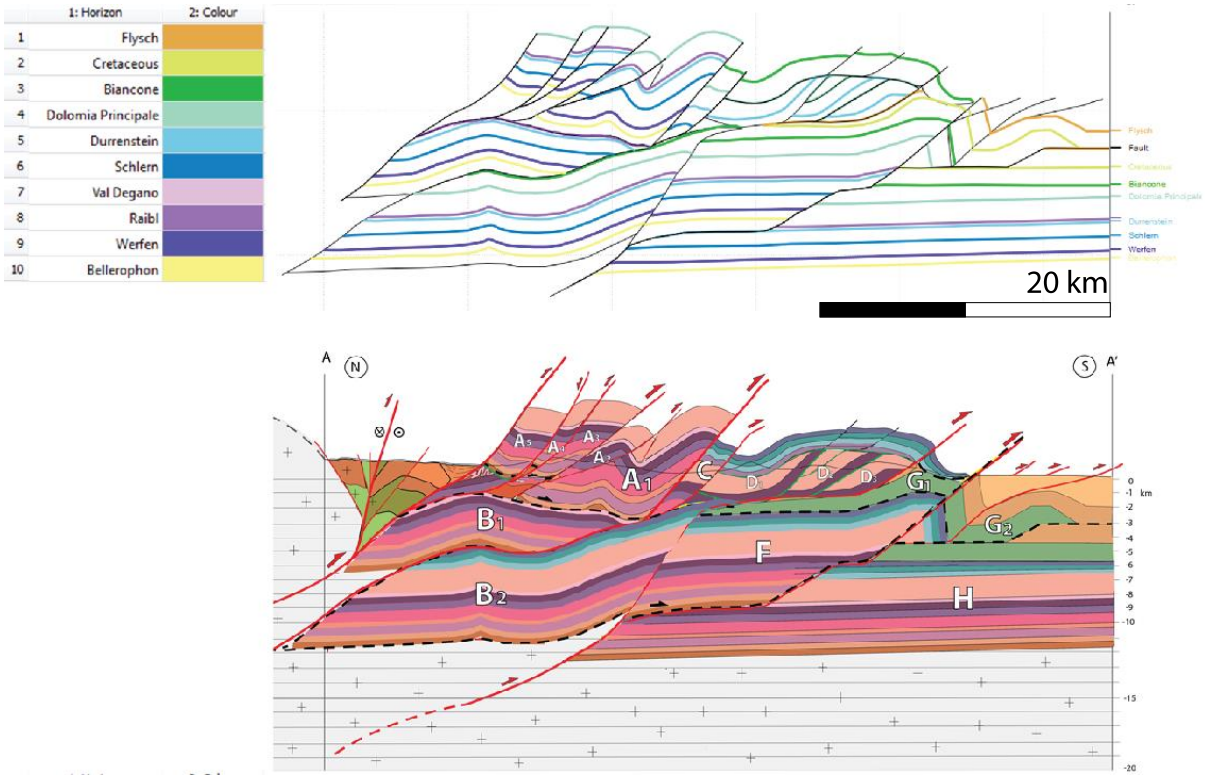

Figure 41. *The by hand constructed N-S cross-section is uploaded as an image in MOVE after which the main horizons and all faults are digitized by use of the 2D model building panel in MOVE.*

From the 2D kinematic modelling options in MOVE, the *unfolding* algorithm is used to restore deformed horizons to its pre-deformation state and the *move along fault* algorithm to deform and restore hanging walls along faults. The main mechanism used for the unfolding of deformed horizons during the restoration was flexural slip, this because field observations as chevron type of folds strongly indicate flexural slip as main folding mechanism for the area. For the restoration of hanging walls along faults, the Simple Shear, Fault Parallel Flow and Fold Bend fold algorithms have been used.

During the restoration, minor space issues in some of the horizons, as well as some small footwall - hanging wall mismatches were exposed and corrected as described by the 2D_Restoration Tutorial (tutorial 14 of MOVE 2014). After correction, the erosional gaps in the top horizons were closed with dashed lines for a more complete overview of the undeformed state of the section. For the maximal shortening model, the total length of the undeformed section amounts 112,5 km, which indicates 57,2 km of shortening (51%) in order to obtain the 55,3 km long present state section (fig. 42).

The total length of the undeformed section of the minimum shortening model amounts 82,5 km indicating 27,2 km of shortening, or 33% (fig. 43).

Based on field observations, the maximal shortening model is favored by the author and will, therefore, be further discussed whereby a step by step evolution is shown by a forward model constructed in MOVE. The presented minimum shortening model is only briefly discussed to indicate the wide range of possible geometries for the deep subsurface and its consequences.

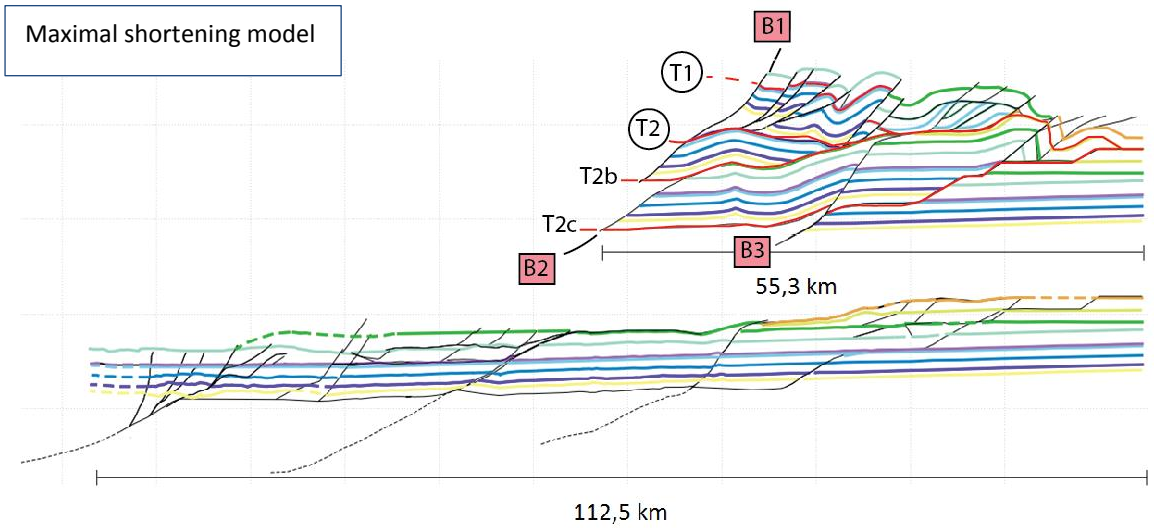

Figure 42. *The present state section of 55,3 km long and the restored undeformed section of 112,5 km long indicating 57,2 km of shortening, or 51% in the maximal shortening model. The encircled faults (T1 and T2) indicate the main thin-skinned faults and B1,B2 and B3 the main basement involved thrusts of the thick-skinned phase.*

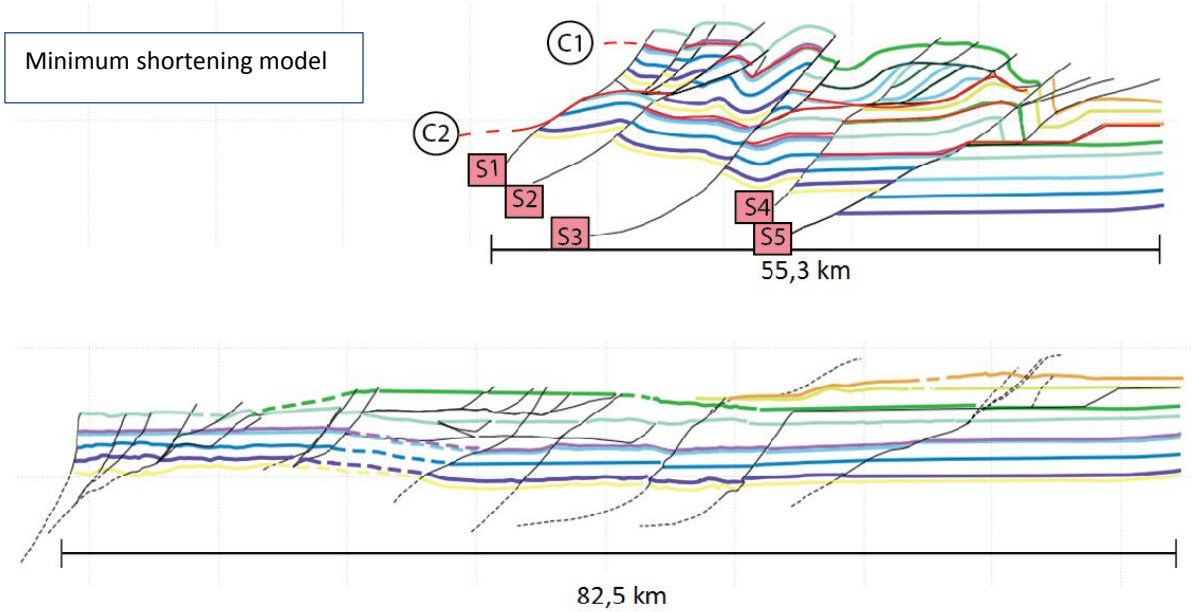

Figure 43. *The present state section of 55,3 km long and the restored undeformed section of 82,5 km long indicating 27,2 km of shortening, or 33% in the minimum shortening model. The encircled faults (C1 and C2) indicate the main thin-skinned faults and S1 – S5 the main basement involved thrusts of the thick-skinned phase.*

Amount of Horizontal (N-S) Displacement along faults					
Maximum shortening model			**Minimum shortening model**		
Stage	**Fault**	**Horizontal displacement**		**Fault**	**Horizontal displacement**
Thin-skinned	T1	49.331 m	Thin-skinned	C1	32.803 m
Thin-skinned	T2	54.580 m	Thin-skinned	C2	35.926 m
Ongoing thin-skinned	T2b	33.635 m			
Ongoing thin-skinned	T2c	8.269 m			
Total thin-skinned		***103.911 m*** *(145.842 m)*	***Total thin-skinned***		***68.729 m***
Thick-skinned	B1	463 m	Thick-skinned	S1	463 m
Thick-skinned	B2	17.907 m	Thick-skinned	S2	993 m
Thick-skinned	B3	8.515 m	Thick-skinned	S3	808 m
			Thick-skinned	S4	1.045 m
			Thick-skinned	S5	3.728 m
Total thick-skinned		**26.885 m**	***Total thick-skinned***		**7.037 m**
Total		**172.727 m**	**Total**		**75.766 m**

Figure 44. *The table above indicates the amount of horizontal displacement along the different main faults in the Maximum shortening model and the Minimum shortening model. The encircled faults correspond to the main thin-skinned faults and the red boxes to the basement involved thick-skinned faults.*

As indicated by the table above (fig. 44), is the total amount of horizontal displacement significantly larger for the Maximum shortening model, 172,7 km, as for the Minimum shortening model, 75,8 km. A logic consequence of the difference in infill of the deeper subsurface, a predominantly flat-ramp-flat thin-skinned style resulting in the tripling of the sedimentary sequences, versus a basement involved thick-skinned style.

The Minimum shortening model involves two main thin-skinned faults, C1 and C2, which follow more or less the same evolution as the equivalents in the Maximal shortening model, T1 and T2. The amount of horizontal displacement however is less, ~69 km compared to ~104 km. But the main difference in the total amount of

horizontal displacement between the two models is caused by the southward continuation of the main basal décollement at the level of the Bellerophon Formation (fault T2b and T2c), which leads in the Maximal shortening model to the tripling of the sedimentary sequence. In the Minimum shortening model is further deformation mainly accommodated by thick-skinned deformation and the sedimentary sequence which had led to only a duplication of the sedimentary sequence (fig. 42 and 43).

5.4.1 Forward modelling

Forward modelling is a useful tool in order to outline and test different structural styles in cases of high geological uncertainty. It enables us to link to the deformation phases based on field data, to the larger scale structural evolution of the area.

During the forward modelling in MOVE, the balanced and restored section will now follow through the proposed order of deformation stages leading to the finite geometry of the section which, in theory, should have the exact same geometry as the input-image of the present state section (fig. 44).

STAGE 0 (Undeformed state)
The Cretaceous Platform formations and the Eocene flysch do not extent over the full length of the 112 km long undeformed section, but only occur in the southern part for about 45 km.

STAGE 1
The first stage accommodates the overall N-S convergent movement by the southward displacement of the Upper-Triassic and Jurassic platform formations along a ~40km long décollement at the level of the Raibl Formation (fault T1). After ~40km of Raibl décollement, fault T1 ramps up through the Upper-Triassic and Jurassic formations and continues along the next décollement layer, the Upper-Jurassic to Late Cretaceous Biancone Formation.

Subsequent to the southward movement of the platform carbonates, is the formation of a basement involved thrust. This thrust follows the Bellerophon horizon before it ramps through the Lower- and Upper-Triassic formations and joins the pre-existing décollement fault at the level of the Raibl Formation (Fault T2).

The overall southward transportation of the Upper-Triassic and Jurassic formations will proceed along a second décollement at the Upper-Jurassic Biancone Formation and will continue until late in the deformational evolution. The basement thrust ultimately results in the stacking of fault-block A on top of block B1 and will eventually bring the lowermost décollement, the Bellerophon Formation, to the surface.

Because of the multiple décollement levels involved during this stage, and the different stages of reactivation of these décollement levels, is a so-called in or out of sequence classification not applicable for this stage.

During the subsequent stages it becomes clear that initially both the thin- and thick-skinned thrusts largely formed in sequence, and only some minor reactivation of preexisting thin-skinned faults caused some out of sequence structures in the section. The thin-skinned thrusts show a normal foreland propagation in the following order; T1, T2, T2b and T2c. The same applies for the subsequent thick-skinned phase with the following fault sequence; B1, B2 and B3. The last stage (STAGE 7) however, shows the formation of the B3 thick-skinned thrust as well as the out of sequence formation of some minor B1 thrust splays in the hinterland. But since these structures are not considered as the main fault structures of the section, the overall fault propagation of this model is regarded to as an in-sequence system.

STAGE 2
The second snap-shot of the deformational evolution includes the initial stages of the formation of the hinterland dipping duplex and the associated roof-thrust in the Upper-Triassic and Jurassic formations. N-S

convergence causes the formation of the duplex systems which is also very well distinguishable on the geological map by a sequence of E-W striking S-vergent thrusts, predominantly exposed in the Dolomia Principale Formation in the southern half of the area. The hinterland dipping duplex of the detached Upper-Triassic platform formations is transported further south via the third décollement level of this ramp-flat system, the Eocene Flysch (T1). The less massif Jurassic formations detach from the Upper-Triassic sequence and move over the duplex via a roof-thrust. The top part of the antiformal-stack is eroded, the duplex system however is still recognizable in the field by a sequence of E-W striking S-vergent thrusts, predominantly exposed in the Dolomia Principale Formation.
Subsequent to the duplex formation is further emplacement of block A on top of B1.

The main thrust fault associated to the second phase is a continuation of the basinal thrust in the Bellerophon gypsum (T2). This thrust fault (T2) ramps through the complete Triassic and Jurassic sequence and connects to the pre-existing thrusts of phase 1 and causes the emplacement of block B1 on top of block B2.

Till this point, basement involved thrusting has only occurred in the hinterland area in the north (along some splays of fault T2).

STAGE 3

The formation of the hinterland dipping duplex has progressed and the detachted Jurassic formations have transported over the duplex along the roofthrust. Besides the continuation of the in-sequence stacking of block-A on top of block-B1 and block-B1 ontop of block-B2, the displacement along the large frontal thrust of the Southern Alpine systems initiates. This large thrust fault is in fact a contiuation of the basinal thrust in the Bellerophon décollement and causes the duplication of the Eocene flysch in the foreland. Future development of the frontal thrust will result in the large fault-progradeding-fold structure in the foreland.

STAGE 4
Stage 4 shows the further southward emplacement of the earlier formed hinterland dipping duplex and due to building pressure from the hinterland the further displacement of block-A over Block-B1. But what especially characterizes this phase is the formation of a second basement involved thrust (B2), which cuts through the pre-existing basinal thrust and emplaces the above lying fault-blocks further to the South.

STAGE 5
Stage 5 describes the further evolvement of stage 4, no new large scale structures have formed.

STAGE 6
During stage 6 the fold-propagation-fold forms due to the continuation of the southward motion along the frontal thrust. In the hinterland, a new splay of the pre-existing basinal thrust (B1) cuts through Block-A and causes further uplift of the northern part of Block-A and its basement material.

STAGE 7 (Present state)
The final stage is characterized by minor southward displacement and involves mainly basement thrusts displacing previously formed décollement horizons and the further uplift of block-A and Block-b1 in the hinterland. A new basement thrust (B3) emerges and cuts through a pre-existing weak zone in the hinge of the fault-bend-fold of block-A. In the foreland new splays of the large frontal thrust form, representing the most recent S-vergent thrust deformation associated to the ongoing N-S convergent and causes minor displacement in the Eocene flysch and the Miocene molasses sequence on top.

Figure 45. *Overview of the forward modeling of the Maximum shortening model in 7 stages:*

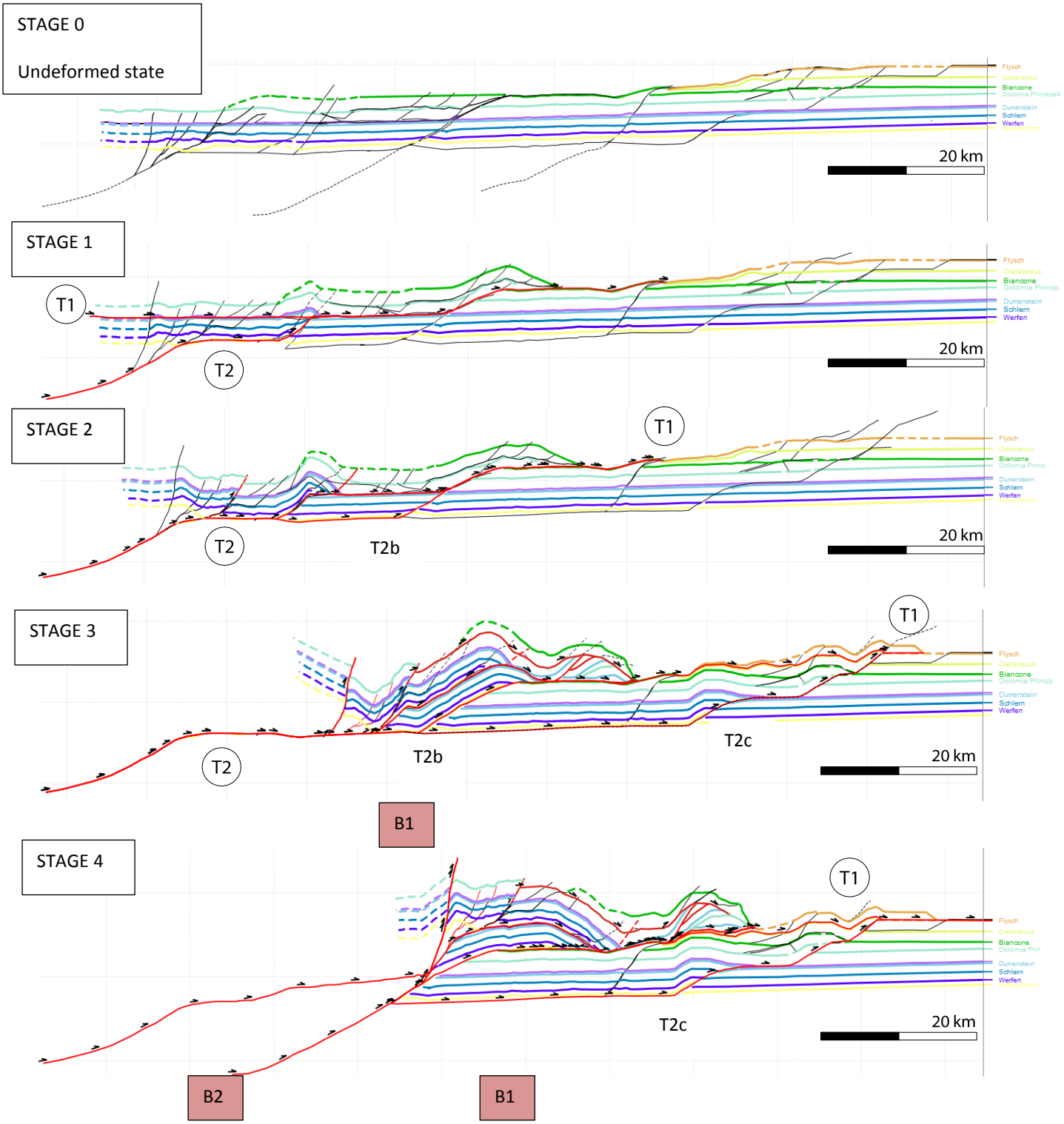

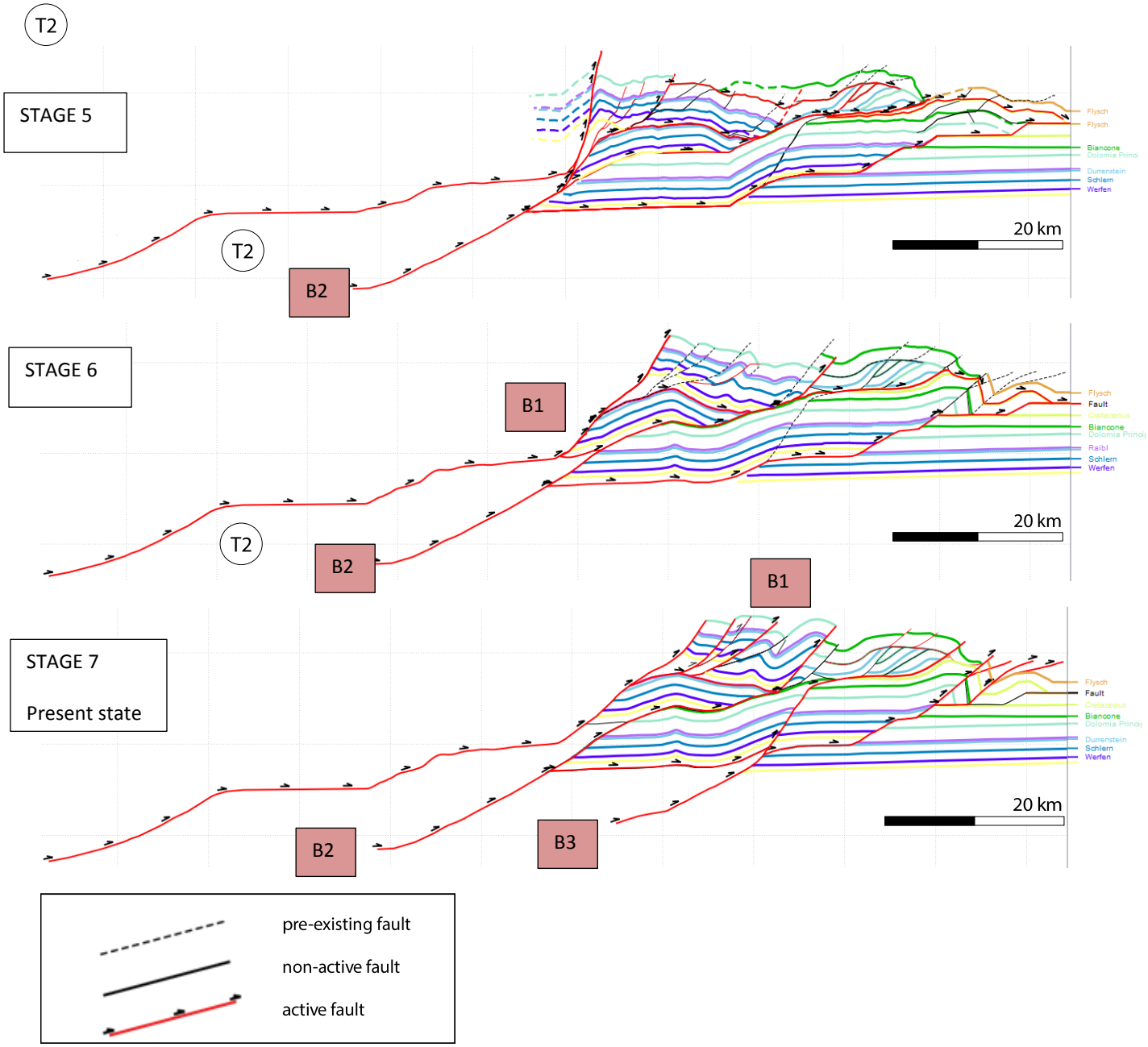
T2
STAGE 5
T2
B2
20 km
Flysch
Flysch
Biancone
Dolomia Princi
Durrenstein
Schlern
Werfen
STAGE 6
B1
T2
B2
20 km
Flysch
Fault
Cretaceous
Biancone
Dolomia Princi
Raibl
Schlern
Werfen
B1
STAGE 7
Present state
B2
B3
20 km
Flysch
Fault
Cretaceous
Biancone
Dolomia Princi
Durrenstein
Schlern
Werfen
pre-existing fault
non-active fault
active fault

5.4.2 Conclusive remarks form the kinematic model

From the restored and balanced sections in MOVE, the following conclusive remarks can be made.

The shortening of the sedimentary sequence in the eastern Southern Alps is largely accommodated by two thrust systems. The T1-thrust system, which is responsible for the southward transport of the Upper-Triassic and Jurassic carbonates along multiple décollements. And the T2-system, of which all splays converge into the major basal thrust in the evaporitic sequence of the Upper-Permian Bellerophon Formation. Subsequent basement involved thrusting along steep fault planes resulted in the exposure of the former deeply situated Bellerophon décollement and basement material at the surface in the hinterland in the North. This means that thick-skinned basement thrusts cut through some former décollement levels, but also use the pre-existing thin-skinned structures for the accommodation of the ongoing shortening. The final stage of basement involved thrusting causes some minor displacements in the hinterland area (block A) and offset along the large frontal thrust creates some new fault splays in the Eocene flysch and Miocene molasses sediments.

The location for thrusts to ramp through the formations may be related to the occurrence of Triassic normal faults, which provide pre-existing natural weaknesses in the stratigraphy. This topic will be further discussed in section 6.6 (*Inherited structures*) of the next chapter.

Maximal shortening model:

- A total of 57,2 km of shortening (51%) along a 55,3 km long N-S transect.
- Pre-dominantly ramp-flat style of deformation with two thrust systems T1 and T2 (accommodates ~50 km of shortening).
- Followed by a minor phase of basement involved thrusting B2 and B3 (accommodates ~7 km of shortening).
- A total amount of **172,7 km of horizontal displacement** along the major faults
- ~145,8 km of horizontal displacement along four main décollement levels
    - Bellerophon Formation
    - Raibl Formation
    - Biancone Formation
    - Eocene flysch
- Greatest amount of displacement experienced by the Upper-Triassic platform formations (i.e. Dolomia Principale Formation) T1-thrust system.
- Basement involved thrusting starts earlier in the hinterland (B1)
- Two large basement involved thrusts (B2 and B3) deform the area during the final stages, simultaneously further development along the earlier basement thrust B1.

Minimum shortening model:

- A total of 27,2 km of shortening (33%) along 55,3 km long N-S transect.
- Flat-ramp-flat style of deformation along two major faults C1 and C2
- Followed by a major phase of basement involved thrusting along five main faults S1 – S5
- A total amount of **75,8 km of horizontal displacement** along the major faults
- ~68,7 km of horizontal displacement along four main décollement levels
    - Bellerophon Formation
    - Raibl Formation
    - Biancone Formation
    - Eocene flysch
- Greatest amount of displacement experienced by the Upper-Triassic platform formations (i.e. Dolomia Principale Formation) C1-thrust system.
- Five large basement involved thrust systems (S1 – S5).

6. Discussion

There is a wide agreement on the general evolution of the eastern Southern Alps, which would consist of a poly-phase compressional evolution involving three main thrust systems (Schönborn, 1999; Castellarin and Cantelli, 2000; Nussbaum, 2002). Multiple names have been used for more or less the same thrust systems in the different research papers. However, a clear distinction concerning the style of deformation (thin-skinned or thick-skinned), is largely lacking. Castellarin and Cantelli (2000) propose a model in which each thrust system contains its own basement unit and the maximum amount of shortening is no more than 35 km. Such a model, with a rather small amount of shortening is not in agreement with the field measurements and observations gathered during this research nor with 2D kinematic model constructed in MOVE, which strongly suggest a great amount of southward transport, especially of the rigid carbonate platform formations, along multiple décollements on various stratigraphic levels. The southward movement is largely accommodated by one thrust system of which multiple splays converge into one floor thrust at the level of the evaporitic sequence of the Bellerophon Formation. Subsequent phases of basement involved thrusting overprint some of these thrust-splays and bring former deeply situated material to the (sub) surface.

Besides the pre-dominantly S-vergent Alpine structures, SW-vergent Dinaric structures have also been clearly distinguished in the field. The N-S oriented cross-sections in this report cut the area parallel to the dominant direction of Alpine movement and therefore provide clear insights on the pre-dominantly southward directed Alpine structures and the associated transport. As a consequence of the N-S oriented sections, the dominant SW-vergent transport associated to Dinaric deformation, is not clearly distinguishable from the S-vergent Alpine structures. The lack on a cross-sectional view parallel to the Dinaric transport direction, makes integration of map- and field-data, and data obtained from the kinematic models, essential, in order to provide a clear overview of both the Dinaric and Alpine phases.

6.1 Thin-skinned versus Thick-skinned deformation

Since it is one of the main objectives of this study to distinguish between the different styles of convergent deformation, thin-skinned and thick-skinned, it is first of all important get clear what the characteristics of these two styles are, in order to finally distinguish between them.

The general subdivision between thin- and thick-skinned deformation, as a result of collision related compressional stresses in the foreland of an orogenic wedge, is determined by the level at which decoupling takes place (formation of the décollement). Thin-skinned deformation is typically the result of a décollement at the level of the basement- (sedimentary) cover transition, whereas thick-skinned deformation is usually the result of decoupling within the basement of the upper crust, or within the lithosphere at even greater depth (Ziegler et al., 2002; Madritsch et al., 2008). The detachment of the sedimentary cover usually occurs along a gently dipping horizon of a rheological weak rock, often salt or shales, and deforms independently from the basement below. The basement rocks below this horizon are not affected by the deformation of the cover but become shortened elsewhere, usually closer to the more internal parts of the orogen (Chapple, 1978; Madritsch et al., 2008).

During Thick-skinned deformation, the contrary takes place and the basement together with the sedimentary sequence undergoes the deformation as a whole. For basement involved shortening in the foreland of an orogen, a crustal-scale décollement allowing the transmission of compressional stresses, is required (Coward, 1983). The angle of these thick-skinned thrusts is usually very steep and involve little horizontal displacement, in contrast to the generally gently dipping thin-skinned fault planes which accommodate great amounts of shortening. Crustal décollements occasionally ramp through the crustal sequence into shallower upper crustal levels or extend far out into the foreland and might cause inversion of sedimentary basins. In both scenarios, thick-skinned deformation is typically associated with the inversion of pre-existing structures in the crust (Chapple, 1978; Davis et al., 1983).

The pure thin- and thick-skinned tectonics represent the two extremes of a wide range of possible combinations lying in between (Pfiffner, 2006, p. 153). For a good understanding of the dynamics of foreland deformation, it is of great importance to unravel the interaction of thin- and thick-skinned tectonics in both space and time (Madritsch et al., 2008).

In conclusion, there is a large agreement in literature on the existence of two general classical styles of thrust tectonics, thin-skinned and thick-skinned. The thin-skinned, tectonic model involves thrust faults that flatten out at depth and join together in some sort of decoupling horizon, which works its way back by a staircase trajectory to the original source of the thrust movement (Coward, 1983). Since thin-skinned deformation is generally associated with low angle thrusting and relatively great amounts of displacement along décollement horizons, we expect to recognize this in the field by intensely deformed relatively soft layers situated in-between more rigid and less deformed sequences. The thick-skinned tectonic model typically involves high angle thrust faults, near vertical movement at depth and hence little horizontal displacement, the steep thrust presumable fade out in the brittle-ductile transition in the lower crust (Coward, 1983). Thick-skinned deformation is associated to inversion and transpressional structures (Chapple, 1978; Davis et al., 1983). Which we therefore expect to be recognizable in the field by different types of faulting, strike-slip, normal and thrusts faults, fitting to one transpressional stress regime, and by the presence of inverted structures. The high degree of vertical displacement is expected to be indicated by the exposure of material that was originally situated deep in crust, such as basement material initially underlying the sedimentary cover.

6.2 Shortening estimates and uncertainties

Generally, for any thin-skinned cross-section is the amount of shortening determined by the amount of area between the surface geology and the basal décollement, and the way this space has been filled. For instance, the area could be filled with duplicated sedimentary sequences, due to a ramp-flat style of thrusting, which would increase the amount of shortening in contrast to basement involved thrusting, which would significantly reduce the amount of shortening (Gotberg et al., 2010). Schönborn (1999) also recognizes this major uncertainty which has great consequences for the estimation of the shortening (fig. 46).

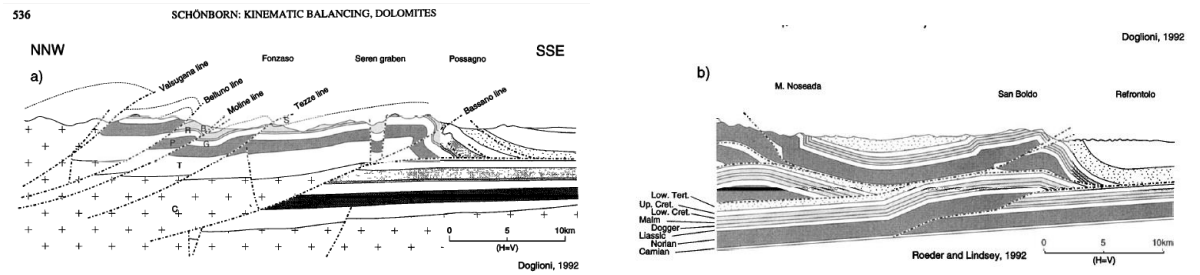

Figure 46. *Two different interpretations of the (sub)surface geology, a minimal shortening model and a maximal shortening model.* ***A)*** *No décollement at all, shortening is accommodate by basement thrusting. Redrawn by Schönborn (1999) after Doglioni (1992).* ***B)*** *An important décollement in the carnian horizon results in a stack of thrust sheets formed from the sedimentary sequence. Redrawn by Schönborn (1999) after Roeder and Lindsey (1992) .*

The main uncertainties for estimation of the shortening come from the following factors; décollement depth and the dip of the décollement, the amount of basement thrusts and unknown fault displacement (by absence of matching hanging wall and footwall cut-offs) (Gotberg et al., 2010).

A major uncertainty is the basal décollement depth and dip, since the choice for a décollement in the evaporitic sequence of the Bellerophon provokes a thin-skinned deformational response, which results in a greater amount of shortening than when the décollement would be situated at the brittle-ductile transition resulting in

a thick-skinned response. However, the last uncertainty, the amount of displacement along faults, is believed to have a great impact on the final shortening estimate as well. First of all because of the often unpreserved hanging wall cut-offs of multiple faults, which often results in a minimum estimate of displacement along such faults. And a second major uncertainty regarding fault displacement issues, is the footwall cut-off of the main basal thrust. This because the extent of the main basal thrust towards the North is unknown and a longer décollement would result in an even greater amount of shortening (fig. 47). The proposed present state situation, whereby basement material is exposed in the northern part of the area, allows multiple scenarios and does not exclude a longer basal décollement. This means that the estimated shortening of 57,2 km, obtained from the "Maximum shortening model", is in fact not fully constrained and that the total maximum shortening could be even more. Also should be taken into account that the length of the transect, used during this study, does not cover the full extent of the eastern Southern fold-and-thrust belt, since the northern end of the section could be extended for ~10 km further to the north to the Periadriactic fault and the southern end could be extended further southward towards the most frontal S to SW-vergent structures in the area.

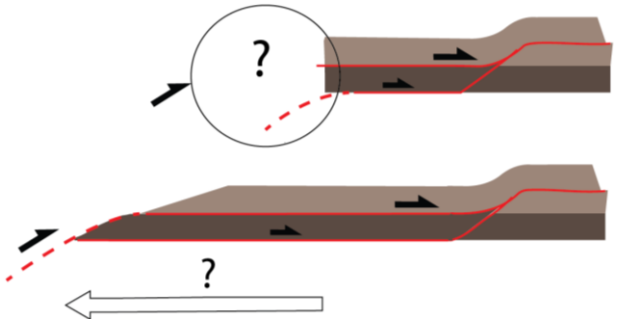

Figure 47. *The extent of the décollement faults in the Bellerophon and Raibl Formations is unknown, allowing multiple scenario and thus different shortening estimates. The uncertainty of the timing of the basement involved thrust, cutting through the basal décollement, leaves the possibility for scenarios with originally longer décollements open.*

Therefore the estimate of the maximal shortening model of 57,2 km of shortening in the Friuli Alps since the Miocene, is probably still an underestimation, which means an even further deviation from the interpretation of the 35 km of shortening proposed by Doglioni for the Italian Dolomites. Although this difference can probably not be attributed just to a lateral difference, it is important to keep in mind that the study of Doglioni focused on a different area, located kilometers west of the Friuli Alps, and can therefore not be compared too strictly. The shortening estimate of Schönborn (1999) and Nussbaum (2009) of ~50 km along a 66 km long section is more consistent with the 57,2 km proposed by the maximal shortening model of this study. However 50 km it is still considered to be at the lower end, especially since the 57,2 km is regarded as a minimum shortening estimate.

Can WSW to SW-transport be projected in a N-S (NNE-SSW) section?

As discussed before, is the ideal strike of a transect parallel to the transport direction in order to express the deformational structures optimally. In the case of the Friuli Alps, which is a rather complex area where two different compressional phases with almost perpendicular directions of transport have occurred, Schönborn proposed an approach in which each event is examined separately, by use of two distinct sections. One running parallel to the Dinaric direction of transport, and one running parallel to the Alpine direction of transport. As this research only includes a N-S striking cross-sectional view through the area, it is questioned here if this N-S striking viewpoint can be of value for insights in the WSW- to SW-vergent Dinaric evolution?

Could the early WSW to SW Dinaric-movement be represented in the N-S kinematic model, or are the kinematic insights display by the forward modeling purely restricted to stages from the Alpine evolution? If Dinaric phases are included in the kinematic model, it would mean that the Southward transport, during the first stages of the kinematic model, is in fact an apparent southward transport and in reality a more SW directed transport (fig. 48C). Kinematic field data indicate WSW- to SW directed transport over two main

décollements, the Bellerophon and Raibl formation, and thus supports the interpretation of a thin-skinned Dinaric phase of deformation. However, it is unlikely that this WSW to SW-vergent phase is displayed in the N-S section, especially when the amount of shortening emerging from the model during this phase is considered. The first two stages in the model account for ~45 km of shortening, which would mean that if this would be an apparent amount of shortening, the true amount must be even more after correction. Also considering that the true fault angles would have unconventional steep orientations, it is more likely that the kinematic evolution, as displayed by the forward modelling in MOVE, is strictly a representation of the S- and SE-vergent D3 and D4 deformation stages rather than the (WSW) SW-directed D2. Which was in the first place already strongly indicated by field data, for instance by the frequent occurrence of large scale S-vergent D3 thrusts in the area and the absence of large scale (map-scale) WSW to SW-directed thrusts.

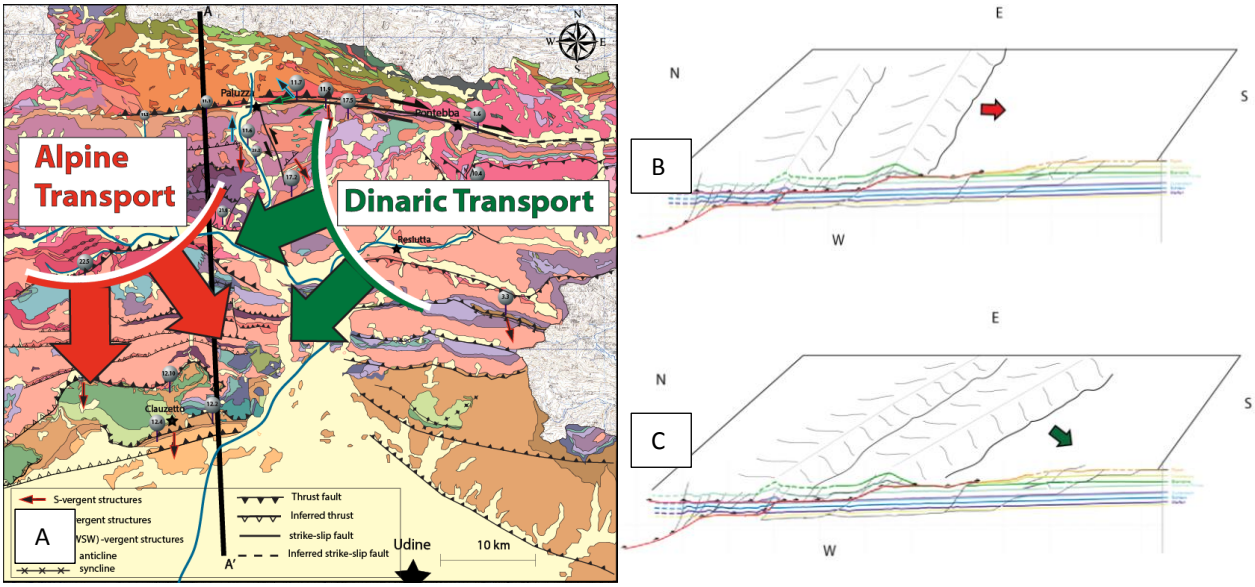

Figure 48. A) *The map illustrates the main directions of transport associated to the Dinaric and Alpine system. The section line runs more or less parallel to the mainly Southward direction of Alpine transport, but makes a great angle (nearly perpendicular) with the Dinaric direction of transport.* ***B)*** *This 3D sketch illustrates how the cross-section view cuts through the Alpine structures, more or less parallel to the Southward direction of movement.* ***C)*** *A 3D sketch of how the cross-section would cut through SW-vergent Dinaric structures.*

6.3 Neogene shortening and shortening constraints

Current discussions revolve around the amount of shortening since the Miocene in the eastern Southern Alps. Doglioni (1987) proposes 5 km of shortening for the sedimentary cover of the Dolomites during the NNW-SSE compressional regime. Whereas Nussbaum (2002) estimates the macro scale shortening in the eastern Southern Alps to be 50 km since the beginning of the Late Miocene.

The structural study of Castellariin and Cantelli (2000) estimates the total shortening of the Valsugana and Montello belts, which are believed to be the corresponding structures of the D3 structures, in the order of 35 km or more (Castellarin et al., 1998; Castellarin and Cantelli, 2000), which is significantly lower than the at least 45 km of shortening during D3 deformation indicated by the kinematic model in this research. However, there is an agreement that this phase is responsible for the greatest amount of shortening in the eastern Southern Alps (Caputo, 2010; Castellerain & Cantelli, 2000).

From the kinematic model it is clear that the majority of the total shortening is accommodated during the D3 thrusting & folding phase, which amounts to at least 45 km and possible more, of the in total 57,2 km of shortening. Despite the match between the characteristics and orientation of the D3 structures and the

corresponding structures of the SSE-vergent thrust systems described by previous work (Doglioni, 1978; Schönborn, 1999; Castellerain and Cantelli, 2000; Nussbaum, 2002), there is a clear deviation when it comes to the amount of shortening. The reason for this is almost certainly the lack of basement involved thrusting in the kinematic model during the D3 phase. These previous studies propose a thin-skinned style of thrusting which is expressed by three in sequence thrust-systems. These three systems however, have all three their own basement unit which limits the amount of shortening substantially.

The interpretation of the field data gathered during this study however indicate the presence of a large basal décollement in the Bellerophon Formation at the sedimentary cover – basement transition. The multiple thrusts, which are believed to be in fact all splays from one large thin-skinned thrust-system, all join in the basal thrust, which finally ramps through the complete sedimentary sequence via a staircase trajectory in the foreland. A subsequent phase of thick-skinned deformation involves the deeper situated basement in the Alpine deformation and reactivates some of the existing structures but also cuts through and displaces some others. However, this idea, which validity has been tested by balancing and forward modeling by means of MOVE software, is not yet constrained due to the uncertainty regarding the extent of the basal décollement as mentioned in an earlier chapter of this report. In order to constrain the maximal amount of shortening, other methods must be used.

The full extent of the eastern Southern Alpine fold-and-thrust belt (with the PA as northern boundary) exceeds the length of our cross-section by ~10 km. Which means that the maximal length of the basal décollement would probably also exceed another 10 km towards the north (fig. 49). For the Southern end of the transect, it is the décollement at the level of the Eocene flysch, that exceeds the range of the cross-section. Based on the most frontal fault structures indicated by the geological map, the maximal extent of the décollement in the Eocene flysch is estimated to exceed the cross-section by ~5 km (fig. 49). This would add a total of 15 km to the length of two main décollements in the cross-section, which means that if we assume the same percentage of shortening (51%) for this new length, the shortening would amount 73,2 km for the full extent of the eastern Southern Alpine fold-and-thrust belt. However, as indicated by multiple cross-sections, including the TRANSALP transect and the EASTERN ALPS transect (fig. 4) by Schmid et al. (2004), increases the thickness of the crustal wedge towards the internal part of the belt in the north, which means there is more space available for the stacking of crustal slices in the 10 km long area between the northern end of our cross-section and the Periadriatic Fault than previously assumed. Schmid et al. (2004) estimates the upper-crustal Southern Alpine retro-wedge to be 10-15 km thick. Due to the increasing thickness towards the internal parts of the belt, we assume 15 km for the thickness of the northern part (the added 10 km) of the crustal wedge, which results in a maximal shortening estimate of 78,4 km for the full extent of the Southern Alpine thrust belt.

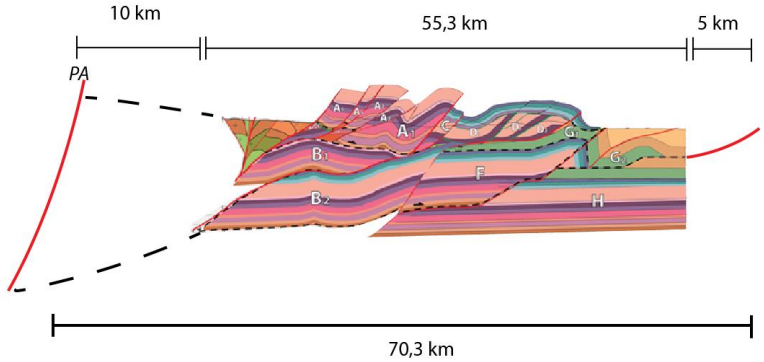

Figure 49. *The maximal shortening model (55,3 km) does not cover the full extent of the Southern Alpine fold-and-thrust belt. The Periadriatic Fault exceeds the model with 10 km, and the most frontal thrust is located 5 km South of the southern end of the cross-section. The thickness of the crustal wedge increases up to 15 km towards the internal parts of the belt, which results in a maximal shortening estimate of 78,4 km for the eastern Southern Alps.*

6.4 Data interpretation and correlation

In the following chapter, the different types of data (field data, insights from the kinematic model and data from previous research) will be interpreted and linked together to provide a new and complete overview of both the Dinaric and Alpine deformational evolution in the Friuli Alps since the Eocene.

The integration of various kinds of data has the advantage that it enables us to examine and express each aspect of the geological evolution in an obtimal way. The kinematic model for instance provides a perfect view for distinghuishing stages of thin-skinned and thick-skinned style of deformation, and is capable of showing the structural evolution of the area in a orderly way. However, the characteristics of the structures and their exact orientation and indicated direction of movement, is not clear from the models view and is in turn much better constrained by field measurements and observations (D1 – D5). And for organized overview of the main orientation of the sturctures, and their spatial distribution in the area, is the geological map most convenient.

After the interpretation and integration of these different types of data, our interpretations are compared to the findings from previous research. Correlation with the absolute dated eventes/sediments from other reporst enabled us to put absolute time constraints on the deformational events (D1 – D5. This, and further discussion on important similarities and/or differences regarding the structural evolution of the eastern Southern Alps as proposed by other research papers, will be adressed in the last following paragraphs.

Figure 50 below shows an event chart with the main tectonic events, from Early-Jurassic till recent time, affecting the eastern Southern Alps. New structural data, gathered during this study, is added to the figure and will form the basis for a new interpretation of the structural evolution of the eastern Southern Alps since the Eocene. The absolute timing of the D1- D5 deformation structures has been determined by correlation with the corresponding events described in earlier publications.

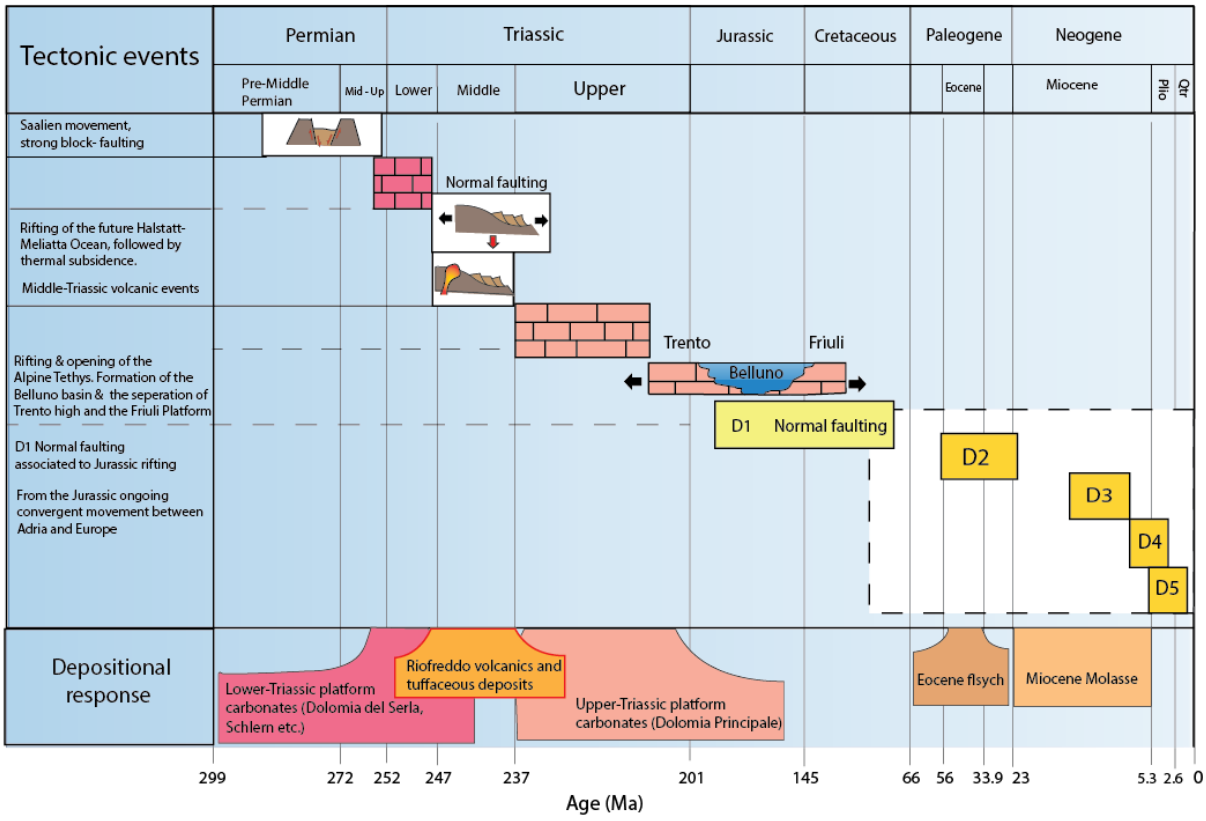

Figure 50. *Event chart of the tectonic evolution since the Permian in the eastern Southern Alps. The sequence of tectonic events is modified after Nussbaum (2002). The dashed box in the lower left corner is enlarged on the next page and provides an detailed overview of the ongoing convergent movement in the eastern Southern Alps since the Jurassic*

6.4.1 Pre-convergent structures (Pre-Paleogene evolution)

The D1 normal faults are not shown on the geological map, or in the cross-sections because of the limited number of D1 structures encountered and the occurrence of only small-scale (outcrop-scale) structures. It is determined that the D1 structures pre-date the main convergent evolution, of the eastern Southern Alps. And since the main focus of this study lies with the amount of shortening since the Eocene, the small scale pre-existing extensional structures of the D1 phase, are considered to be relatively unimportant. However, because these small scale structures may reflect large scale extensional structures which actually could have affected the course of the subsequent convergent phase, the D1 and possible associations with recorded tectonic events, are briefly discussed in the first paragraph of the geological history chapter.

D1 - Triassic and Jurassic extension and normal faults

Small scale D1 normal faults with unconventional fault plane angles are exposed in the Lower-Triassic Werfen and lower Upper-Triassic Val Degano Formation. The unconventional steep and low angles (0° - 30° and 70° - 90°)have been interpreted as the result of an extensional phase pre-dating the tilting of the bedding. Two extensional events have been mentioned by previous research and are related to the Triassic rifting phase and Early-Jurassic rifting associated to the opening of the Alpine Tethys.

The Middle-Triassic rifting phase, associated to the evolution of the passive margin of the Hallstatt-Meliata and Vardar oceans (Nussbaum, 2002; Ziegle, 1989; Stampfli et al., 1991), caused a large scale syn-sedimentary environment where E-W trending normal faults developed. The Middle-Triassic normal faults have previously been described by Nussbaum (2002) as growth faults, which are not easily recognizable in the field since they are only indicated by thickness variations in the post-tectonic sedimentary cover. Considering the deviant structural characterization and orientation of the Middle-Triassic normal faults with respect to the rather small scale (cm-dm scale) NE-SW oriented D1 normal faults, correlation between the Middle-Triassic rifting stage and the D1 normal fault is very unlikely. And moreover, the Middle-Triassic extension pre-dates the lower Upper-Triassic, D1 structures bearing, Val Degano formation, which fully excludes correlation between the D1 normal faults and the Middle-Triassic rifting stage.

The Early-Jurassic rifting is well documented by growth faults indicated by abrupt thickness variations in the Lower Jurassic syn-sedimentary strata, and also by the local accumulation of breccia material (Nussbaum, 2002). Doglioni (1987) also describes a phase of Jurassic extension involving tilted blocks causing angular unconformities in the Jurassic sediments and relates large scale N-S striking normal faults to the Jurassic extension.

Although the orientation of the D1 normal faults is not entirely in agreement with the, by Doglioni (1987) proposed, N-S oriented extensional Jurassic structures, it is likely that these are related. Also because of previously interpreted seismic data (Cati et al., 1987) indicates an intermediate basin separating the Friuli platform in a southwestern and northeastern part (Schönborn, 1999) indicating NE-SW extension (fig. 51).

The NE-SW extension, indicated by boudinaged structures in the Raibl Formation, point out strongly in the direction of a relatively early phase of NE-SW extension, because of the required minimum depth for such structures to form (10 km). Therefore, it is excluded that the NW-SE oriented structures, the high angle normal faults and the boudinaged structures, are in fact, deviant D5 transtensional structures, since this deformation phase took place late in the deformational evolution and thus at a too shallow depth. Another indication is the observed inversion of some of the normal faults, indicating an extensional phase pre-dating the convergent movement responsible for the inversion.

In summary, the NW-SE orientation of the D1 structures is not entirely in accordance with the N-S orientation registered by Doglioni in the adjacent Dolomites but are in accordance with the NE-SW Early-Jurassic extension, indicated by an NW-SE striking basin separating the Friuli platform (Cati et al., 1987; Schönborn, 1999). Nussbaum (2009) as well indicates describes a two-split of the Friuli Alps by a N to NNE trending normal fault of Early-Jurassic age. Along with the exclusion of correlation with the Middle-Triassic rifting, due to the previously discussed constraints, and the strong indications for extensional deformation prior to compressional deformation, correlation of the D1 extensional phase with the Early-Jurassic rifting, is favored.

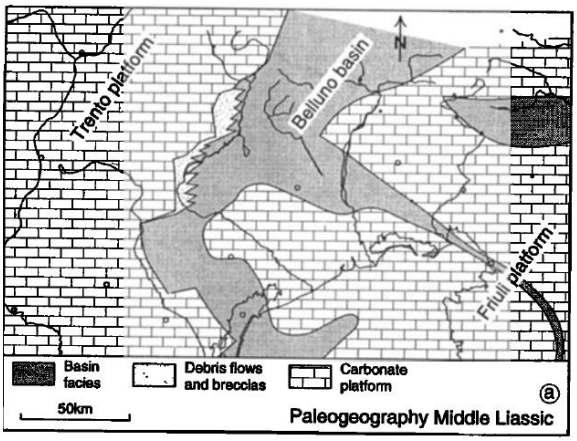

Figure 51. *An intermediate basin separates the Friuli platform into a northeastern and a southwestern part during the Early-Jurassic (modified after Bosellini et al., 1981; Cousin, 1981; Cati et al., 1987 and Schönborn, 1999).*

6.4.2 Cenozoic convergent evolution of the Friuli Alps

The absolute timing of the convergent evolution, phases D2 - D5, is determined by correlation with tectonic events and by information provided by the depositional response. Both data from precious research as well as new data collected during this research have been used.

The figure 52 below shows the event chart of the tectonic evolution from the Eocene onward. The timing and characteristics of the different phases will be discussed in the following chapter.

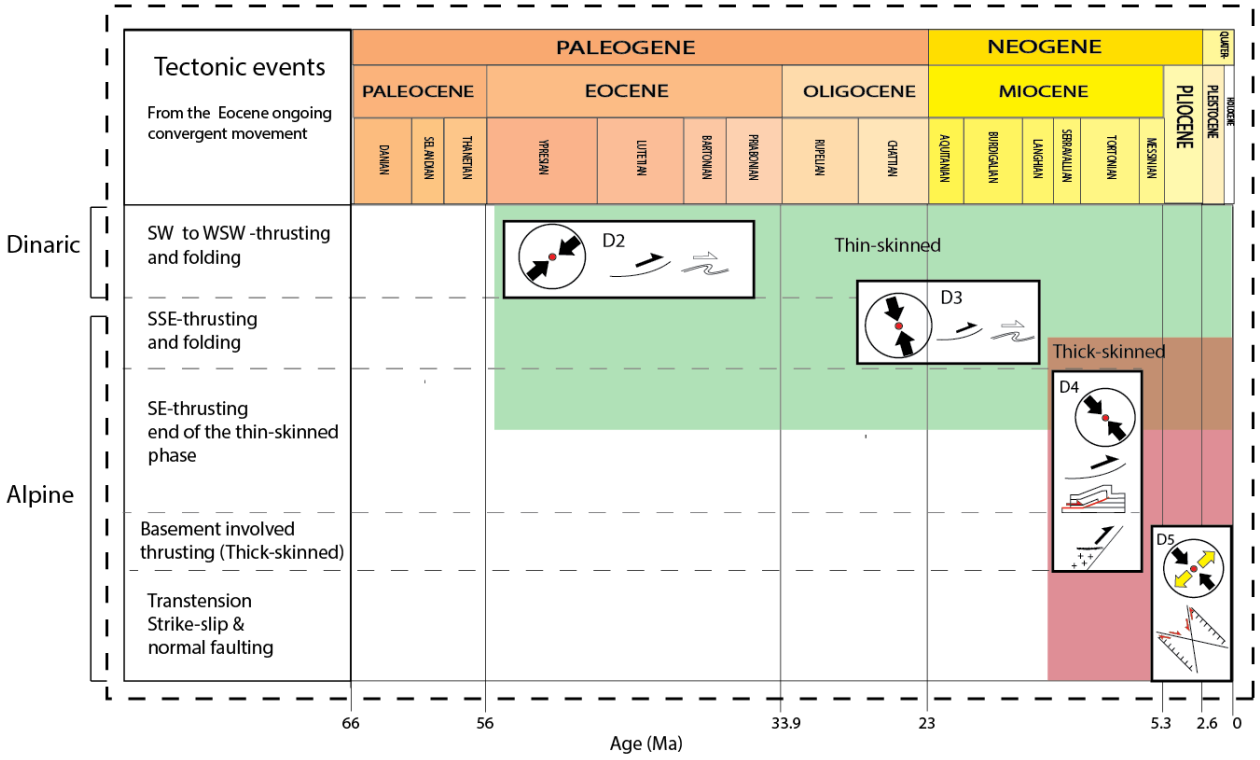

Figure 52. *Event chart of the Tectonic events since the Eocene encountered during this research in the western part of the Friuli Alps.*

D2 – Dinaric shortening
Late Paleocene (59,2 Ma) to Early Miocene (16 Ma)

From the map view it is clear that the exposure of large scale NW-SE striking Dinaric structures is very scarce in the Friuli area. Evidence of large scale SW to WSW-vergent structures is only found in the foreland flysch in the eastern part of the area (fig. 53). These thrusts have an overall NW-SE orientation in contrast to the ENE-WSW striking Alpine thrusts in the both the eastern and western part of the area. Another notable observation is that the eastern part contains a number of N-vergent thrusts, or back-thrusts, as opposed to the western part where only S-vergent thrusts have been encountered.

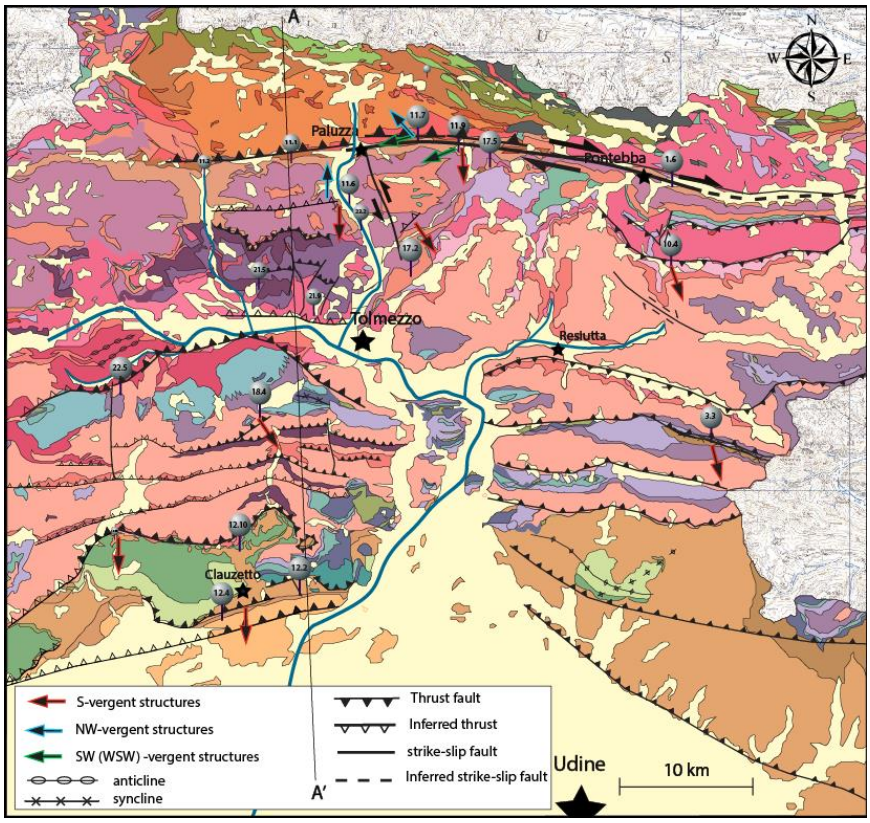

Figure 53. *Geological map of the Friuli Alps. The western part of the area consists exclusively of S-vergent thrusts, while the eastern part shows both S- and N-vergent thrusts. The foreland flysch and molasses sequences in the east expose NE-SW oriented, Dinaric-strike, structures in contrast to the almost exclusively S to SSE-vergent structures in the western part.*

The geological map already indicates, that S-vergent structures predominate in the area, and trackable large Dinaric structures are scarce, is also confirmed by observations and measurements from the field. Apart from the D1 extensional phase, all phases are associated with convergent stress regimes. The eldest convergent deformation phase determined during this research is the D2, which comprises NE-SW shortening and is probably associated to the overall SW-vergent Dinaric deformation affecting the area from the East. D2 structures are observed in four relatively "soft" formations, the Bellerophon, Werfen and Buchenstein and Raibl Formation, which strongly suggests that these were in fact former décollement horizons. The scale of the D2 structures is relatively small, especially when compared to the 30-40 meters wide fault zones associated to the D3 southward thrusting.

The influence of, predominantly Eocene, shortening in the External Dinarides on the Southern Alps, prior to the mainly N-S directed Alpine stages, is widely mentioned in previous studies on the Italian Dolomites (Doglioni, 1987) and eastern Southern Alps (Nussbaum, 2002) and is the oldest deformation during the Cenozoic evolution recorded in the area. The observed (W) WSW- to SW-vergent D2 structures are consistent with the Paleo-Alpine phase, previously described by Doglioni (1987), with W to WSW-vergent thin-skinned thrusts with

detachment horizons in the evaporites of the Bellerophon Formation, the Werfen, and the Lusnizza Formations in the west and the Raibl Formation farther east. Also Nussbaum (2002) describes a dominant SW-directed Dinaric deformation, which has had substantially affected the easternmost part of the Southern Alpine belt, and reaches till the central Dolomites where Dinaric thrusts are still well preserved despite the subsequent Alpine deformation. However, the majority of these structures have been overprinted by the Alpine phases, resulting in the discontinuation and local rotation of Dinaric structures (Doglioni, 1987). Field observations collected during this research support the interpretation of severe overprinting of pre-existing Dinaric structures by subsequent S-directed Alpine deformation. The overall top W to SW D2 shearing (fig. 54) indicated in both the Bellerophon and Raibl formations have been interpreted as the relics of former Dinaric décollements for the overall WSW- to SW- transport of the overlying strata by means of a thin-skinned fault system. However, the lack of map-scale, trackable D2 structures in the field, and the wide range of the Dinaric directions, SW to W- directed (fig. 54), indicate severe overprinting by subsequent deformation phases and consequently local rotation of Dinaric structures.

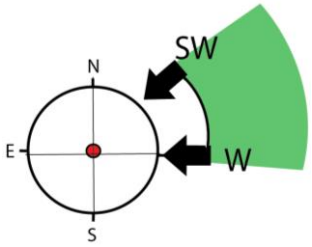

Figure 54. *Overview of the range of Dinaric directions found in the area.*

Nussbaum (2002) argues for two décollements for the SW-directed Dinaric transport, the Bellerophon gypsum and the Upper-Jurassic to Lower-Cretaceous Biancone Formation. New field observations gathered during this study show evidence for SW- to WSW- directed Dinaric transport along three décollement levels, in the Bellerophon, Raibl and Biancone Formation. The strongly deformed décollements indicate a thin-skinned style of deformation with flat-ramp thrust systems prior to the dominant south directed Alpine deformation.

Despite the large agreement on directions and characteristics of the Dinaric transport, as described by previous researchers, and the new field evidence gathered during this research, is the generally proposed amount of Dinaric shortening in the eastern Southern alps rather low.

Doglioni (1978) proposes an amount of at least 10-11 km of shortening (15%) along a 70 km long E-W section through the Dolomites, formed due to an E-W (ENE-WSW) compression possibly related to the folded foreland of the Dinaric chain. However, regarding the thin-skinned nature of the Dinaric deformation, which is typically associated with a high degree of horizontal displacement, we suspect a larger amount of Dinaric shortening in the eastern Southern Alps. However, since this the Dinaric transport have only been examined by means of field observations and not by the construction of a Dinaric (NE-SW) cross-section or a Dinaric kinematic model, no proper conclusions on this topic can be made.

The onset of the Dinaric deformation is roughly indicated by the Dinaric flysch deposits which were deposited onto the Friuli platform from the East. The first appearance of Dinaric flysch deposits varies from Thanetian age (59,2 – 56 Ma) in the NE of the Friuli platform, to uppermost Lutenian (47,8 – 41,2 Ma) in the SW (Cousin, 1981; Nussbaum, 2002). The subsequent deposition of Dinaric molasses sediments continued till the Early Miocene (23 – 16 Ma) before the sedimentation area was integrated in the newly, northward thickening, Alpine foredeep which formation started during the Middle-Miocene (16 – 11,6 Ma). Cross-cutting relationships clearly indicate the predating of the Dinaric structures, which constraints the absolute timing Dinaric D2 phase to be between Late Paleocene (59,2 Ma) to Early Miocene (16 Ma).

6.4.3 Alpine Neogene deformation, D3, D4 and D5

Both Castellerain and Cantelli (2000), and Caputo (2010) describe four main tectonic events during the Neogene in the eastern Southern Alps. However, Caputo distinguishes 4 sub-events within the fourth event during the Pliocene-Pleistocene interval referred to as “tectonic pulses”. These tectonic pulses will be discussed later on in this section because of the possible correlation with the minor thrusts in the flysch and molasse of the Southern Alps.

The forward modeling stages in MOVE clearly indicate a pre-dominantly thin-skinned deformational response, especially in the early stage of the overall N-S shortening. Since Dinaric thrusting is not included in the cross-sectional view, the kinematic model indicates a Neogene deformation accounting for a minimum amount of 57,2 km of shortening.

The first event in the Neogene is commonly referred to as the Insubric event (or Chatian – Burdigalian event) which mainly affected the northern area of the eastern Southern Alps and the nowadays central and foreland areas, the Veneto and Friuli areas, which represented during that stage a distal foreland basin (Caputo, 2010; Fatoni et al., 2002). Caputo (1996) makes a distinction between the early, Eocene age, Dinaric system with NE-SW shortening, and a late Dinaric system with NNE-SSW directed shortening during Chatian to Burdigalian time. Fission-track analyses indicate a cluster of exhumation ages between 21.7 (±3.4) Ma and 16.5 (±1.0) Ma. (Monegato et al., 2010). However, this late Dinaric event is not clearly registered during this study, which is possible explained by the focus of this research lying with the central and frontal regions of the eastern Southern Alps instead of the more internal regions in the North. The table below (fig. 56) indicates the main deformation phases distinguished in the Southern Alps (Castellerain & Cantelli, 2000; Caputo, 2010) correlated with the D3, D4 and D5 phases from this research.

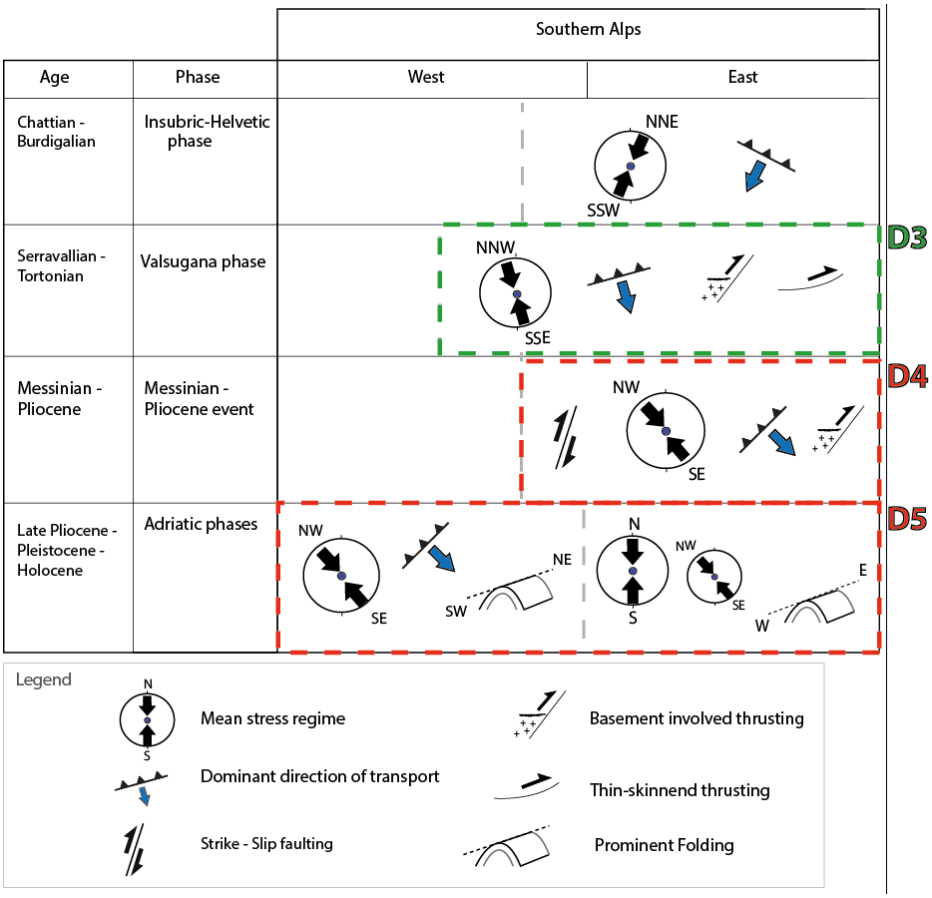

Figure 56. *Overview of the different directions of shortening in the Southern Alps modified after Castellarin and Cantelli (2000).*

D3 – Middle-Late Miocene (13,8 – 7,2 Ma) N-S Alpine shortening (Thin-skinned)

The D3 structures encountered in the field include large scale thrust faults, hectometer scale E-W oriented anti- and synclinal structures and dm-m scale E-W oriented asymmetric folds, all indicating Southward movement. The dm-m scale folding is in particular encountered in the Bellerophon, Raibl and Biancone Formations, which are therefore the proposed main décollements for the S-vergent movement of the D3 phase. In the frontal part of the belt, the Eocene Flysch acts as a fourth décollement horizon for the southward movement. The near vertical bedding planes of the flysch of stop 12.4 for example strongly indicate a footwall syncline of one of the large frontal S-vergent thrusts in the area. A minor D3 décollement is indicated by the consistent asymmetric folding expressed in outcrops of the Buchtenstein Formation, indicating an overall Southward direction of movement.

The majority of the large scale brittle fault zones is encountered in the Upper-Triassic Dolomia Principale, and is linked to the D3 S-vergent ramp-thrusts. The brittle fault zones in the carbonate formations indicate the places where the thrust faults ramp through the rigid carbonate body, while in the "softer" formations the southward movement is expressed by small scale S-vergent structures like; asymmetric folding and kinkbands, semi-brittle top south shearing and cm-scale thrust faults (fig. 57).

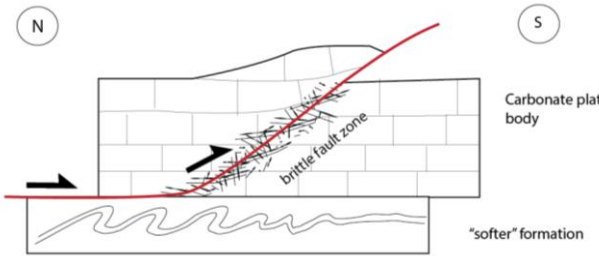

Figure 57. *Sketch illustrating the relationship between the small scale, cm-m scale, structures in the "softer" formations and the large scale cataclastic fault zones in the carbonate platform formations.*

The kinematic model clearly shows the three, and at a later stage, four décollement levels involved in the D3 thin-skinned thrusting (fig. 49). The D3 convergence is accommodated by one fault system, which has its basal décollement in the Upper-Permian evaporitic sequence of the Bellerophon Formation. However, the first phase of shortening is accommodated by the detachment of the Upper-Triassic platform formations, by a large décollement thrust in the Raibl Formation. It is believed that this décollement thrust is the most frontal splay of a previously in sequence formed thrust system located closer to the internal part of the orogen in the North. The southward movement of the associated thrust sheet of this system is the driving force behind the transport of the Upper-Triassic carbonates. Due to subsequent thick-skinned thrusting (D4), the most internal thrust sheet, becomes vertically uplifted and, therefore, subjected to intense erosion.

The forward modeling in MOVE gives insights in the kinematic evolution of the D3 thrusting, which indicates an in-sequence propagation of thrusts towards the south. Shortening is firstly accommodated by the southward displacement of the detached Upper-Triassic and Jurassic formations along a ~45km long décollement at the level of the Raibl Formation. While this main thrust ramps through the Triassic sequence and evolves further along the second décollement in the Upper-Jurassic to Lower Cretaceous Biancone Formation, substantial displacement along the secondly formed lower splay, at the level of the Bellerophon, initiates and starts the emplacement of the first thrust-sheet (Block-A).

The timing of the displacement of the basement material, which is presently exposed in the northern part of the area, remains unknown. The earlier presented kinematic model indicates a scenario where the basement is displaced during the creation of the large basal thrust, which means that it has always been attached to thrust-sheet A and only got uplifted to the surface during a late stage of thick-skinned deformation (D4). This scenario is followed to obtain the minimum shortening estimate of 57,2 km. Other scenarios, involving a longer basal décollement and a later phase of basement emplacement, could increase the amount of thin-skinned shortening significantly (up to 78,4 km).

The possibility of a longer basal thrust in the lowermost décollement makes a strict constraint of the amount of shortening impossible. However, it can be stated that the Neogene deformation accounts for a minimum amount of 57,2 km of N-S shortening (Dinaric thrusting is not included), of which the majority (~45-50km) is accommodated during the D3 thin-skinned thrusting and folding phase during the Middle-Late Miocene.

The second tectonic event in the Neogene, mentioned in literature, is the so called Valsugana (or Serravallian-Tortonian) event, which involves new southward thrusting including the Valsugana and Belluno thrusts (Castellerain et al., 2006). As shown by the table above, we correlate the D3 structures with the SSE-vergent structures associated to the Valsugana compressional event during Serravalian to Tortonian time. This interpretation is well supported, considering that besides the corresponding paleostress direction (NNW-SSE), also the scale and geometries of the structures is in agreement. The ramp-flat geometries, frontal splays and SSE-directed slip and the associated large amount of shortening, described by Caputo 2010 (and references therein), is in agreement with the field observations of large scale E-W striking, sub-horizontal fault zones, where structures in the surrounding formations strongly indicate overall S-directed movement. Ramp-flat style of deformation along multiple décollement levels in southward direction, is also clearly indicated by the kinematic model (fig. 54). D3 décollements have been found in the evaporitic sequence of the Bellerophon Formation, the alternations of marls with thinly bedded limestones in the Raibl Formation, the marls and limestone beds of the Biancone Formation and in the Eocene flysch deposits.

D4 – Late Miocene – Pliocene (7,2 – 2,6 Ma) NE-SW Alpine shortening (Thick-skinned)

The SE-directed thrusts planes and the refolding of N-S plunging folds, strongly indicate SE-vergent thrusting subsequent to the main S-vergent phase (D3). The encountered NE-SW striking thrust planes are of dm-scale up to several meters, usually with a cm - dm scale offset, which is relatively small compared to the large scale fault-zones and large offsets associated to the D3 thrusting. The relatively less prominent deformational expression at the surface and the relatively late timing of the D4, fit to a thick-skinned style of deformation. The insights from the forward modeling strongly indicate a late phase of basement involved thrusting, subsequent to the thin-skinned D3 phase. The reactivation and rearrangement of pre-existing structures, and the brought-up basement material and former thin-skinned décollements, fit to the general thick-skinned tectonic model which usually involves high angle thrust faults, near vertical movement at depth and hence little horizontal displacement (Coward, 1983). The high angle basement thrusts may ramp up into pre-existing thin-skinned décollements and may partly reactivate these structures, which is regarded as a common result of thick-skinned deformation (Lacombe & Mouthereau, 2002; Ziegler et al., 2002; Pfiffner, 2006). The relatively great amount of vertical displacement is indicated by the exposure of basal décollement levels (Bellerophon outcrops in the Northern part of the area) and crystalline basement material which originally underlie the sedimentary cover, is now exposed at the surface in the Northern part of the area, close to the Italian-Austrian border.

The reactivation of pre-existing structures, such as D3 fault planes, instead of creating new fault structures, might explain the restricted expression of the NW-SE oriented faults in the surface geology, however there are multiple example of NE-SW plunging fold axes. As described by Molinaro et al. (2005) it is a common characteristic of thick-skinned deformation to initiate during a late stage of deformation and to follow initial thin-skinned tectonics, resulting in refolding of shallow thin-skinned thrust nappes.

The paleostress directions indicated by the D4 structures are NE-SW oriented, which is in accordance with the Messinian-Pliocene event (Castellarin et al., 1992) or “Adriatic” event (Castellarin et al., 2006a). The Messinian-Pliocene structures are related to late post-collisional neo-Alpine evolution of the Adriatic-Po plain compressional events. Castellerain & Cantelli (2000) described strong reactivations and consequently rearrangements of pre-existing structures in the frontal zones of the Friuli region. Which is in line with new field observations, insights from the kinematic modelling and common attributes with thick-skinned models

described in literature. Therefore the D4 phase has been interpreted as a phase of thick-skinned deformation in a NW-SE directed compressional regime.

D5 - Tranpression, strike-slip (NNW-SSE) & normal faulting (NNW-SSE)

The D5 is widely observed throughout the entire Friuli Alps. On the larger scale (map-scale) it is mainly strike-slip deformation (NW-SE to N-S oriented planes) that has affected the area, while normal faulting (NNW-SSE oriented planes) is particularly represented by relatively small scale structures. The D5 phase is also characterized by the reactivation of older structures. Various outcrops have been encountered which indicate the strike-slip reactivation of large thrust faults, resulting in large brecciated zones, with often non-consistent kinematic directions. These zones often contain the so called mirror planes, eye-catching smooth surfaces which presumably represent intensely polished paleo-fault surfaces.

From the field it is clear that the D5 structures cut through, or reactivate all other structures, which puts them last in the deformational evolution. In the kinematic model however, is this phase not clearly expressed, due to the oblique orientation of the D5 structures with respect to the section line. Further interpretation of the D5 phase is therefore entirely based on the field observations only.

In the northern part of the area, a large scale E-W shear zone with a dextral displacement is exposed and has clearly affected the surrounding area. The relative orientation of the NNW-SSE oriented strike-slip planes and the large dextral E-W trending shear zone in the northern part of the area, correspond very well to the general fault configuration of a dextral transpressional system (fig. 58). This fault zone is therefore considered to be a Riedel of the Periadriac fault, the so called Fella Sava fault. The general orientation of the smaller strike-slip structures corresponds to the orientation of the R' shears, which are related to R-shears, which in turn are related to the large scale dextral E-W oriented transpressional system (fig. 59).

Therefore the is the D4 interpreted as the late transpressional response to the continuing NW – SE (NNW-SSE) thick-skinned deformation (D4) due to the ongoing convergent movement between Europe and Africa. The compressional to transpressional reactivation, and inversion of pre-existing crustal discontinuities, by thick-skinned deformation is after all a common feature (Lacombe and Mouthereau, 2002; Ziegler et al., 2002; Pfiffner, 2006).

Concerning the timing constraints for the D5 phase, no clear field indicates were found for the exact onset of deformation. However, since the overall dextral strike-slip deformation is related to the Fella Sava fault and the Periadriatic fault, can these structures be used in order to constrain the timing of the D5 phase. Fodor (1998) did research after the Miocene to Pliocene tectonic evolution of the Slovenian Periadriatic fault and reports a first transpressional event, corresponding to the first phase of lateral extrusion of the East Alpine-Western Carpathian-Northern Pannonian block, during the Early-Miocene (24 – 17,5 Ma). And a second phase of dextral strike-slip is related to a Late Miocene phase of extrusion (Fodor et al., 1998). Castellarin & Cantelli (2000) describe NW-SE sinsistral transfer faults that are in contact with Messinian-Pliocene syntectonic clastic sediments associated tot the Montello-Friuli thrust system. The internally deformed conglomerates of the S. Bartolomeo Hill have been uplifted along with their marine Pliocene cover, which constraints the age of deformation on Messinian – Pliocene (7,2 – 2,6 Ma), the same age as the thrust system responsible for the syntectonic sediments. Based on this information, the D5 structures are likely to be formed in the time span from Early Miocene to Pliocene time (24 – 2,6 Ma).

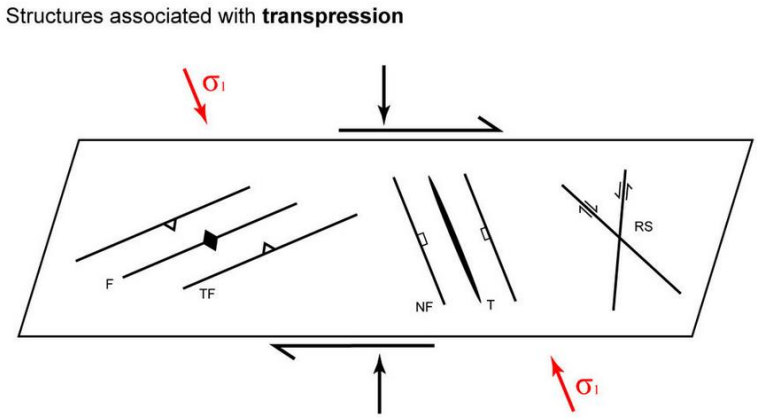

***Figure 58**. **A)** Schematic illustration of the different structures and their orientations within one stress regime. The main direction of compression indicated by the red arrows and the extensional directions by orientation of the normal fault symbols (after the transpression model by Sanderson & Marchini, 1984).*

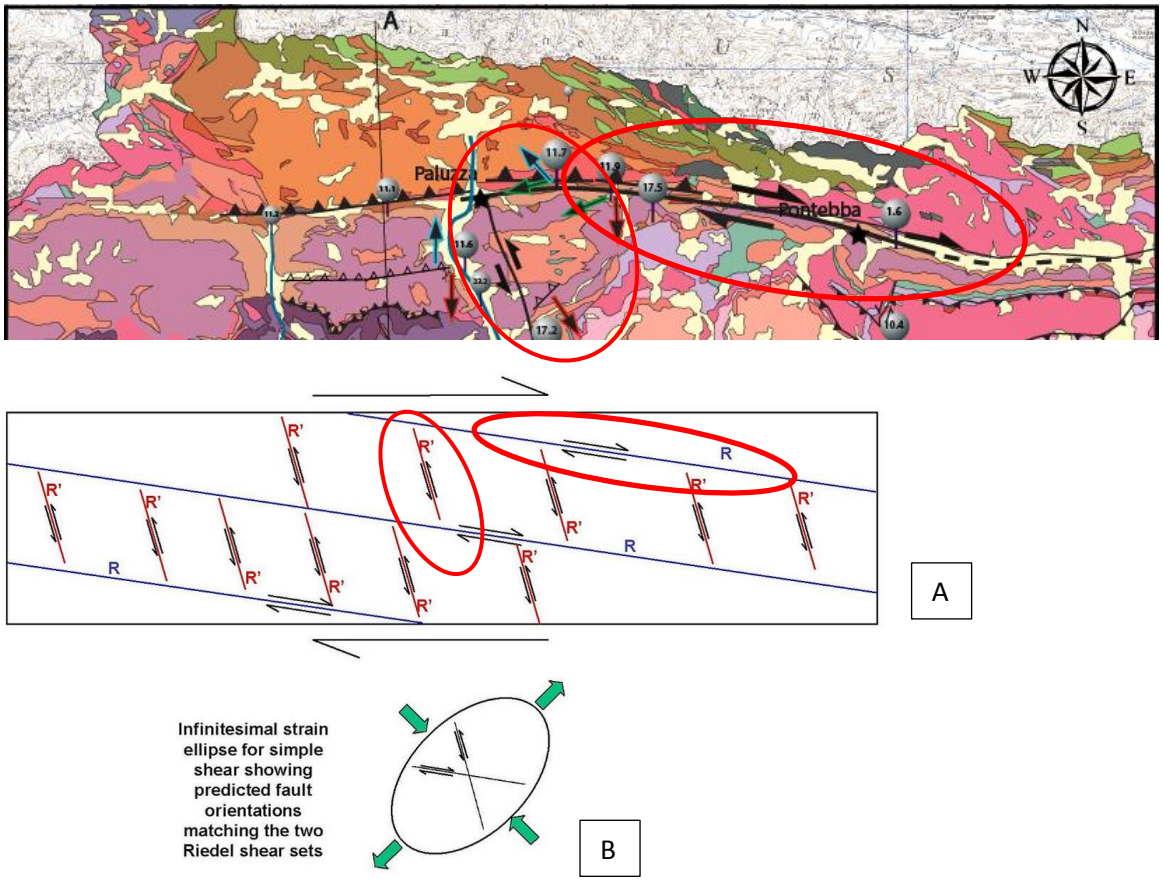

***Figure 59. A)** The northern part of the geological map is shown in order to indicate the large E-W dextral strike-slip fault in the area. The smaller NNW-SSE striking strike-slip faults have been interpreted as being the R'-shears of the large dextral E-W strike-slip regime. **B)** Infinitesimal strain ellipse for simple shear showing predicted fault orientations matching the two Riedel shear sets of figure A.*

Figure 60. Overview of the deformation phases in a N-S cross-sectional view.

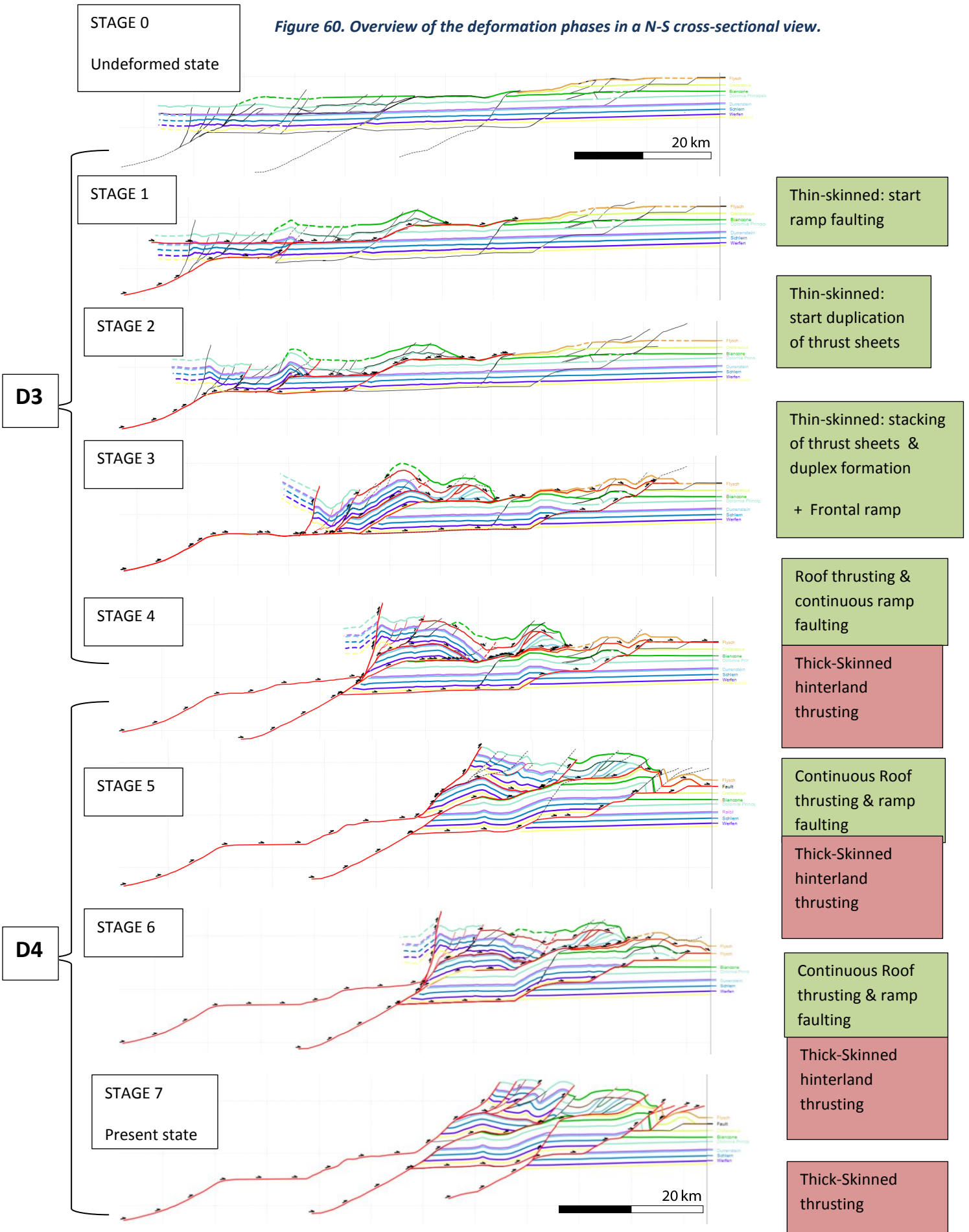

7. Regional implications

In this chapter we address the implications of the findings from this study on the regional tectonics of the Friuli Alps. The interpretation of the field-data enabled us to construct a geologically sound N-S cross-section, as tested by a balancing exercise in MOVE software for 2D kinematic modeling. The insights from the restored section and the forward modeling, suggest that the present-day configuration of the eastern Southern Alps is the result of Alpine thin- and thick-skinned phases of deformation. The earlier thin-skinned phase of deformation accommodated the majority of the total shortening amounting to at least 57,2 and maximum ~105 km and took place during the Middle -Late Miocene. This phase was followed by a late thick-skinned deformation phase with minor shortening of late Miocene – Pliocene age. The most recent deformation in the area is associated to an overall dextral transpressional movement in the eastern Southern Alps.

Especially the higher degree of thin-skinned tectonics, and the associated higher shortening estimate 57,2 to ~105 km proposed during this study, may lead to new developments and insights on the tectonic setting of the region. This increase in crustal shortening in the eastern Southern Alps might be related to the possible subduction of the Adriatic lithosphere underneath the Eastern Alps and the counter clockwise rotation of the Adriatic indenter.

7.1 Polarity switch of subduction

The European Alps is a classic example of an collisional orogen displaying along-strike variations in orogenic wedge geometry, shortening and/or surface uplift patterns, indicating the 3D character of the mountain building process (Luth et al., 2013). In the case of the European Alps, the Western- and Central Alps contain relatively large scale pro-wedges overlying the subducting European plate and rather narrow retro-wedges, in contrast to the Eastern Alps where crustal deformation is more evenly distributed above the collision zone resulting in a maximum width of the orogen along the TRANSALP profile (fig. 61). A possible explanation for this difference along the Alpine chain may be the switch of subduction polarity beneath the Eastern Alps.

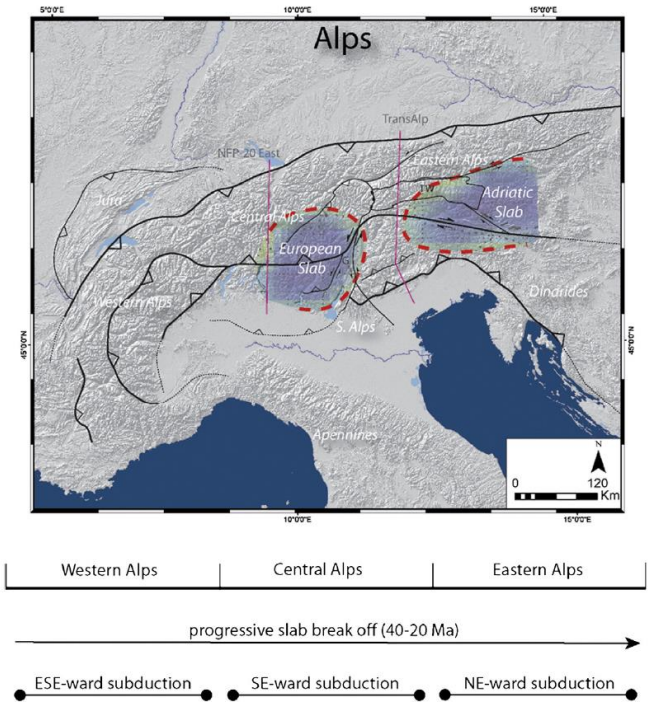

Figure 61. Section lines of the TRANSALP profile through the Eastern Alps, indicating the more symmetric pro- and retro-wedge formation compared to the Western and Eastern Alps where the retro-wedge on the European side relatively larger than the pro-wedge (from Luth et al., 2013).

The Southern Alps are generally considered to be the retro-wedge response of the Alpine mountain building, which is associated to the S-directed subduction of Europe below Adria. However, Teleseismic tomographic research by Lippitsch et al. (2003) indicates SE-directed subduction of the European mantle below the Central Alps, but NE-directed subduction of the Adriatic mantle lithosphere below the Eastern Alps (Luth et al., 2013; Kissling et al., 2006; Lippitsch et al., 2003). The observations of Lippitsch et al. (2003) where confirmed by a tomographic study of Mitterbauer et al. (2011), its interpretation however differs. Mitterbauer et al. (2011) relates the observed anomalies below the Eastern Alps to the subduction of European lower lithosphere instead of to the subduction of Adriatic mantle lithosphere, which illustrates the ongoing debate about the existence of a polarity switch beneath the Eastern Alps.

Luth et al. (2013) investigated the surface expression of lateral polarity change of continental mantle lithosphere subduction by the use of lithosphere scale physical models. The models have been compared to the along-strike differences known in the European Alps, the asymmetric wedge in the Western and Central Alps compared to the more symmetric wedge in the Eastern Alps. This study led to the general conclusion that large-scale lateral variations of the crustal architecture in mountain belts may indicate a subduction polarity switch at mantle depth (Luth et al., 2013).

7.2 Subduction & amount of shortening

The total amount of post-collisional shortening in the Eastern Alps has been estimated to be 210 km during the last 20 Ma (Schmid et al., 2004), which is in accordance with the 210 km long NE-dipping slab, representing the subducted Adriatic lower lithosphere (Schmid et al., 2004). However, the subduction of Adriatic continental lithosphere beneath the Eastern Alps, reaching to a depth of 200 km or more, is regarded as controversial on dynamic grounds (Handy et al., 2014). Especially when the subduction occurred without attachment to oceanic lithosphere, providing the gravity to let the slab sink. Teleseismic tomography shows a $+V_p$ anomaly below the Eastern Alps, indicating slab material at a depth of 210-240 km, and even deeper, 350-600 km beneath the Pannonian Basin further to the east (Handy et al., 2014). A possible explanation for the great depth could be that the subducted slab got significantly deformation and stretched, achieving the indicated depth of 210-240 km (Handy et al., 2014). This stretching may be caused by just the weight of the slab, or may be pulled down by the adjacent subducted European plate (Handy et al., 2014). A different explanation may be that the anomaly indicating the depth of 210-240 km, may be induced by a compound of European and Adriatic slabs (Handy et al., 2014). However, both cases require a considerable amount of subduction, which is expected to be reflected by the amount of crustal shortening in the eastern Southern Alps. The current shortening estimates of the eastern Southern Alpine crust of 30 to 50 km are therefore clearly not in accordance with the proposed amount of subduction (Handy et al., 2014).

Regarding the conclusion of Luth et al. (2013), that the lateral variations of the crustal architecture in a mountain belt may be linked to a lateral switch of the subduction polarity, we will now discuss the possible consequences of our research for the insights on the plate tectonic configuration below the Eastern (Southern) Alps, and in particular with respect to the previously mentioned polarity switch theory.

Shortening in the eastern Southern Alps initiated early in the Miocene, coeval with sinistral displacement of the Periadriactic lineament by the Giiudicarie line and with the shortening and exhumation of the Tauern Window in the Eastern Alps (e.g. Luth et al., 2013; Fügenschuh et al., 1997; Laubscher, 2010). The general estimation of the total amount of shortening in the eastern Southern Alps ranges between 35 and 50 km (Castellarin et al., 2006; Schönborn, 1999), which is less, but still comparable to the 30 to 70 km of shortening estimated for the western Southern Alps (Castellarin et al., 2006; Roeder, 1992; Schönborn, 1999). However, as mentioned earlier in this report, the amount of shortening in the eastern Southern Alps is poorly constrained, mainly due to the lack of Miocene sediments (Castellarin et al., 2006; Roeder, 1992).

Regarding the conclusion of Luth et al. (2013), that the lateral variations of the crustal architecture in a mountain belt may be linked to a lateral switch of the subduction polarity, would a higher amount of shortening in the eastern Southern Alps compared to the western Southern Alps, support the idea of continental subduction of Adria below the Eastern Alps during the Miocene.

The, during this research proposed, shortening estimate of 57,2 – 78,4 km for the eastern Southern Alps still also falls significantly short in meeting the ~210 -240 km of subducted slab. However, Miocene crustal shortening is not only accommodated in the southern Eastern Alps, but also in the northern Eastern Alps, and an additional 64 km of shortening registered in the Eastern Alps by a balancing study of Linzer (2002), brings

the total Miocene shortening in the Eastern Alps up to 142,4 km. Despite that this amount of shortening, still does not meets up to the ~210 – 240 km, as indicated by the amount of subducted slab, we consider this increase in shortening in the eastern Southern Alps, along with the consequently larger deviation between the Western and Eastern part of the Alps, as supporting evidence for the subduction polarity switch below the Eastern Alps during the Miocene.

Handy et al. (2014) proposes widespread horizontal decoupling at the crust-mantle boundary and/or within the crust itself, in order to explain several anomalous structures related to the indentation of Adria. Horizontal decoupling below the Tauern Window, would explain the preservation of the pre-Miocene southward dipping Moho beneath the crustal wedge, as indicated by the TRANSALP section (Kummerow et al., 2004; Lüdschen et al., 2004, 2006). But more relevant for this study, it may explain the differences in style and location of the N-S Miocene shortening along the strike of the eastern Adriatic indenter. In the west, the amount of shortening was the largest north of the PA, and was localized in front of the crustal wedge near the Tauern Window. In the eastern part, Miocene and Pliocene shortening was mainly accommodated south of the PA and is expressed by thrusting, strike-slip deformation and block-rotations (Handy et al., 2014).

In summary, we propose a tectonic setting involving a polarity switch of the subducting plate below the Eastern Alps, first Europe and later Adria, accounting for the along-strike difference of the higher amount of Miocene shortening in the eastern Southern Alps. The higher amount of (upper-) crustal shortening may be the result of horizontal decoupling at the upper-lower crustal boundary as a consequence of the subduction of Adria beneath the Eastern Alps initiating during the early Miocene. The evaporites of the Upper-Permian Bellerophon Formation provides the ideal sliding surface for the thin-skinned deformation of upper crustal cover which has detached from the lower crustal basement, leading to a thin-skinned deformation of the upper crustal cover and to underthrusting and partial subduction of the lower crust associated to the northward subduction of Adria beneath the Eastern Alps. The later phase of thick-skinned tectonics led to the uplift of basement material in the northern part of the eastern Southern Alps and reactivated some of the pre-existing thin-skinned structures (fig. 62 A,B and C).

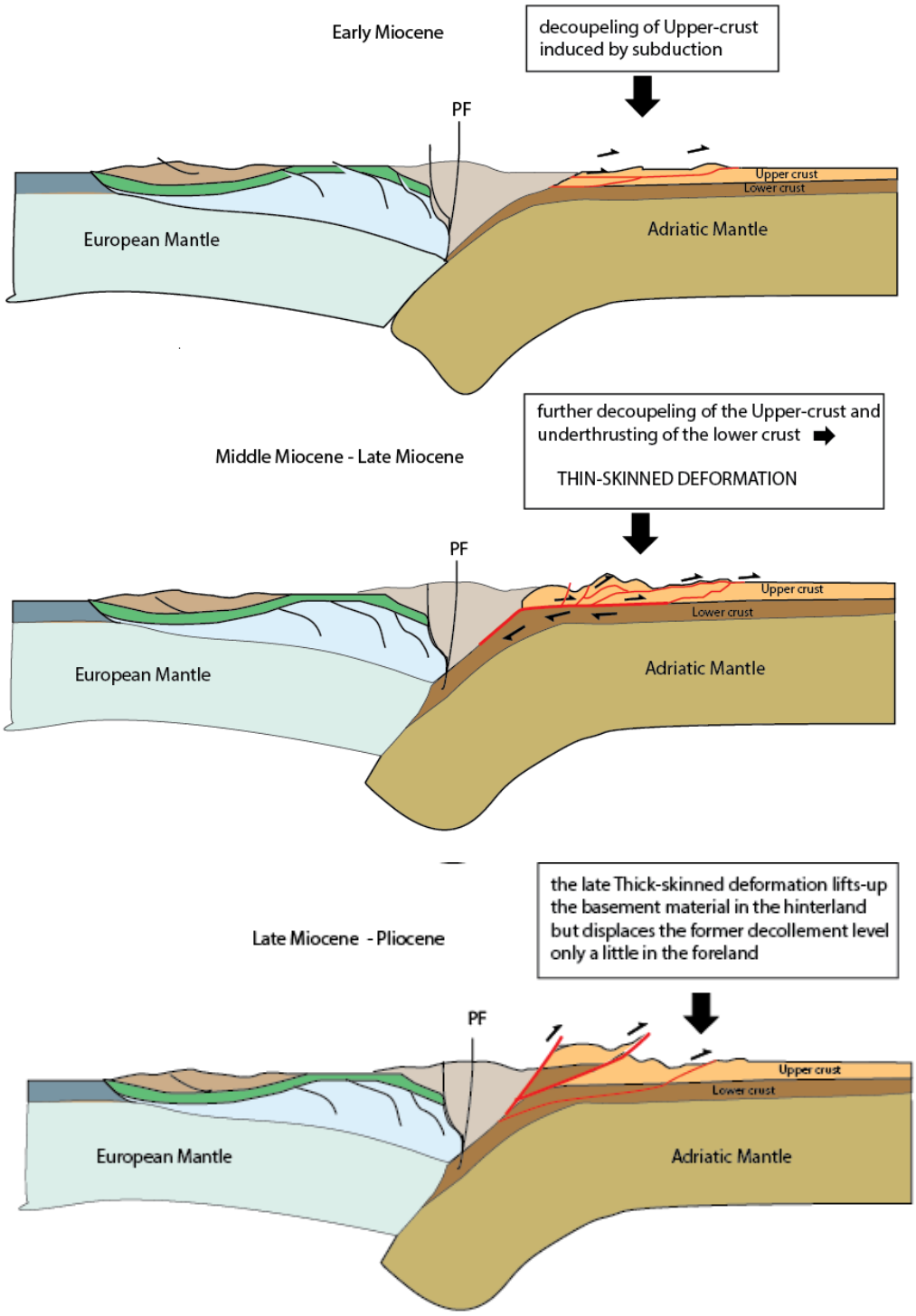

Figure 62. *Overview of the tectonic evolution since the Miocene (modified after Handy et al., 2014).* ***A)*** *During the early Miocene, The subduction of Adria initiates beneath the Eastern Alps.* ***B)*** *In Middle-Late Miocene time, the ongoing subduction of Adria below the European plate caused horizontal decoupling at Upper- lower-crust boundary and crustal shortening is accommodated by S-vergent thin-skinned tectonics in the Southern Alps.* ***C)*** *A late phase of thick-skinned deformation causes the basement-uplift in the northern part of the ESA and displaces pre-existing thin-skinned décollements.*

8. Conclusions

Based on field data, five distinct deformation phases (D1- D5) have been defined. Due to the additional insights from the restoration and forward modelling in MOVE, a clear distinction could be made between thin- and a thick-skinned phase of deformation.

- D1- Prior to the compressional phases is the D1 NW-SE extensional phase, which is expressed by NNW-SSE oriented normal faults, which have been related to the NE-SW platform separation during the Early-Jurassic.
- D2 - The D2 NE-SW to E-W directed Dinaric shortening started during the Eocene and continued till early Miocene time and is expressed by SW to W-vergent thrusting and folding. The thin-skinned nature of Dinaric deformation is strongly indicated by kinematic evidence found in three Dinaric décollement horiozons; Bellerophon, Raibl and Biancone Formation. The Dinaric structures are largely overprinted by three Alpine deformation phases, what possibly led to the local rotation of Dinaric structures.
- D3 – The D3 N-S thin-skinned Alpine shortening (Middle- to Late-Miocene), is characterized by large scale S-vergent thrusting along flat-ramp-flat trajectories, resulting in great amounts of transportation of the Upper-Triassic and Jurassic platform formations along four main décollements (the Bellerophon, Raibl and Biancone Formation, and the Eocene flysch) and ultimately to tripling and folding of the sedimentary cover. The thin-skinned faulting was accommodated by one major thrust system with its basal décollement horizon in the Upper Permian evaporates of the Bellerophon Formation. The multiple fault-splays in this thrust-system originate all from the main basal décollement in the Bellerophon Formation, and developed in sequence from north to south.
- D4 - The D4 NE-SW thick-skinned Alpine shortening (Late Miocene – Pliocene), is expressed in the field by thrusting and folding and led to the reactivation, cross-cutting and uplift of former thin-skinned structures and basement material.
- D5 - The D5 Transpressional phase (initiated during the Early –Miocene and is probably still active), has been interpreted as the transpressional continuation of the D4 thick-skinned deformation and involves large scale strike-slip deformation and minor normal faulting.

- Due to the clear distinction between thin- and thick-skinned deformation, we were able to make an estimation of the total amount of N-S shortening since the Eocene. The balancing and reconstruction of the thin-skinned dominated model in MOVE indicates a minimum shortening of 57,2 km (51%) for the Friuli Alps. The maximum shortening, based on an estimation of the extent of the main décollement levels and some simple crustal-wedge budget calculations, is estimated on ~78,4 km. These newly proposed shortening estimates are significantly higher than the previously proposed 30 – 50 km of N-S shortening for the eastern Southern Alps during the Miocene and provide new insights on the plate tectonic setting below the Eastern Alps.

- This newly proposed, larger amount of shortening for the eastern Southern Alps, enhances the lateral variation between the western and eastern part of the Southern Alps. Further differentiation between the western and eastern Southern Alps supports the idea that lateral variations of the crustal architecture in a mountain belt may be linked to a lateral switch of the subduction polarity and may indicate the horizontal decoupling of the Adriatic upper crust and the underthrusting and possible stacking of the lower crust, associated to the subduction of the Adriatic plate beneath the Eastern Alps.

9. Future work

The choice of the cross-section line

In order to investigate an interference area like the Friuli Alps, it would be best to construct at least two cross-sections parallel to the two expected interfering directions of shortening. In the case of the Friuli Alps would that be a NE-SW to E-W cross-section, to investigate the Dinaric structures, and an N-S cross-section to illustrate the Alpine structures. But to unravel the true nature of the interfering structures, a 3D restoration of the area by use of multiple, more or less, perpendicular cross-sections is needed. However, such an approach would require a lot of field-data in a large area, and is therefore expected to be very time consuming, nonetheless of great value for the understanding of the area.

Analogue (sandbox) models

The construction of analogue models (sandbox) in order to investigate the proposed decoupling scenario in combination with a polarity switch of the subducting slab (Adria below Europe) would give new insights on the validity of the scenario and the possible correlation with the Eastern Alpine tectonic setting. What also could be tested is the validity of the pure thin-skinned response to the convergent movement, followed by a later stage of thick-skinned deformation. The focus of such research would be on the foreland deformation structures, what type of deformation mechanism developed the geometries and is it comparable to the exterior of the eastern Southern Alps?

10. Acknowledgements

First of all I would like to thank Inge van Gelder for all the helpful tips and feedback during the fieldwork and during the process of writing. I would like to thank Ernst Willingshofer for his feedback, advice and for providing excellent local food during field lunches. I would also like to thank Liviu Matenco, for his feedback on the cross-section and thesis presentation. Special thanks to my fieldbuddy Anissa Smits, for being my sparring partner during the fieldwork and for the great company. Finally I would like to thank my friends, family and girlfriend for their support during the writing.

References

Bartel, E., et al., 2014, States of paleostress north and south of the Periadriatic fault: Comparison of the Drau Range and the Friuli Southalpine wedge, Tectonophysics 637, pp. 305–327

Bosellini, A. and Doglioni, C., 1986, Inherited structures in the hangingwall of the Valsugana Overthrust (Southern Alps, Northern Italy), Journal of Structural Geology, Vol. 8, No. 5, pp. 581-583

Carulli, G. et al., 2006, Carta Geologica del Friuli Venezia Giulia, Università degli sturdy di Trieste e Udine

Castellarin A., et al., 1998, La tettonica delle Dolomiti nel quadro delle Alpi Meridionali Orientali, Mem. Soc. Geol. 53, pp. 133-143

Castellarin, A. and Cantelli, L., 2010, Geology and evolution of the Northern Adriatic structural triangle between Alps and Apennine, Rend. Fis. Acc. Lincei 21 (Suppl 1): S3–S14

Cati, A. et al., 1987b, Carbonate platforms in the subsurface of the northern Adriatic area, Mem. Soc. Geol. It., 40, pp. 295-308

Chapple, W. M., 1978, Mechanics of thin-skinned fold-and-thrust belts, Geol. Soc. Am. Bull., 89, 1189 – 1198

Coward, M.P., 1983, Thrust tectonics, thin skinned or thick skinned, and continuation of thrust to deep in the crust, Department of Earth Sciences, Leeds Univeristy, Leeds LS2(JT,U.K. Journal of Structural Geology, Vol. 5, No. 2, pp. 113 to 123, 1983

D'argenio B., Catalano R., Channell J.E.T., 1980, Palaeomagnetism and deformation of the Mesozoic continental margin in Sicily, Tectonophysics Volume 61, Issue 4, 10 January 1980, Pages 391-40

Delvaux, D., 2014, Win_Tensor 5.0.5., Royal Museum for Central Africa, Dept. Geology & Mineralogy, Tervuren, Belgium

Doglioni, C., 1986, Tectonics of the Dolomites (Southern Alps, Northern Italy), Journal of Structural Geology, Vol. 9, No. 2, pp. 181 - 193

Frisch, W., Dunkl, I., Kuhlemann, J., 2000, Post-collisional orogen-parallel large-scale extension in the Eastern Alps, Tectonophysics 327, pp. 239-265

Flügel H.W., Jaeger H., Schönlaub H.P. & Vai, G.B., 1977, Carnic Alps. In: Martinson, A (ed.) The Silurian-Devonian Boundary: IUGS Series A, 5, 126-142

Fügenschuh B., Seward D., Mancktelow N.S., 1997. Exhumation in a convergent orogen: the western Tauern window. Terra Nova: 9, pp. 213-217, 1997

Gotberg, N., McQuarrie, N., and Caillaux, V.C., 2010, Comparison of crustal thickening budget and shortening estimates in southern Peru (12–14°S): Implications for mass balance and rotations in the "Bolivian orocline": Geological Society of America Bulletin, v. 122, p. 727–742, doi :10 .1130 /B26477 .1 Handy, M.,

Ustaszewski, K. and Kissling, E., 2014, Reconstructing the Alps–Carpathians–Dinarides as a key to understanding switches in subduction polarity, slab gaps and surface motion, Int. J. Earth. Sci., Geol. Rundsch., DOI 10.1007/s00531-014-1060-3

Janák, M., et al., 2004, First evidence for ultrahigh-pressure metamorphism of eclogites in Pohorje, Slovenia: Tracing deep continental subduction in the Eastern Alps, Tectonics, vol. 23, TC5014, doi: 10.1029/2004TC001641

Kissling, E. et al. 2006, Lithosphere structure and tectonic evolution of the Alpine arc: new evidence from high-resolution teleseismic tomography, Geol. Soc. Lond. Mem. 32, pp. 129–145

Krainer, K., 1993. Late-and Post-Variscan Sediments of the Eastern and Southern Alps. In: *Pre-Mesozoic geology in the Alps*, edited by J.F. von Raumer and F. Neubauer, 537-564, Springer Verlag Berlin.

Lacombe, O. and Mouthereau, F., 2002, Basement-involved shortening and deep detachment tectonics in forelands of orogens: Insights from recent collision belts (Taiwan, Western Alps, Pyrenees). *Tectonics 21: doi: 10.1029/2001TC901018. issn: 0278-7407.*

Linzer, H.G., Decker, K., Peresson, H., Dell'Mour, R., Frisch, W., 2002, Balancing lateral orogenic float of the Eastern Alps, Tectonicphysiscs 354 (2002) 211-237

Lippitsch, R., Kissling, E., Ansorge, J., 2003, Upper mantle structure beneath the Alpine orogen from high-resolution teleseismic tomography, J. Geophys. Res., Vol. 108, No. B8, 2376, doi:10.1029/2002JB002016

Luth, S., et al., 2013, Does subduction polarity changes below the Alps? Inferences from analogue modelling,Tectonophysics 582, pp. 140–161

Monegato, G., Stefani, C., Zattin, M., 2010. From present rivers to old terrigenous sediments: the evolution of the drainage system in the eastern Southern Alps. Terra Nova 22 (3), 218e226. doi:10.1111/j.1365-3121.2010.00937.x.

Nussbaum, C., 2002, Neogene Tectonics and Thermal Maturity of Sediments of the Easternmost Southern Alps (Friuli Area, Italy), Institut de Géologie Université de Neuchâtel

Ratschbacher, L., Merle, O., Davy, P., Cobbold, P., 1991, Lateral Extrusion in the Eastern Alps, part 1: boundary conditions and experiments scaled for gravity, Tectonics 10(2), pp. 245–256

Schmid, S.M. et al., 1996, Geophysical-geological transect and tectonic evolution of the Swiss-Italian Alps, Tectonics, Vol.15, No. 5, pp. 1036-1064

Schmid , S.M. et al., 2004, Tectonic map and overall architecture of the Alpine orogen, Eclogae geol. Helv. 97,pp. 93–117

Schmid, S.M. et al., 2008, The Alpine-Carpathian-Dinaridic orogenic system: correlation and evolution of tectonic units, Swiss J. Geosci. 101, pp. 139–183

Schönborn, G., 1999, Balancing cross sections with kinematic constraints: The Dolomites (northern Italy), Tectonics, Vol. 18, No. 3, pp. 527-545

Sanders, D.J., Marchini W.R.D., Transpression, Department of Geology, The Queen's Univeristy, Belfast BT7 INN, U.K. Journal of Structural Geology, Vol. 6, No. 5, pp. 449 to 458, 1984

Stampfli, G., Mosar, J., 1999. The making and becoming of Apulia. Mémoires Science Géologie (University of Padova). Special Volume, Third Workshop on Alpine Geology, Padova 51/1, 141e154

Ustaszewski, K. et al., 2008, A map-view restoration of the Alpine–Carpathian–Dinaridic system for the Early Miocene, Swiss J. Geosci. 101(1), pp. 273–294

Van Gelder, I., 2011, Lateral extrusion in the Eastern Alps: a matter of pushing or pulling? Part II: Insights from analogue crustal scale models, Master Thesis VU Amsterdam

Venturini, C. (Ed), 1990a. Field workshop on Carboniferous to Permian sequence of the Pramollo-Nassfeld basin (Carnic Alps). Guidebook Pramollo 1990. *Arti Grafiche Friulani, Udine*, 1-159.

Willingshofer, E., Neubauer, F. and Cloetingh, S., 1999, The Significance of Gosau-Type Basins for the Late Cretaceous Tectonic History of the Alpine-Carpathian Belt, Phys. Chem. Earth (A), Vol. 24, No. 8, pp. 687-695

Zampieri D., Massironi M., 2007, Evolution of a poly-deformed relay zone between fault segments in the eastern Southern Alps, Italy.

Ziegler, P. A., G. Bertotti, and S. A. P. L. Cloetingh, 2002, Dynamic processes controlling foreland development - Role of mechanical (de)coupling of orogenic wedges and forelands, in Continental Collision and the Tectono-sedimentary Evolution of Forelands, EUG Stephan Mueller Publ. Ser., vol.1, edited by B. Bertotti, K. Schulmann, and S. A. P.L. Cloetingh, pp. 17 – 56, Copernicus, Katlenburg-Lindau, Germany.

Appendices

APPENDIX A: Geological map *(modified after Carulli et al., 2006)*

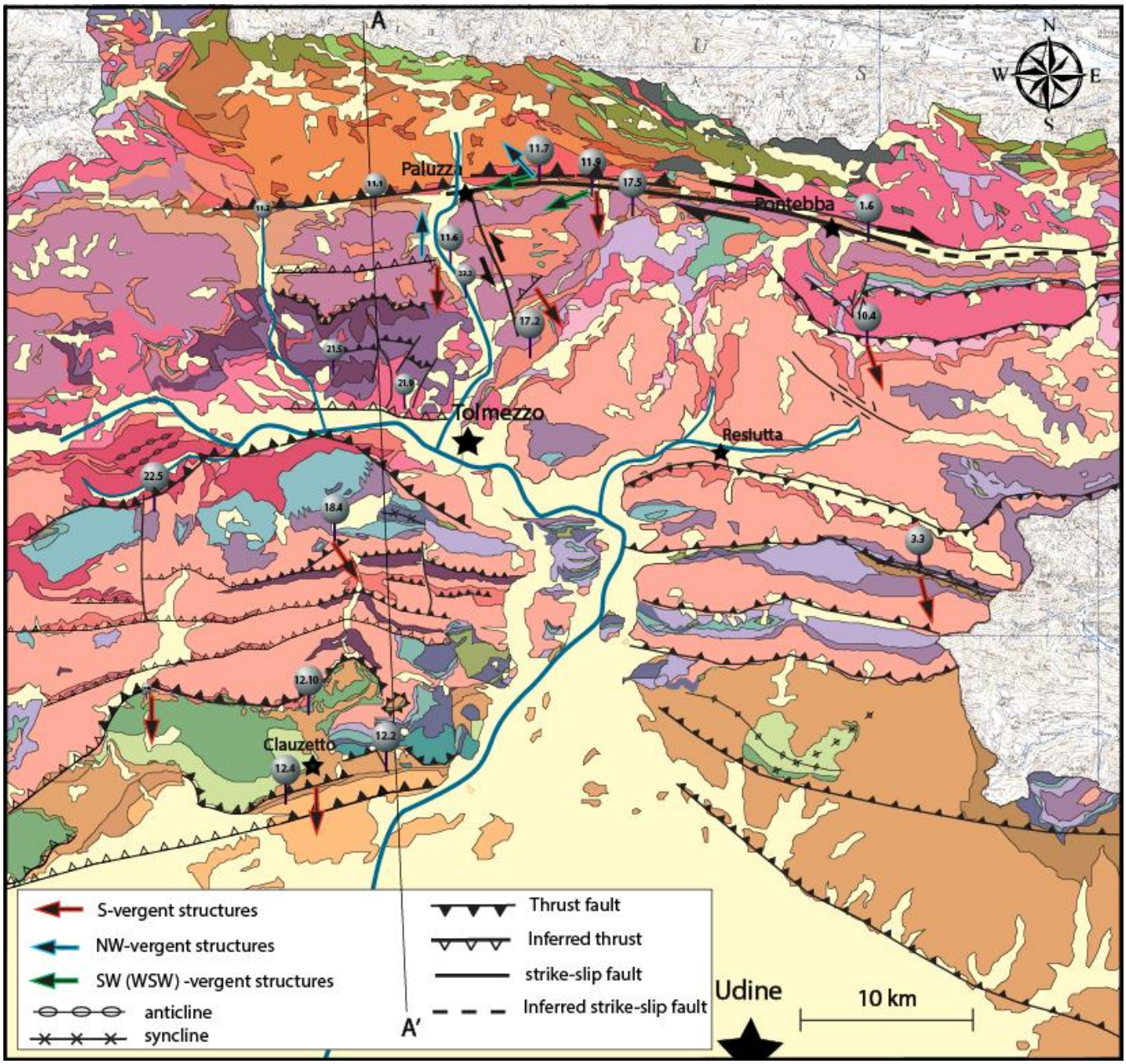

Geological map of the Friuli area. This map gives an overview of the large scale geological structures and key outcrops in the western part of the research area. The colors of the structures corresponds with the structures in the cross-sections of chapter 7.

APPENDIX B: Legend of the geological map

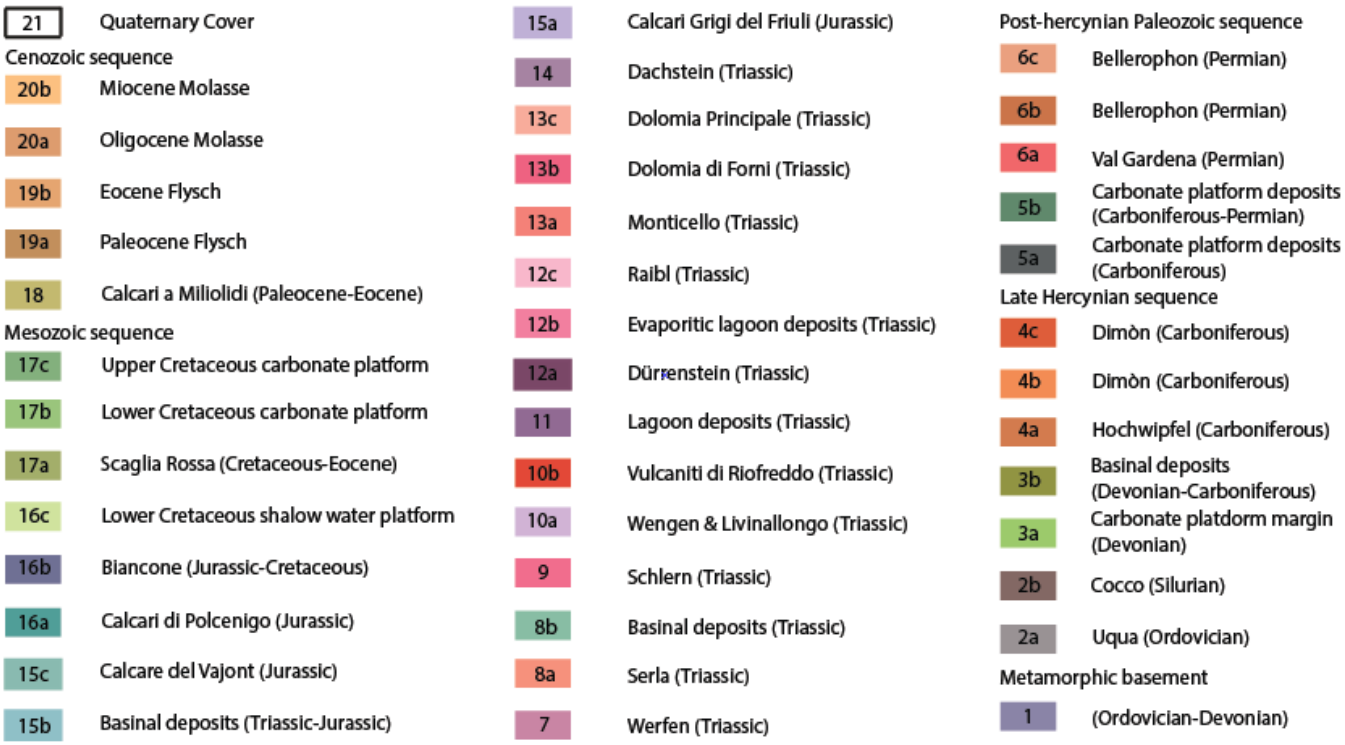

APPENDIX C: Geological map of the Friuli Alps *(Carulli et al., 2006)*

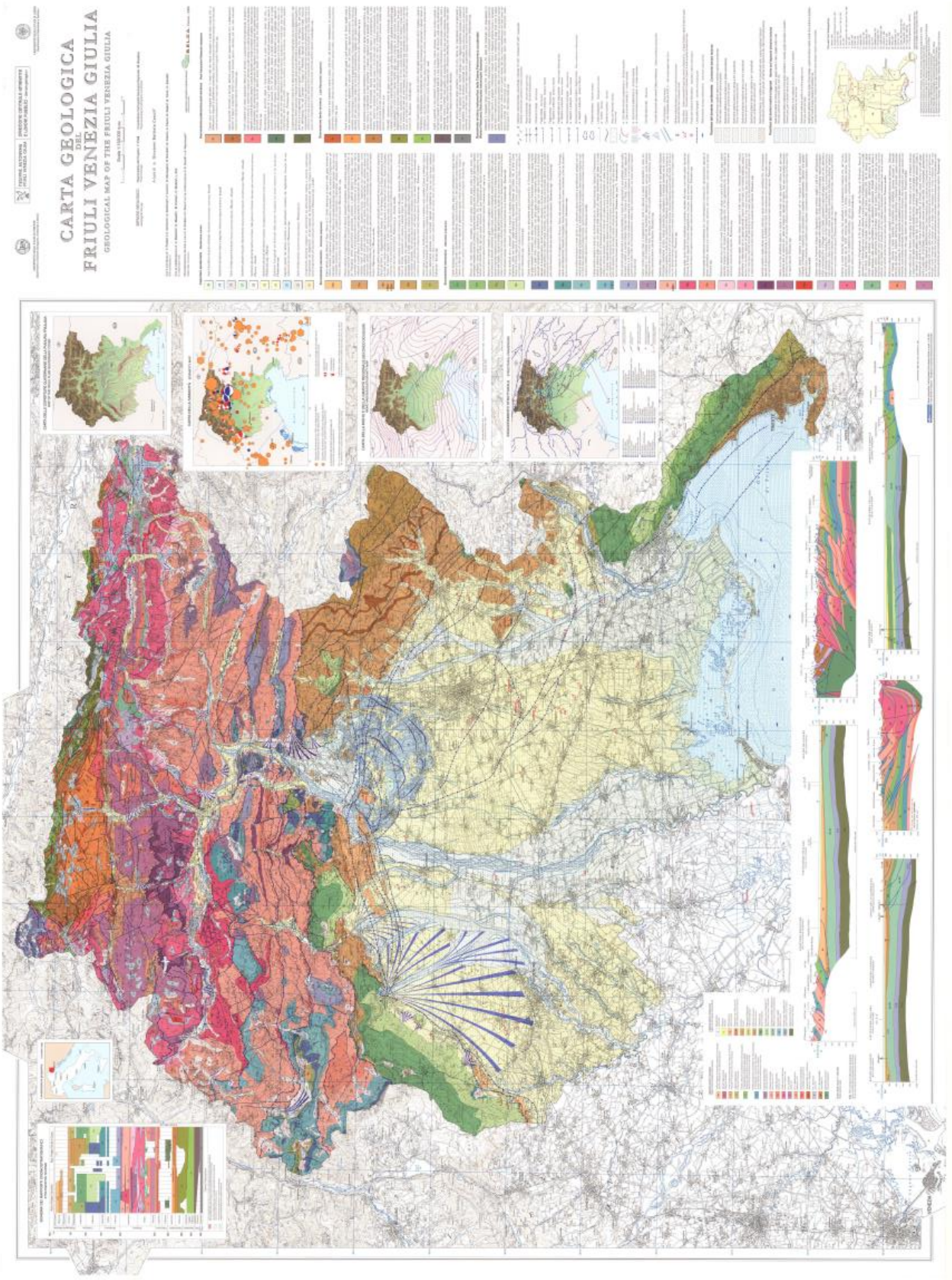

APPENDIX D: Map overview of all the field stops

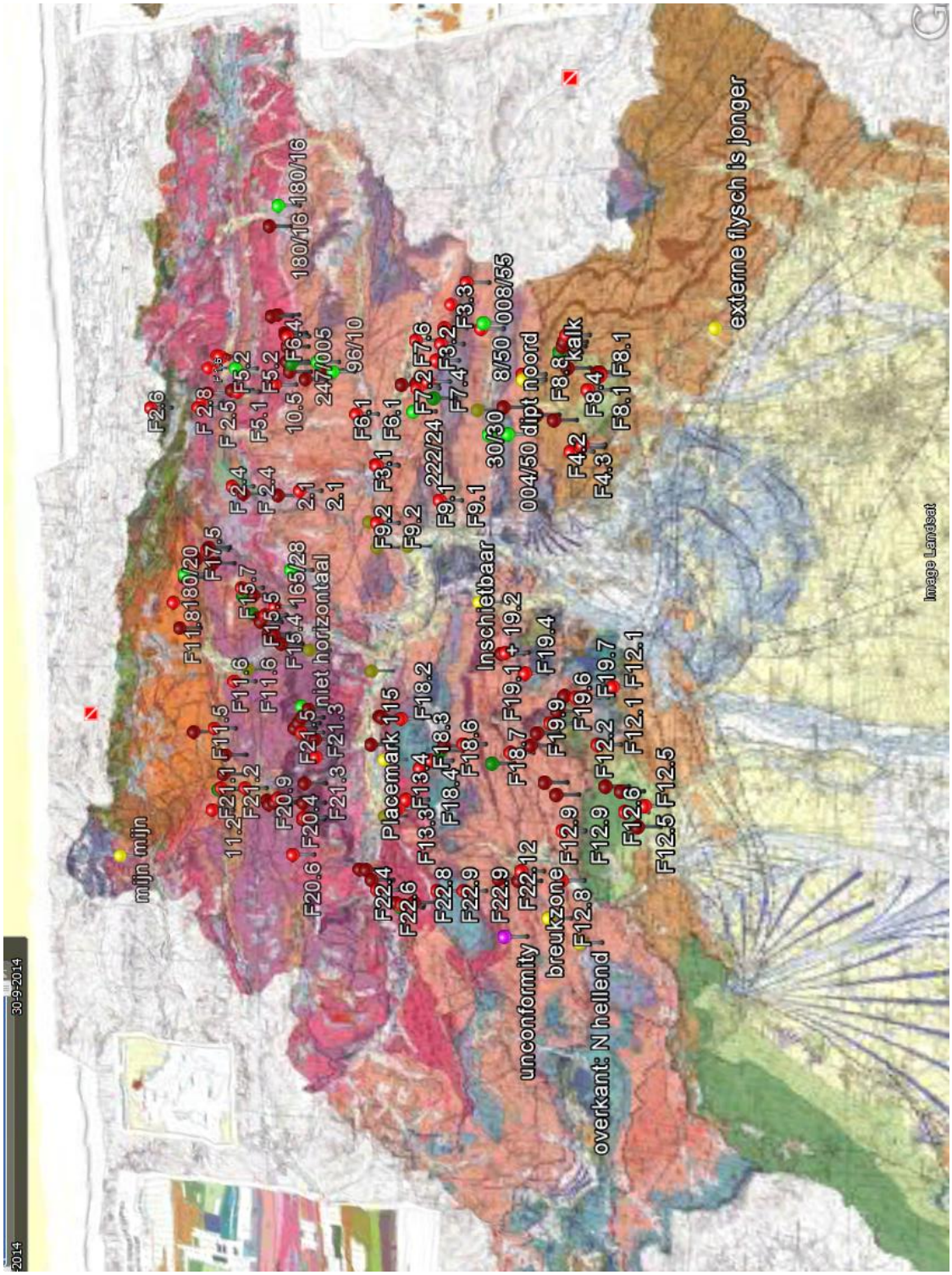

A total of 141 field stops have been made in the Friuli area.